EFFECTS OF DYNAMIC LOADING ON NEOCARTILAGE FORMATION

A THESIS SUBMITTED TO
THE GRADUATE SCHOOL OF NATURAL AND APPLIED SCIENCES
OF
MIDDLE EAST TECHNICAL UNIVERSITY

BY

GÜLÇİN ÇİÇEK REZAEİTABAR

IN PARTIAL FULFILLMENT OF THE REQUIREMENTS
FOR
THE DEGREE OF DOCTOR OF PHILOSOPHY
IN
BIOMEDICAL ENGINEERING

AUGUST 2022

Approval of the thesis:

EFFECTS OF DYNAMIC LOADING ON NEOCARTILAGE FORMATION

submitted by **GÜLÇİN ÇİÇEK REZAEİTABAR** in partial fulfillment of the requirements for the degree of **Doctor of Philosophy in Biomedical Engineering, Middle East Technical University** by,

Prof. Dr. Halil Kalıpçılar
Dean, Graduate School of **Natural and Applied Sciences** _____

Prof. Dr. Vilda Purutçuoğlu
Head of the Department, **Biomedical Eng.** _____

Prof. Dr. Ayşen Tezcaner
Supervisor, **Biomedical Eng., METU** _____

Prof. Dr. Korhan Altunbaş
Co-Supervisor, **Histology and Embryology, Afyon Kocatepe University** _____

Examining Committee Members:

Prof. Dr. Sreeparna Banerjee
Biological Sciences, METU _____

Prof. Dr. Ayşen Tezcaner
Biomedical Eng., METU _____

Prof. Dr. Eda Ayşe Aksoy
Basic Pharmaceutical Sciences, Hacettepe University _____

Prof. Dr. Pınar Yılgör Huri
Biomedical Eng., Ankara University _____

Asst. Prof. Dr. Senih Gürses
Engineering Sciences, METU _____

Date: 09.08.2022

I hereby declare that all information in this document has been obtained and presented in accordance with academic rules and ethical conduct. I also declare that, as required by these rules and conduct, I have fully cited and referenced all material and results that are not original to this work.

Name Last name : Gülçin Çiçek Rezaeitabar

Signature :

ABSTRACT

EFFECTS OF DYNAMIC LOADING ON NEOCARTILAGE FORMATION

Çiçek Rezaeitabar, Gülçin
Doctor of Philosophy, Biomedical Engineering
Supervisor: Prof. Dr. Ayşen Tezcaner
Co-Supervisor: Prof. Dr. Korhan Altunbaş

August 2022, 141 pages

Cartilage tissue engineering has gained attention to meet the increasing demand for articular cartilage treatment in ageing populations. In this study, a visible light crosslinkable Methacrylated Glycol Chitosan (MeGC)-Fibrinogen (Fib) hydrogel system which can potentially be used in cartilage tissue engineering applications was developed. Incorporation of Fib into MeGC hydrogel structure decreased the swelling, led to increase in stability and improved the mechanical properties of hydrogels. Besides Fib addition enhanced proliferation of encapsulated chondrocytes and improved cartilagenious extracellular matrix (ECM) deposition within hydrogels. To investigate the effect of incremental dynamic compressive loading on the development of cartilage tissue constructs, rabbit chondrocytes were entrapped in 1 MeGC-Fib based hydrogels and cultivated in a custom-built mechanobioreactor. Investigations revealed that, not just dynamic cultivation but applied mechanical stimulation regime is also crucially important on viability and cartilage-specific ECM production by chondrocytes. At the end of 21 days of cultivation, compared to free swelling and DC-1 regime, hydrogel-entrapped chondrocytes cultivated under incremental dynamic compressive loading regime (DC-2) increased cell proliferation and chondrocyte functionality. To further evaluate the chondrogenic

potential of MeGC-Fib hydrogels and DC-2 regime, in-vivo studies were performed by hydrogel implantation to chondral defect models created on New Zealand White Rabbits. The histological and immunoflorescent examinations revealed the positive impact both MeGC-Fib hydrogels and DC-2 regime on neocartilage formation with a higher s-GAG, total collagen and collagen-II content compared to other groups. These findings demonstrate the potential of developed MeGC-Fib hydrogels and incremental dynamic compressive loading regime to promote cartilage regeneration.

Keywords: Cartilage, Tissue Engineering, Mechanical stimulation, Dynamic culture, Biomaterials

ÖZ

NEOKIKIRDAK OLUŞUMUNDA DİNAMİK YÜKLEMENİN ETKİLERİ

Çiçek Rezaeitabar, Gülçin
Doktora, Biyomedikal Mühendisliği
Tez Yöneticisi: Prof. Dr. Ayşen Tezcaner
Ortak Tez Yöneticisi: Prof. Dr. Korhan Altunbaş

Ağustos 2022, 141 sayfa

Populasyonların yaşlanmasıyla artan artiküler kıkırdak tedavisi ihtiyacını karşılamaya yönelik kıkırdak doku mühendisliği çalışmaları dikkat çekmektedir. Bu çalışmada, kıkırdak doku mühendisliği uygulamalarında potansiyel olarak kullanılabilecek yeni bir görünür ışık altında fotopolimerize olabilen Glikol Kitosan Metakrilat (MeGC)- Fibrinojen (Fib) hidrojel sistemi geliştirildi. Fibrinojenin MeGC hidrojel yapısına girmesi hidrojel sisteminin şişmesini azaltmış, stabilitesini artırmış mekanik özelliklerinde iyileşmeye yol açmıştır. Fibrinojenin MeGC hidrojel yapısına eklenmesiyle hidrojel sistemine hücre tutunması iyileşmiş, hücre canlılığı ve proliferasyonunda, sGAG ve kolajen II içeren kıkırdak-spesifik ECM birikiminde artış sağlanmıştır. Artımlı dinamik basma yüklemesinin kıkırdak doku konstrüktlerinin gelişimi üzerindeki etkisini araştırmak için, tavşan kondrositleri 1 MeGC-Fib bazlı hidrojellere hapsedilmiş ve özel olarak yapılmış bir mekanobiyoreaktörde kültive edilmiştir. Mekanik stimülasyonun hücre canlılığı üzerindeki etkisine ilişkin araştırmalar, sadece dinamik kültivasyonun değil, aynı zamanda uygulanan mekanik stimülasyon rejiminin de hücrelerin canlılığı ve kıkırdağa özgü ECM sentezinde oldukça önemli olduğunu ortaya koymuştur. 21 günlük kültivasyonun sonunda, statik kültür ve DC-1 rejimine kıyasla, artan dinamik

sıkıştırma yükleme rejimiyle (DC-2) uyarılan kondrositlerin hücre çoğalmasında ve kondrosit işlevselliğinde artış görülmüştür. MeGC-Fib hidrojellerinin ve DC-2 rejiminin kondrojenik potansiyelinin daha da araştırılması için, Yeni Zelanda Beyaz Tavşanları üzerinde oluşturulan kondral defekt modellerine hidrojel implantasyonu gerçekleştirilerek in-vivo çalışmalar yapılmıştır. Histolojik ve immünfloresan incelemeler, diğer gruplara kıyasla daha yüksek s-GAG, toplam kollajen ve kollajen-II içeriği ile hem MeGC-Fib hidrojellerinin hem de DC-2 rejiminin neo-kıkırdak oluşumu üzerindeki olumlu etkisini ortaya koymuştur. Elde edilen bulgular, kıkırdak rejenerasyonunu artırmak için geliştirilen MeGC-Fib hidrojellerinin ve artımlı dinamik sıkıştırma yükleme rejiminin potansiyelini göstermektedir.

Anahtar Kelimeler: Kıkırdak, Doku Mühendisliği, Mekanik Uyarım, Dinamik Kültür, Biyomalzemeler

To my beloved family...

ACKNOWLEDGMENTS

I would like to express my special thanks to my supervisor Prof. Dr. Ayşen Tezcaner for her guidance, advice, encouragement, and support throughout this research. She will always be my lighthouse that inspires me to keep going forward and to contribute to this beautiful world with my skills and values.

I thank to my co-supervisor Prof. Dr. Korhan Altunbaş for his valuable contribution and support. I also thank to Tayfun Dikmen for his help for histological investigations.

I deeply thank my dear friend İdil Uysal for her wonderful friendship, support and for continuous help in every possible way. I also would like to express my special thanks to Gerçem Altunordu and Deniz Atila for their valuable friendship, and for all the fun we have had during all these years.

I would like to express appreciation to all other current and graduate members of Esbio Research Group, Dr. Ali Deniz Dalgıç, Dr. Ayşegül Kavas, Dr. Reza Moonesi Rad, Mustafa Nakipoğlu, Nazlı Seray Bostancı, Duygu Akolpoğlu, Sema Akababa, Dr. Özge Erdemli, Bahadır Güner, Sepren Öncü, Büşra Yedekçi, Funda Can, Engin Pazarçeviren, and Gülhan Işık for their friendship and sharing their knowledge whenever I needed.

I would like to express my deepest gratitude to my family. I would like to thank my dear husband Yousef Rezaeitabar for his endless support and understanding he showed during my thesis work. I would like to thank my lovely baby, Aren for

choosing me as a mother and everyday giving me the joy of having him. I would like to thank my parents for their unconditional love, and their effort to develop my scientific curiousity and enterpreneural nature.

Lastly, I gratefully acknowledge The Scientific and Technological Research Council of Turkey (TUBITAK) for the financial support they provided through the project “Photopolymerized Hydrogel-Based Cartilage Regeneration System” (Project no: 217S463).

TABLE OF CONTENTS

LIST OF TABLES

TABLES

LIST OF FIGURES

FIGURES

LIST OF ABBREVIATIONS

ACI	Autologous Chondrocyte Implantation
CS	Chondroitin Sulphate
DAPI	4', 6-diamidino-2-phenylindole
DC-1	Constant Cyclic Compressive Loading Regime: 21 kPa of Cyclic Compressive Loading Throughout the Culture
DC-2	Incremental Cyclic Compressive Loading Regime: Initial Cyclic Compressive Loading (7 kPa) Stepwise Increased Every Seven Days to the Values of 14 kPa and 21 kPa During the Culture
DMEM	Dulbecco's Modified Eagle Medium
DMMB	Dimethyl Methylene Blue
DMSO	Dimethyl Sulfoxide
DN	Double Network
ECM	Extracellular Matrix
EDTA	Ethylenediaminetetraacetic Acid
FBS	Fetal Bovine Serum
FGF	Fibroblast Growth Factor
Fib	Fibrinogen
FS	Free Swelling
FTIR	Fourier Transform Infrared Spectroscopy
Gel	Gelatin
GC	Glycol Chitosan

GCH	Gelatin/Chondroitin Sulphate/Hyaluronic Acid
GCHC	Gelatin/Chondroitin Sulphate/Hyaluronic Acid/Chitosan
GG	Gellan Gum
GelMA	Methacrylated Gelatin
^{1}H-NMR	Proton Nuclear Magnetic Resonance Spectroscopy
HA	Hyaluronic Acid
hMSC	Human Mesenchymal Stem Cells
IPN	Interpenetrated Polymer Network
MeGC	Methacrylated Glycol Chitosan
MCS	O-methacrylate Chondroitin Sulphate
MCH	Maleic Functionalized Chitosan
MSC	Mesenchymal Stem Cell
MSF	Methacrylated Silk Fibroin
PBS	Phosphate Buffered Saline
PDLLA	Poly -D, L -Lactic Acid
PEG	Polyethylene Glycol
PI	Propidium Iodide
PRP	Platelet-rich plasma
RF	Riboflavin
ROS	Reactive Oxygen Species
s-GAG	Sulfated Glycosaminoglycan
SBF	Simulated Body Fluid

SEM	Scanning Electron Microscope
SF	Silk Fibroin
TE	Tissue Engineering
UV	Ultraviolet
VBL	Visible Blue Light
VEGF	Vascular Endothelial Growth Factor
Vit-B2	Vitamin B2
VL	Visible Light

CHAPTER 1

INTRODUCTION

Articular cartilage defects are one of the most important problems in orthopedics due to the cartilage's limited ability to self-repair. Current treatment methods do not provide long-term clinical solutions, and there is no successful and widely accepted therapy for cartilage degeneration. Patients with cartilage degeneration can only be treated symptomatically, and total joint replacement appears to be the only option for end-stage degenerative joint pathology. Surgical treatments for articular cartilage defects, such as osteotomy and autologous osteochondral graft transplantation, have not been shown to be consistently effective in preventing damage recurrence [1, 2]. The development of neocartilage-based therapy methods through tissue engineering approaches has become critical in fulfilling the demand for articular cartilage treatment.

Tissue engineering techniques are used to develop adequate biomaterials for cartilage regeneration, which is critical for successful autologous chondrocyte implantation (ACI) applications. It's crucial to use a material that closely resembles the native environment of articular cartilage, particularly the ECM structure, to make an effective three-dimensional scaffold. Biocompatible, porous, biodegradable, absorbable scaffolds that mimic the mechanical properties of natural tissue and act as a guide for new tissue formation are ideal [3-5]. Furthermore, the scaffold should allow nutrients and metabolic waste products to diffuse [6].

1.1 Stucture of Articular Cartilage

The main function of articular cartilage is to provide lubricated articular movement on joints and to act as a shock absorber against cyclic compressive loadings encountered during joint movement [7]. Articular cartilage is avascular, aneural and alymphatic tissue which has only one cell type named chondrocyte. The perichondrium which is a fibrillar and highly veinous structure surrounding the upper layer cartilage is responsible of supplying nutrients and oxygen to chondrocytes, as well as removing waste products [8]. The extracellular matrix (ECM) built by chondrocytes is predominantly made of collagen type-II (10-30%) and proteoglycans (3-10%) of which 65–80% of the volume consists of water [7, 9]. Unfortunately, cartilage has limited regenerative capacity when damaged [10].

Chondrocytes constitute only 1% of the tissue volume and 95% of the collagen in the extracellular matrix is composed of collagen type II fibrils, which contribute to the tissue's tensile strength [8]. The high negative charge arising from glycosaminoglycan (GAG) biomolecules present in the proteoglycan structure gives cartilage its ability to swell and lubrication [11]. Through its depth, cartilage is organized zonally, with a distinct arrangement of collagen type II fibers and cells that lead to a calcified-cartilage area and then to subchondral bone [12]. Figure 1.1 illustrates the basic structure of cartilage.

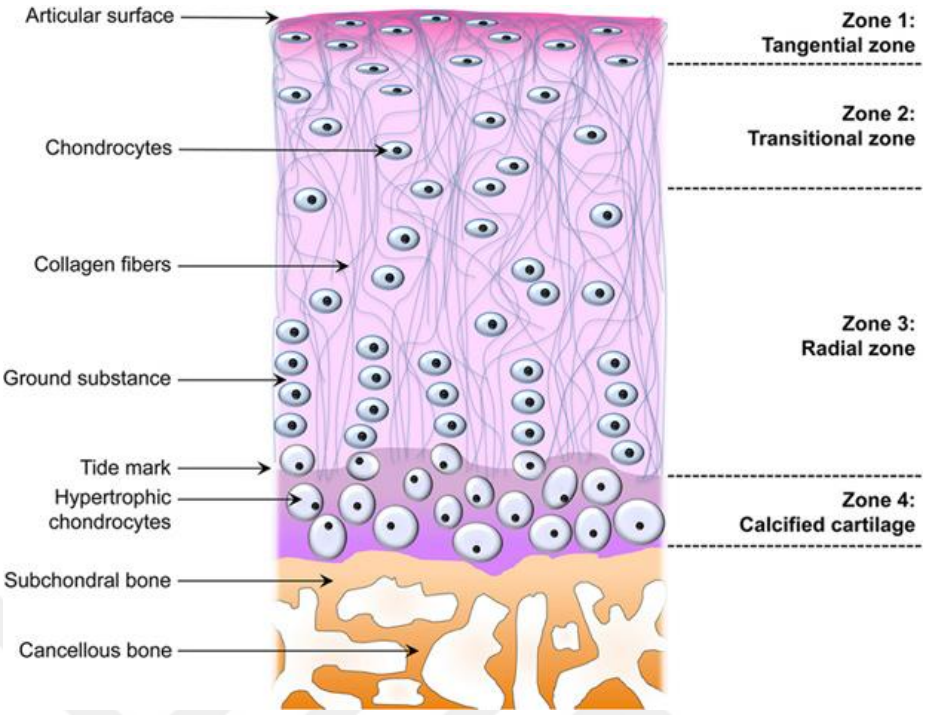

Figure 1.1. Illustration of the cartilage structure [3]

1.2 A Brief Overview on Articular Cartilage Biomechanics

The articular cartilage is a dynamic tissue that requires mechanical stimulation to function properly [13]. As a result of physiological loading *in vivo*, a variety of mechanical stimuli, ranging from compressive and shear strains to stress, hydrostatic pressure, and fluid flow, are generated in cartilage [14]. During loading, complex and nonuniform patterns of fluid flow, strain, and pressure develop, which can be attributed to the anisotropic and zonal organization of the matrix, as well as the fact that the tissue is confined by the surrounding matrix and subchondral bone [13, 15]. Cartilage exhibits mechanical properties that are site- and depth-dependent as a result of its highly anisotropic viscoelastic and poroelastic properties [13]. Due to the tissue's diminishable porosity and water retention capacity, physiological loading compacts the matrix, allowing the application of high pressures to the cartilage [16].

Articular cartilage can be subjected to stress values of 10-20 MPa and compressive strain up to 45% during daily physiological activities [17, 18]. Average compressive strain values of more than 13% have been measured for the articular cartilage of in the hip and knee (the major weight-bearing joints) during daily functions [19-21].

The cartilage is subjected to dynamic loading during daily phyiological activities and as consequence, mechanical stimuli of varying magnitudes stimulate chondrocytes to regulate cellular activities [15, 16]. Chondrocytes' ability to sense their mechanical environment is important for cartilage's structural and functional adaptation to loading. Compressive forces applied to a single chondrocyte result in nuclear deformation, which is critical for mechanotransduction and gene expression [15, 22]. Chondrocytes respond to compressive forces dosage-dependently by modulating the gene expression of ECM proteins that have role on ECM biosynthesis [15, 23]. Leipzig et al. demonstrated that incrementing the compressive force applied to a single chondrocyte results in a metabolic shift in mRNA levels of collagen-IIa and aggrecan [23].

Various mechanisms have been proposed for clarifying mechanical signal transmission and resultant metabolic responses of chondrocytes. Chondocytes may detect external stimuli via the stress–strain shift created at the cell boundary owing to differences in the mechanical properties of the matrix and the cell [15]. A variety of mechanisms, including integrin receptors and stretch-activated activated ion channels, are directly influenced by cellular strains and fluid shear stress arising from compression of the tissue [24-26]. Accompanied by primary cilia, the pericellular matrix may also act as a signal transducer for cells [25]. On the chondrocyte surface, the primary cilium can function such as an antenna, detecting mechanical and biochemical signals within the tissue matrix [27, 28].

1.3 Regenerative Engineering of Cartilage

Today, the most common treatments for cartilage damage include GAG-containing medications, hyaluronic acid injections, platelet-rich plasma (PRP), and surgical procedures (mosaicplasty, microfracture, prosthesis, etc.) [29, 30]. Unfortunately, none of these methods can provide a permanent solution to the problem and there is a tremendous need for the development of alternative new therapies [29]. Consequently, biomaterials and tissue engineering approaches to stimulate neocartilage formation have attracted a huge research interest [31, 32].

Autologous chondrocyte implantation (ACI) is a technique that involves *in-vitro* expansion and following re-implantation of harvested chondrocytes [33, 34]. In the third generation ACI applications, tissue engineering techniques were employed to produce cartilage-like tissue within a autologous chondrocyte seeded biodegradable scaffolds and subsequently the obtained tissue construct is transplanted to the defect site [33, 35]. In 1998, Behrens et al. performed the first third generation ACI implantation using a porcine collagen I/III matrix as a scaffold [36].

The development of suitable biomaterials for cartilage regeneration is critical for successful third generation ACI applications, and it is at this point tissue engineering techniques comes into play [34]. To be able to construct a successful three-dimensional scaffold, using a biomaterial that closely resembles the native articular cartilage environment, particularly the ECM structure is essential [5, 32]. The ideal scaffold should be biocompatible, biodegradable, porous, and function as a guide for new tissue development [5]. Additionally, the scaffold should mimic the mechanical properties of the native cartilage and enable diffusion of nutrients and metabolic waste producs [37].

1.4 Chitosan for Cartilage Tissue Engineering

Because of its biocompatibility and structural resemblance to glycosaminoglycan (GAG) molecules found in the native cartilage ECM, chitosan, a naturally produced polysaccharide, is a promising biomaterial for cartilage tissue repair [38, 39]. Because of this structural similarity, chitosan appears to stimulate the bioprocesses observed in cartilage for GAG production, and biodegradable biodegradation products of chitosan are thought to be involved in the synthesis of articular cartilage components like chondroitin sulphate, hyaluronic acid, and type II collagen [40]. Furthermore, chitosan's amino groups enable the formation of ionic complexes with anionic polymers or chemical modification with various crosslinkable groups [41].

Chitosan has been shown to have a high potential for use in cartilage regeneration through experimentation. Chitosan was injected intra-articularly and an increase in epiphyseal cartilage was observed in the tibia and femoral joints, along with an increase in chondrocyte proliferation [42, 43]. Additionally, it has been demonstrated that chitosan scaffolds support culturing chondrocytes *in vitro*, maintain their viability, and promote proliferation [44-46]. Chondrocytes cultured *in vitro* on chitosan substrates preserved a round morphology and retained the ability to synthesize cell-specific ECM molecules [47, 48].

Despite its numerous advantages, chondrocytes are not able to adhere well to chitosan structure [49]. It is critical to incorporate bioactive materials that facilitate chondrocyte adhesion and chondrogenesis into the chitosan network in order to obtain effective chitosan-based hydrogels for cartilage tissue engineering applications [38]. In a previous study, fibronectin was covalently attached to the surface of chitosan membranes and it was demonstrated that the presence of fibronectin stimulated cell adhesion on chitosan [50]. Correia et al. prepared freeze-dried composite scaffolds of chitosan and hyaluronic acid (HA) at various weight ratios and demonstrated that the addition of HA enhanced chondrocyte adhesion and

cartilage ECM production *in vitro* [51]. Additionally, other natural biomaterials such as gelatin, alginate, galactose, and lactose have been used to create hybrid/complex chitosan hydrogels/scaffolds with enhanced chondrocyte adhesion and proliferation [48, 52-58]. Borgogna et al. prepared a polyanion-polycation based bioactive hydrogel scaffolds which were composed of alginate and a lactose-modified chitosan (chitlac) for potential use in cartilage reconstructive surgery applications. In the study, porcine articular chondrocytes were entrapped in the hydrogel structure and characterization results showed that chitosan containing polyanion-polycation hydrogels were able to maintain chondrocyte phenotype, significantly stimulate and promote chondrocyte growth and proliferation compared to pure alginate hydrogels [55]. In another study, Lee et al. produced hydrogels by physically blending glycol chitosan (GC) with gellan gum (GG) for cartilage tissue engineering (TE). Primary articular chondrocytes isolated from New Zealand white rabbits were encapsulated in the hydrogels and histological analysis demonstrated a high-level of GAG synthesis and proliferation of cells [48]. In another recent study, Sahai et al. prepared 3D printed chitosan-gelatin-alginate composite hydrogel scaffolds with controlled porosity and architectures for use in patient-specific degenerated cartilage regeneration therapies [58]. Human mesenchymal stem cells (hMSC) entrapped in 3D printed scaffolds revealed a good proliferation and chondrogenic differentiation. The study concluded that 3D printed chitosan-based hydrogel scaffolds had chondrogenic potential and are suitable for use in hMSC-derived cartilage regeneration therapies.

1.5 A Brief Overview on Photopolymerization of Biomaterials

Photopolymerization is a method using light to initiate and continue a polymerization reaction which results in the formation of a linear or crosslinked polymer network. To photocrosslink the polymers, it is required to generate free radicals in the system, which will cause monomers and oligomers to undergo free radical chain polymerization. Photoinitiators are very important in this mechanism, hence they are

excited by light to generate the active radicals which initiate the polymerization process. [59, 60]. Following interaction with these active radicals, reactive groups on the monomer or the polymer structure are created and crosslinks are formed.

The most important advantages of photopolymerization of biomaterials over conventional polymerization methods are fast polymerization rate, ease in production and implantation, possibility adapting complex shapes, low-degree polymerization temperature and ability of entrapping a wide range of cells and substances [61].

As a result of UV irradiation, reactive oxygen species (ROS) and free radicals are formed and their presence can induce and DNA damage [62]. Therefore, using visible-region photoinitiators and hydrogel photocrosslinking under visible light (VL) rather than using UV light is favorable for biomedical applications [63]. The most widely employed VL photoinitiators in cell entrapment are triethanolamine, eosin-Y, and camphorquinone [60, 63, 64].

Another important aspect in cell survival in cell-entrapped photopolymerized hydrogel systems is the biocompatibility of the photoinitiator. Recently, Vitamin B2 (riboflavin, vit-B2) attracted attention as a VL photoinitiator due to its excellent biocompatibility. Application of riboflavin in VL photocrosslinking enable producing hydrogels with high cell viability and safe for human health [63, 65, 66]

In 2017 Koh et. al prepared riboflavin-initiated photocrosslinked collagen-hyaluronic acid hydrogels and entrapped tonsil-derived mesenchymal stem cells in this hydrogel system [67]. *In vitro* and *in vivo* results demonstrated that when supplemented with TGF-β3, the hydrogel system had great potential for regeneration of meniscus In 2018, Lee et al. reported the crosslinking of hyaluronic acid hydrogels in the presence of riboflavin phosphate via the thiolene reaction under visible blue light [68]. The cytocompatibility of the hydrogels system was investigated using corneal fibroblasts, and the resultant gel material had no negative effect on cell viability. In another study

carried out in 2020, riboflavin was used to initiate the crosslinking of silk fibroin molecules under visible light [69]. The results revealed that the crosslinked silk fibroin based hydrogel system was a suitable bioink candidate for 3D printing. to form an silk fibroin hydrogel through dityrosine bonding. Monfared et al developed a dual crosslinkable hydrogel composed of poly(ethylene glycol) (PEG) star polymer and nanocellulose fibers [70]. The network of cellulose nanofibers prepared by ionic crosslinking with calcium ions while a PEG hydrogel network was formed via VL crosslinking by thiol-ene photoreaction in the presence of riboflavin as a photo initiator. The obtained hydrogel system enhanced cell viability and proliferation of L929 fibroblasts. The developed hydrogel system had easy to tailor viscoelastic and mechanical properties and may be used in a wide range of regenerative medicine applications.

1.6 Photocrosslinking of Chitosan For Cartilage Tissue Engineering

The addition of photoreactive side groups to chitosan structure enables the polymer chains to cross-link when exposed to UV or visible light. It's important note that chitosan is insoluble in both alkaline and neutral pH values, as well as in water. By grafting glycolic acid or methacrylate groups to the primary amine groups, chitosan can be made water-soluble [40, 71]. As a water-soluble chitosan derivative, glycol chitosan, have gathered considerable research interest to prepare photocrosslinkable chitosan-based hydrogels for cartilage therapies, owing to its enhanced solubility in physiological solvents, which enables direct cell encapsulation. Hu et al. developed photopolymerizable methacrylated glycol chitosan (MeGC) hydrogels in 2012 using riboflavin (RF) as a photoinitiator that enables gelation in response to visible blue light exposure [72]. In the study, hydrogels constructed using RF with only 40 s irradiation time supported 80–90% cell viability. In addition, increasing irradiation time up to 300 s had no negative effect on cell viability. Besides, RF-photoinitiated hydrogels supported proliferation of encapsulated chondrocytes and cartilafe-specific extracellular matrix deposition. The study demonstrated that MeGC

hydrogels prepared using RF initator offer a promising hydrogel system for tissue engineering applications.

Later, the same group created a favorable chondrogenic microenvironment which allows chondrocytes to maintain their phenotype and enhance neocartilage formation by incorporating extracellular matrix (ECM) components of cartilaginous tissues to modifiy this photopolymerizable MeGC hydrogel. Park et al. (2014) developed a MeGC-based hydrogel containing Collagen type II and Chondroitin sulphate (CS) to repair cartilage defects. The photopolymerized hydrogels were demonstrated to be cytocompatible, and their incorporation into a crosslinked chitosan network significantly increased cell proliferation and cartilage-specific ECM production by chondrocytes entrapped in MeGC hydrogels [73]. Choi et al. incorporated collagen type II and TGF-1 into MeGC via simple entrapment and affinity binding in another study [74]. They entrapped chondrocytes and, mesenchymal stem cells (MSCs), and synovium-derived MSCs (as promising stem cell type for cartilage tissue engineering due to their high chondrogenic potential) in this hydrogel and loaded TGF-1 to hydrogel structures to stimulate deposition of cartilaginous extracellular matrix and chondrocyte differentiation. The results demonstrated that hydrogels containing Collagen type II enabled the controlled release of TGF-1 over time in chondrogenic medium which further enhanced the proliferation and cartilage-specific ECM production of encapsulated chondrocytes and MSCs. Additionally, when cell-entrapped hydrogels were implanted subcutaneously to the mice for 3 weeks, neocartilage formation was significantly improved in the constructs loaded with TGF-1 compared to controls. Hayami et al developed a photopolymerizable hydrogel system by blending N-methacrylate glycol chitosan (MGC) and O-methacrylate chondroitin sulfate (MCS) prepolymers to enhance cartilaginous biosynthesis for cartilage tissue engineering applications [75]. In the study primary articular chondrocytes entrapped in MCS-MGC hydrogel system formed multicellular aggregates which were surrounded by cartilage-specific matrix containing elevated amounts of s-GAG and collagen II compared to control groups.

There is also a large body of the literature employing other chemically modified light-curable chitosan forms to design biomaterials with suitable physico-chemical, mechanical and biological properties which have a great potential for cartilage regeneration. In 2018, Chichiricco et al. developed a new photochemically cross-linked hydrogel membrane formulation composed of silanized hydroxypropyl methylcellulose and methacrylated carboxymethyl chitosan for guided tissue regeneration [76]. The hydrogels were photopolymerized using riboflavin photoinitiator under visible light during 2 min of irradiation. In order to test barrier properties of the membranes, human primary gingival fibroblasts were seeded and cultured on the hydrogel membranes and analyzed with confocal microscopy and histological staining. Both confocal microscopy and hematoxylin & eosin staining results confirmed that the cells could not infiltrate the cross-linked hydrogels. Results of the study confirmed the suitability of the hydrogel membranes for guided tissue regeneration applications. Zhou et al. prepared photocrosslinkable and water-soluble maleic-functionalized chitosan (MCH) and methacrylated silk fibroin (MSF) biopolymers [77]. Photopolymerization of the MCH-MSF interpenetrated polymer network (IPN) hydrogel was carried out under UV light in the presence of Darocur 2959 as the photoinitiator. The IPN hydrogel composed of 6 % (w/v) MCH and 0.1 % MSF (w/v) had a compressive modulus of 0.32 MPa which is in the range of compressive modulus of articular cartilage (0.1-2 MPa). Cytocompatibility of the same hydrogel group was tested by culturing primary mouse articular chondrocytes with hydrogel extraction medium and revealed good cytocompatibility (80% cell viability of the negative control.) In 2020, Shao et al. prepared a similar photopolymerized TGF-β loaded IPN hydrogel which consists of water-soluble maleilated chitosan (MCH) and methacrylic esterified silk fibroin (MSF) as a drug-carrier for cartilage tissue regeneration [78]. In cell culture studies, hydrogels showed good cytocompatibility with human bone marrow-derived mesenchymal stem cells and significantly enhanced cell adhesion and proliferation. In another study reported last year, Tannic acid-containing MeGC/methacrylated silk fibroin double-network hydrogels were prepared and photopolymerization was carried out with Lithium

phenyl (2,4,6-trimethylbenzoyl) phosphinate photoinitiator under UV light [79]. Introduction of tannic acid to this dual reinforced the hydrogel system and significantly decreased the photopolymerization time. The cell viability investigations performed by seeding NIH 3T3 Fibroblasts on hydrogels revealed good cytocompatibility and the hydrogel system was shown to be promising for accelerating wound healing.

1.7 A Brief Overview on Fibrinogen as a Biomaterial

Fibrinogen (Fib) is a soluble plasma glycoprotein synthesized by the liver and required for normal blood clotting, inflammation, cell–matrix interactions, wound healing, and neoplasia [40, 80-82]. Fib is derived from blood and possesses intrinsic characteristics that promote cellular interactions and tissue healing, making it particularly valuable in tissue engineering, hemostasis, and wound dressing applications [81]. Fib contains integrin binding sites such as RGD and has been shown to bind to vascular endothelial growth factor (VEGF), fibroblast growth factor (FGF), and various other cytokines with high affinity [82-85]. Glycoprotein-based Fib promotes cell adhesion by binding to integrin receptors and ECM proteins [86-88]. Furthermore, growth factors bind to Fib, which promotes cell proliferation and differentiation [85, 89].

Fibrinogen is frequently used in hybrid fibrous tissue scaffolds, and these hybrid scaffolds e mostly contain polymers such as poly(L-lactic acid), poly(epsilon-caprolactone) and poly(ethylene glycol) elastomers, which have been demonstrated to enhance cell adhesion and proliferation *in vitro* [81]. In 2020, Woods et.al developed a rolled-sheet graft from polycaprolactone-reinforced porcine blood-derived fibrinogen scaffold to be used this as tissue-engineered vascular grafts [90]. *In-vitro* cell culture study showed that umbilical artery-derived smooth muscle cells seeded on the grafts resulted in neotissue formation within the scaffold. In another

study, electrospun poly (L-lactide-co caprolactone) and porcine fibrinogen scaffolds were used for reconstruction of abdominal wall and tested in canine hernia model [91]. To investigate cell viability, canine superficial vein endothelial cells were seeded on the surface of hybrid scaffolds with different ratios of poly (L-lactide-co caprolactone) and porcine fibrinogen and cultured for 16 days. Poly (l-lactide-co caprolactone) and porcine fibrinogen scaffolds which were prepared using a blend ratio of 4:1(w:w) revealed almost 9 fold increase in cell proliferation compared to negative tissue culture plate group. Resorbable poly (L-lactide-co caprolactone)-porcine fibrinogen scaffolds were shown to be effective for restoring abdominal skeletal muscle 36 weeks after in vivo implantation. P&P Biotech Company try to commercialize this electrospun nanofiber-based porcine fibrinogen and poly(L-lactide-co-caprolactone) patch for abdominal wall regeneration as class III medical device [92].

Several studies have established the advantages of combining fibrinogen with other polymers in hydrogel structures. For example, fibrinogen and gelatin hydrogels have been demonstrated to stimulate osteogenic differentiation human adipose-derived MSCs and improve chondrogenesis potential of bone-derived MSCs [93]. In the study, MSC-containing cubes with the size of 1 cm^3 were 3D printed and analyzed by immunochemistry for cell survival and production of a calcified extracellular matrix was investigated by alizarin red staining. Cell containing hydrogel cubes (concentration of fibrin 6.66 mg/mL and gelatin 33.33 mg/mL) demonstrated good mechanical stability and encapsulated MSCs in 3D cubes were viable (survival rates of more than 87% compared to negative control) and able to calcify the hydrogel after bioprinting. In another study, Almany and Seliktar developed photo crosslinked fib-PEG hydrogel system. They synthesized a biosynthetic hybrid hydrogel network with a fib backbone and difunctional PEG side chains [94]. They used PEG diacrylates to modify denatured fib fragments, mixed them with a photoinitiator, and exposed them to UV light to obtain a cell entrapped hydrogel network [94]. The

findings indicated that amino acid domains within the fibrinogen backbone act as adhesion motifs for endothelial and smooth muscle cells.

Today it's well known that that fibrinogen in PEG-based Fib containing hydrogel systems chondrogenic activity is mainly provided by Fib because bare PEG hydrogel has poor performance in tissue regeneration due to its poor cell adhesion [94-98]. Gelrin C, a cartilage regeneration product developed by Regentis Biomaterials (Israel) for knee cartilage treatment, consists of UV-photopolymerized hydrogel composed of PEG diacrylate and Fib. Gelrin-C has been demonstrated to be chondrogenic on both porcine models and clinical trials. It significantly increased type II collagen and proteoglycan biosynthesis [97]. Loebel et al developed a fibrinogen containing double network hydrogel system that can be applied for the repair of viscoelastic tissues [99]. In the study they formulated double network (DN) hydrogels through a combination of supramolecular and covalent networks to tailor hydrogel viscoelastic properties. The primary network was photopolymerized fibrinogen modified with acrylated poly(ethylene)glycol while for the secondary network, supramolecular guest–host interactions was used to build the network through a combination of β-cyclodextrin (host) and adamantane (guest), which were both and individually linked to hyaluronic acid. The results revealed that the bioactivity and degradability of the fibrinogen backbone was preserved after the double network hydrogel formation. High viability and proliferation of bovine mesenchymal stromal cells (MSCs) that were entrapped in hydrogel network were observed. This dual coupling of supramolecular and covalent interactions allowed the tuning of dynamic hydrogels with tailorable characteristics for various possible tissue repair applications.

It was reported that fibrinogen incorporation showed enhanced bone formation and stimulated angiogenesis [100]. Peled et al. (2007) also demonstrated that PEGy-lated fibrinogen material can promote the healing of bone defects and sustained release of Fib fragments induce bone regeneration at the injury site [101]. Based on all the

previous findings mentioned above, we hypothesize that incorporation of cell RGD-rich fibrinogen to into the chitosan-based hydrogel is expected to enhance chondrocyte specific ECM synthesis and cartilage regeneration.

1.8 Dynamic Culture and Compressive Loading in Cartilage Tissue Engineering

Dynamic culture conditions provide a superior environment for the organization of 3D cellular networks compared to static culture conditions in which cells are restricted to two dimensions. *In vitro* culture of three-dimensional cell-scaffold constructs in bioreactors under conditions that promote efficient cell nutrition and in combination with the mechanical stimulation to direct cellular activity and phenotype, is a crucial step towards the production of tissue engineering constructs that are functional [102]. Previous research well documented that, stimulation of cartilage tissue engineering constructs with dynamic compressive loading has the potential to modulate ECM composition and influence neocartilage properties. Compressive loading has been shown to enhance chondrocyte viability, gene expression, and extracellular matrix biomolecule synthesis and influence neocartilage properties [103-105]. Previously various short- and long-term studies have been reported applying unconfined dynamic compression with a wide range of strains (2-23 %), frequencies (0.001 to 5.0 Hz), and stresses (0.005-2.5 MPa) on a variety of cartilage tissue engineering systems based on hydrogels or macroporous scaffolds [106].

Mauck et al. carried out the first long-term research on the effect of dynamic compressive loading on the matrix properties of chondrocyte-entrapped hydrogels [107]. Four weeks of dynamic unconfined compression (10 % axial strain, 1 Hz, for three consecutive 1 h on-off cycles per day, five days per week) of chondrocyte-seeded agarose hydrogels resulted in a twofold increase in the equilibrium aggregate

modulus (24.5 kPa, compared to free-swelling controls) and also significantly increased the collagen and GAG content of the constructs [107]. Another pioneer study using chondrocyte-entrapped peptide gels demonstrated that even a very low level of compressive stimulation were sufficient to enhance chondrogenesis on a long-term culture [108]. Compressive loading (1 Hz, 2.5 % strain, 45 min stimulation followed by 5.25 h of free-swelling, four times per day, one day off, one day on) on peptide gels for 39 days resulted in an 18% increase in young modulus, a 22% increase in GAG, and a 60% increase in dynamic compressive stiffness when compared to non-loaded controls. The results revealed that mechanical stimulation increased both the number of cells and the amount of GAG biosynthesis of chondrocytes. In 2018, Sawatjui et al developed porous scaffolds composed of silk fibroin (SF) and SF with gelatin/chondroitin sulfate/hyaluronate (SF-GCH) [109]. They seeded human chondrocytes isolated from osteoarthritic joints and investigated chondrogenesis obtained in the tissue constructs with and without dynamic compression. For dynamic culture studies, all scaffolds were subjected to uniaxial dynamic compressive loading with 10% strain at 1Hz of frequency, 1 hr/day for 2 weeks. The results revealed that dynamic compression elevated chondrocyte expression of aggrecan and collagen X (COL10A1) five times higher than free swelling controls. Additionally, uniaxial dynamic compression significantly enhanced chondrogenesis and anabolic activity of chondrocytes in both SF-GCH and SF scaffolds, as evidenced by GAG, GAG/DNA and collagen type II content of the scaffolds. In another study published in the same year, cryogels consisting of gelatin/chondroitin-6-sulfate/hyaluronan/chitosan (GCHC) was produced to investigate the effects of dynamic compressive loading on chondrocyte functionality (cartilaginous ECM production). In dynamic culture experiments, primary porcine chondrocytes entrapped in GCHC gels were subjected to dynamic compressive stimulation with 10% to 40% strain at 1 Hz of frequency (1 to 9 h/day duration) in a multi-chamber mechanobioreactor for 14 days. According to gene expression results, optimum dynamic culture condition was identified as 20% strain with 3 h/day stimulation duration to preserve the chondrogenic phenotype. Results revealed that

with 20% strain and 3 h/day stimulation resulted in higher gene expression of Col I, Col II, TGF-β1 and IGF-1 markers compared to the other groups. In addition, biochemical analysis results demonstrated that biosynthesis of ECM molecules (GAGs and Col II) increased with the defined optimum stimulation regime. In 2020, Chong et al. dynamically cultivated by applying compressive loading to human osteoarthritic chondrocytes entrapped in agarose hydrogels at a density of 1 x 10^6 cells/ml. [110]. In the study, varying dynamic compressive strains (10% and 20% uniaxial dynamic compression) were employed for 8 days with a 1 Hz of frequency (stimulus was applied 4 times/day for 30 min with pauses of 60 min). Results revealed that dynamically loaded osteoarthritic chondrocytes (entrapped in agarose hydrogels) subjected to 20% compression deposited higher amount of proteoglycan and collagen type-II than 10% compression and free-swelling control. The study demonstrated that, compression regimens can be used to increase the biosynthetic activity of human chondrocytes from osteoarthritic joints. In 2021, Fritch et al. blended poly-D,L-lactic acid/ polyethylene glycol (PEG-PDLLA) and polycaprolactone–poly(ethylene glycol)-polycaprolactone (PEG-PCL-DA) polymers and developed a biodegradable visible light crosslinked hydrogel system to be used for cartilage tissue engineering [111]. Human chondrocytes were encapsulated in hydrogels and to investigate the effect of compressive loading on the chondrogenesis, dynamic culture studies were carried out with 5% strain and a frequency of 0.2 Hz (1 h/day for 14 days). Application of compressive loading enhanced the production of cartilage-like matrix by increasing proteoglycan and collagen-II synthesis of chondrocytes in hydrogel constructs compared to statically cultured control group. In order to investigate *in vivo* chondrogenesis potential, chondrocyte-entrapped hydrogels with or without being stimulated by dynamic compressive loading, were subcutaneously implantated into mice. The results indicated that, chondrocyte phenotype and cartilage-specific ECM biosynthesis both were well preserved in all samples after *in-vivo* implantation.

As demonstrated by previous studies, compressive stimulation has the potential to increase the quality and function of tissue engineered cartilage constructs. However,

each group uses different custom-built bioreactors and due to variations in experimental designs, applied culture conditions and used analysis methods it is not possible to directly compare their outcomes. The precise stimuli, duty cycles and frequencies that are required to obtain an improved chondrogenesis performance are unknown and are hydrogels/scaffold, cell type, and culture time dependent. Even though dynamic compression at physiological levels has been shown to enhance ECM biosynthesis in general, when and at which magnitude the load should be applied and the optimum loading regime is still not clear. According to Khoshgoftar et. Al's a finite element analysis, an increase in applied load would be necessary to maintain cellular loading at the same level as extracellular matrix deposition increased [112]. In a recent study by Finlay et al., during 84 days, dynamic compressive loading (Hz, 1 h per day) was applied to scaffolds seeded with bovine synoviocytes [113]. In the study, the initial strain, which was not fully defined but in the range of 13% -23% , was increased in an uncontrolled manner as the construct developed and at maximum strain level (30%), a maximum load of 0.225 MPa was applied to the constructs. By this method, the compressive modulus of the construct reached 12 MPa, which is comparable to the value of native cartilage. Last year Kwan et al. published a PhD thesis with the objective of examining the effect of incremental compression on cell deformation in native and tissue engineered cartilage in order to have a better understanding of Finlay's hypothesized mechanism for developing tissue engineered cartilage constructs [114]. In the study, one important focus point was to develop a new tool and technical methodology to monitor, track, image and quantify changes in cell morphology within native or engineered cartilage constructs under static compressive strain experiments and a novel compression device was designed to simultaneously allow monitoring of cells within cartilage constructs while applying static compressive strains in real time. Although the same compressive strain values were applied as reported by Finlay, Kwan et al obtained different results. In contrast to Finlay et al., a small quantity of cartilage-like matrix was observed in tissue-engineered constructs which were subjected to incremental compressive loading. The inconsistency of the result was stated as a result of the

difference in initial scaffold porosity and mechanical properties of used constructs highlighting the importance of microenvironment surrounding the cells and understanding the interrelations between scaffold porosity, mechanical properties and cells. In addition, within loaded constructions, no change in synoviocyte morphology and no cell deformation were detected at the highest compressive strain that was applied (28%).

Despite high number of scientific publications on investigation of the effect of various dynamic compressive loads on development of cartilage tissue constructs, up to today, there is not a systematic study on increasing magnitude of the applied load in a controlled manner that would go along with neotissue formation.

1.9 Aim of The Study

Today bioreactors are started to be used in cultivation processes in commercially available therapeutic cartilage tissue engineering products to provide a more rapid and potentially sustained therapeutic effect [115]. The main reason of applying dynamic culture in regenerative therapy product development processes is to simulate the articular joint conditions in patients to increase the functionality, maturity and ECM production yield of autologous neocartilage tisssue before implantation [116, 117]. It is well known that the success of the applied bioprocess regime in mimicking the native tissue development environment plays a critical role on functionality and, cellularity and ECM yield of engineered cartilage tissue [118]. Since cartilage at the knee joint is a tissue which is continously subjected to dynamic compressive loading during daily activities, it is important to define and include an optimal compressive stimulation regime to neocartilage development bioprocesses [102, 118]. However, despite the large body of literature on the effect of compressive loading on cartilage tissue engineering applications, there is no consensus on proper loading regime of the administered stimulus to obtain a cartilage tissue construct

with high functionality. It is well known that, there is a strong dependency between mechanical properties of the hydrogel/scaffold, mechanical stimulus sensed by the cells and metabolic response and ECM biosynhesis of the cells [22, 119-121]. However, mechanical properties of the tissue construct change in time due to increased cellularity and accumulation and maturation of extracellular matrix within the construct [121]. Therefore we hypothesize that, during the neocartilage formation process, the applied load should be increased by time in order to transfer adequate compressive stimulus to the cells present within developing constructs.

First objective of the thesis study was to define a new compressive loading regime that will be applied for engineering cartilage using a hydrogel system. Despite the high number of studies investigating of the effect of various dynamic compressive loads on the development of cartilage tissue constructs, up to today, there is not a systematic study on loading regime that involves increasing the magnitude of the applied load in a controlled manner. In this thesis, the applied load was incremented by time with the development of the neocartilage formation. For this purpose, chondrocyte containing hydrogel constructs was prepared and cultivated in a custom-built mechanobioreactor. Constructs was subjected to increasing unconfined dynamic compressive loads (7 kPa, 14 kPa, 21 kPa) for defined time periods (7 days, each) and the effect of the incremental loading on cartilage tissue construct formation will be investigated.

Second objective of the thesis study was to develop a new fibrinogen-chitosan hydrogel system in which primary chondrocytes can be entrapped via a biocompatible process, visible light crosslinking. Chitosan, a natural polymer (N-acetylglycosamine), draws attention for cartilage regeneration applications due to its structural similarity to natural glycosaminoglycan molecules present in natural cartilage ECM structure, its biocompatibility and antibacterial characteristics [42]. In addition, chitosan has a stimulating effect on the bioprocesses observed for GAG

synthesis and its degradation products of the polymer are involved in the synthesis of articular cartilage components such as chondroitin sulfate, hyaluronic acid and type II collagen [40]. Chitosan-based hydrogels are usually preferred to be prepared with various bioactive materials which promote chondrocyte adhesion, enhance chondrocyte proliferation and facilitate chondrogenesis. Fibrinogen, a bioactive material with the qualities of interest, is a glycoprotein made of the polypeptide chains and it is the precursor of fibrin [122]. Incorporation of fibrinogen into chitosan hydrogel system will help mimicking the polysaccharide-protein content of natural cartilage ECM, improve chondrocyte adhesion to hydrogels, enhance chondrogenesis and improve the mechanical properties of chitosan hydrogel scaffolds [123-125]. Biocompatibility of the photoinitiator and the usage of visible light instead of UV during the photopolymerization are crucial factors which are decisive on viability of cells entrapped in photopolymerized systems. In recent years, use of riboflavin (vitamin B2) as a biocompatible photoinitiator for visible light photopolymerization has attracted attention [126-128]. In this thesis, hydrogels that are highly safe for chondrocyte entrapment will be produced by polymerizing methacrylated glycol chitosan (MeGC) with riboflavin under visible light. Until now, fibrinogen has not been used as a bioactive agent in chitosan hydrogel structures that are formed by visible light photopolymerization.

In sum, there are two primary aims of this study:

1. To investigate the effect of incremental dynamic compressive loading on the development of cartilage tissue constructs, up to today, there has been no systematic study on loading regime that involves increasing the magnitude of the applied load in a controlled manner.

2. To develop a novel fibrinogen-chitosan hydrogel system in which primary chondrocytes can be entrapped via a biocompatible process through visible light crosslinking.

CHAPTER 2

MATERIALS AND METHODS

2.1 Materials

Penicillin-streptomycin and Dulbecco's Modified Eagle Medium were purchased from Biowest (France). Trypsin-EDTA, fetal bovine serum (FBS), L-ascorbic acid, gentamycin, sodium pyruvate, 1,9 dimethyl methylene blue (DMMB), papain, lysozyme, riboflavin, glycol chitosan, chondroitin-6- sulfate were obtained from Sigma Aldrich (USA). L-cysteine, di-sodium hydrogen phosphate dehydrate, di-potassium hydrogen phosphate anhydrous, calcium carbonate, potassium chloride, glucose, HEPES and ethylenediaminetetraacetic acid (EDTA), sodium chloride were purchased from Merck Millipore (Germany). For cell isolation, pronase was obtained from Roche (France) and collagenase type II from Worthington (USA), respectively. Dimethyl sulfoxide (DMSO) (molecular biology grade) was the product of AppliChem GmbH (Germany). Alamar Blue and LIVE/DEAD Viability/Cytotoxicity kit were purchased from Invitrogen (U.S.A). Hoechst 33258 from Abcam (UK) was used for DNA quantitation studies. Chondrogenic Growth Medium from Cell Applications Inc. (USA) were used for chondrocyte cultivation. Total Collagen Assay Kit was the product of BioVision, Inc., USA and Type II Collagen Detection Kit, Multi-Species was purchased from Chondrex, USA. Hematoxylin, eosin and Alcian blue were purchased from Applichem GmbH (Germany). All other chemicals were of analytical grade and were utilized without further purification. All other chemicals were of analytical grade and were utilized without further purification.

2.2 Glycol Chitosan Methacrylation

MeGC was synthesized by reacting glycol chitosan with glycidyl methacrylate. In brief, glycol chitosan (GC) was dissolved in water (20 ml) to give a 2% (w/v) solution, and pH of the solution was adjusted to 9.0 with addition of 1 M NaOH [129]. Following this, Glycidyl methacrylate was added to GC aqueous solution with a 1:1 M ratio to the primary amine groups of chitosan. The reaction medium was allowed to react for 36 h with gentle shaking at room temperature and then neutralized with 0.1 M HCl. Later on, polymer solution was placed in dialysis tubing (MW cutoff of 12 kDa) and dialyzed against DI water for 24 h at room temperature. The medium was refreshed at 2h time intervals. Following this, MeGC solution was lyophilized for 36 h to obtain a white end product.

2.3 Proton Nuclear Magnetic Resonance Spectroscopy (^{1}H-NMR) Analysis

Methacrylation of GC was examined by ^{1}H-NMR analysis. The investigations were performed with 600 MHz high resolution digital ^{1}H-NMR spectrometer (Varian 600 MHz NMR) at TUBITAK National Metrology Institute. Samples were prepared by adding 20 microliters of Trifluoroacetic acid at a concentration of 15 mg/mL in D_2O and after complete dissolution for 2 h samples were analyzed at 50°C.

2.4 Preparation of Photocrosslinked MeGC-Based Hydrogels

Optimization studies were conducted for preparing the chitosan hydrogels. For this purpose, 2%, 3% and 4% (w/v) MeGC solutions containing 12 µM riboflavin were prepared in phosphate buffer (PBS, 0.1 M, pH 7.2) and polymer solutions were casted into a custom made teflon mold which has wells with 5 mm diameter and 3 mm height and photopolymerized for 300 s under visible blue light (400-500 nm, 500 mW / cm ^{2}) [72].

2.5 Characterization of MeGC-Based Hydrogels

2.5.1 Fourier Transform Infrared Spectroscopy (FTIR) Investigations

FTIR-ATR analyzes were performed in METU Central Lab in order to examine the chemical structures of the obtained hydrogels. FTIR analyses were performed with the Perkin Elmer 400 series spectrophotometer (Perkin Elmer, Inc., UK). The analysis was performed with a total of 16 scans per sample at the spectral region 400–4000 cm^{-1} with 4 cm^{-1} resolution.

2.5.2 Gelation Time

Gelation time of MEGC-based hydrogels prepared in PBS containing 3% (w/v) chitosan prepared with different concentrations of riboflavin (6 µM, 12 µM and 24 µM) was determined by the vial-tilting method [130, 131]. Then, different amounts of fibrinogen 0.25%, 0.5% and 1% (v/w) were added to these solutions. The maximum amount of fibrinogen used was 1% (v/w) because higher than this concentration caused solubility problems in the prepolymer solutions. The resulting solutions were placed in glass vials which were then exposed to visible blue light to initiate photopolymerization. Vials were bent every two s until no fluidity was observed then the defined gelation time was recorded. Each data point is an average of three measurements.

2.5.3 Water Uptake Capacity

The time dependent water uptake capacity of hydrogels was determined by measuring the weight of hydrogels in the swollen state and in the dried state [132]. For this purpose, hydrogels were immersed in simulated synovial fluid (SBF) which contains 3 mg/ml hyaluronic acid and 30 mg/ml bovine serum albumin in PBS at 37°C [133]. At certain time points, samples were taken out from SBF and after

removing excess water from hydrogel surfaces weights of wet samples were measured carefully and recorded. As a second step, samples were lyophilized and weighed again to determine the dry weights. Water uptake percentage of each sample was calculated according to the equation given below where Ww and Wd stand for wet and dry weights of the sample, respectively. The synovial fluids used during the experimental period were renewed every 3 days and each group was studied in four replicates.

$$Swelling\ Ratio\ \% = \frac{Ww - Wd}{Wd} * 100$$

2.5.4 Degradation Studies

In order to observe weight loss profile of hydrogels in PBS environment, preweighed hydrogel (n=4) samples (with dimensions ~3 mmx5 mmx4 mm) were incubated in 5 ml PBS containing 2 mg/mL lysozyme at 37°C in a shaking water bath (Nüve Bath NB 5, Turkey). At different time points, samples were removed from PBS; lyophilized and dry samples were weighed. Weight loss percentages were calculated according to the equation given below where W_0 and W_1 represent initial and final weights of the sample at the end of each incubation period, respectively [134]. Degradation media were renewed every 3 days.

$$Weight\ Loss\ \% = \frac{W1 - W0}{W0} * 100$$

2.5.5 Mechanical Tests

Mechanical properties of the cell-free hydrogels were investigated by uniaxial compression test. For the compression test, Univert Biomaterial Mechanical Tester

(Cell scale, Canada) at METU Biomaten was used with 10 N load cell. The preload value for the experiment was selected as 0.1 N and the withdrawal speed was set to 1 mm/min. Cylindrical hydrogel specimens for compression test were prepared as diameter: 7 mm, height: 5 mm. Stress-strain graphs were drawn with the data obtained from compression tests, and Young's modulus values were calculated from the linear region of the obtained tension-strain curves. Each group was studied by using four replicates.

2.5.6 Scanning Electron Microscopy Investigations

The surface and pore morphology of the hydrogels were investigated using a Scanning Electron Microscope (SEM - Quanta 400 FEG, Netherlands). The prepared hydrogels were lyophilized, coated with 10 nm gold layer and then visualized via SEM at METU Central Lab. The average diameter size of MeGC-based hydrogels was calculated using over 50 measurements obtained from SEM images via ImageJ software (National Institutes of Health, Bethesda, USA).

2.6 *In Vitro* Studies

2.6.1 Chondrocyte Isolation and Expansion

Before starting chondrocyte isolation procedure two main isolation stock solutions were prepared as below:

Washing solution: 0.2 g/L KCl, 1.0 g/L $C_6H_{12}O_6 \cdot H_2O$, 0.056 g/L $NaH_2PO_4 \cdot 2H_2O$, 1.0 g/L $NaHCO_3$, 8.0 g/L NaCl,10 mL/L Penicillin/Streptomycin, 3 mL/L Gentamicin, 20 mL/L HEPES buffer 1M, 2 mL/L Phenol red sodium salt in deionized water.

Isolation DMEM: 13.38 g/L DMEM, , 0.11 g/L Na-pyruvate, 3.7 g/L $NaHCO_3$, 3 mL/L Gentamicin, 10 mL/L Penicillin/Streptomycin, 20 mL/L HEPES (1M) in deionized water.

2.6.1.1 Chondrocyte Isolation from Bovine Joints

Joints from a 12-month-old bovine were received directly from the slaughterhouse. The skin around the joints was still intact. The interested leg area shaved and soaped in the first phase. After that, the leg was placed in a laminar flow cabinet to be processed. The fetlock joint was laid loose by opening the skin (Fig. 2.1a). Articular cartilage of the joint areas was aseptically harvested. The harvested cartilage was then chopped into small pieces and placed in dishes with 50 mL of washing solution (1 dish per joint) (Fig. 2.1c). Cartilage samples were taken into flasks containing 60 ml of washing solution as 1 flask per joint. Harvested cartilage pieces were pre-digested for 105–120 min at 37°C in a carbon dioxide incubator with Pronase (7 U/mg,1 mg/mL) in DMEM (10 mL /flask) (EC 160, Nuve, Turkey). The pre-digested cartilage was rinsed three times with 60 mL washing solution before being digested with 600 U/mL Collagenase II in DMEM by stirring overnight (14 h) in T-flasks (10 mL / flask) in a CO_2 incubator (5% CO_2), at 37°C.

To dilute the isolated bovine chondrocyte cell suspension, 20 mL isolation DMEM (containing 25% FBS) was used. Falcon tubes were used to filter the contents of the T-flasks, which were then poured into new falcons and centrifuged for 7 min at 565 G at 4°C (M4808 PR,Electromag, Turkey). Chondrogenic Growth Medium supplemented with 10% (v/v) fetal bovine serum and 1% penicillin-streptomycin were used to culture primary chondrocytes in cell culture flasks at 37°C in a 95% humidified CO_2 (5%) environment. Cells were extracted from the surface using 0.25 % trypsin-EDTA (Sigma, Germany), centrifuged, and resuspended in DMEM for cell cultivation after confluency was reached. The chondrocytes at passage 3 were used in all cell culture studies.

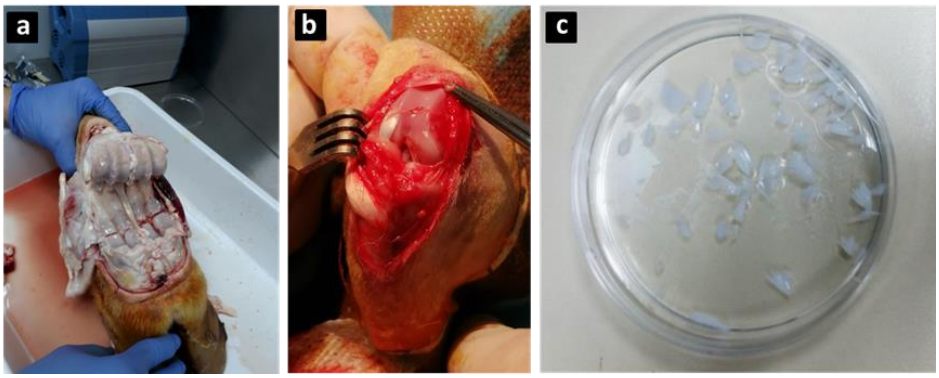

Figure 2.1. Images of **(a)** bovine fetlock joint and **(b)** rabbit hind leg joint areas which cartilage tissues were obtained, **(c)** cartilage particles obtained as a result of the operation (bovine-derived).

2.6.1.2 Chondrocyte Isolation from Rabbit

Rabbit cartilage tissue was were collected under the guidelines approved by the Ethic Committee of Kobay DHL A.Ş . (Ankara, Turkey, ethical committee approval no: 329). Primary rabbit chondrocytes were isolated from the articular cartilage of the New Zealand rabbits by using the isolation method of Willers et al. [135]. For *in-vitro* studies, 4 rabbits were sacrificed and the hindleg cartilage tissue was aseptically stripped from the articular joint region (Fig 2.1b). For autologous chondrocyte isolation which were used in *in-vivo* studies, immediately after surgery, harvested cartilages were separately labeled, transported in serum-free DMEM–F12 medium (supplemented with 0.5% pen–strep) and taken inside the laminar flow cabinet.

Isolated cartilage particles were cut into approximately 1 mm^3 pieces. After washing twice with the washing solution (0.2 g/L KCl, 1.0 g/L $C_6H_{12}O_6 \cdot H_2O$, 0.056 g/L $NaH_2PO_4 \cdot 2H_2O$, 1.0 g/L $NaHCO_3$, 8.0 g/L NaCl,10 mL/L Penicillin/Streptomycin, 3 mL/L Gentamicin, 20 mL/L HEPES buffer 1M, 2 mL/L Phenol red sodium salt in deionized water), ~ 2 g of cartilage pieces were predigested in 7 U/mg pronase containing DMEM at 37ºC for one h. After the first enzyme treatment, the cartilage

samples were washed 3 times with washing solution and subsequently digested with 600 U/ml Collagenase II in DMEM by stirring overnight (10 h) at 37°C, 5% CO_2 in flask (10 ml / flask). After enzymatic treatments, the supernatant containing chondrocytes was passed through 40 µm nylon filters, and after centrifugation, the chondrocytes were stained with trypan blue and counted with a hemocytometer. The chondrocytes obtained were seeded at a cell density of 1 x 10^4 cells / cm^2 to tissue culture flasks (Stoddart et al., 2006).

Primary chondrocytes were cultured in cell culture flasks containing Chondrogenic Growth Medium (Cell Applications Inc., ABD) supplemented with 10% (v / v) fetal bovine serum (FBS, Sigma Co., Germany) and 1% penicillin-streptomycin (Sigma Co., Germany) at 37°C in a humidified CO2 (5%) atmosphere. When confluency was reached, the cells were passaged with 0.25% trypsin-EDTA (Sigma, Germany), centrifuged and resuspended in medium for cell cultivation. Chondrocytes at passage 3 were used in the cell culture studies.

2.7 Preparation of Chondrocyte Encapsulated MeGC-Based Hydrogels

Isolated rabbit chondrocytes were suspended at a concentration of 2 x 10^6 cells/mL in MeGC solutions with and without fibrinogen [136, 137]. Encapsulation of cells in the hydrogels was achieved by exposing the pregels with visible blue light for 300 s. The experimental groups studied are given in Table 3.1.

Table 2.1 List of experimental groups

Group	Concentration of MeGC (w/v %)	Concentration of Fibrinogen (w/v %)	Concentration of Riboflavin (µM)
MeGC	3	0	12
0.25 MeGC-Fib	3	0.25	12
5 MeGC-Fib	3	0.5	12
1 MeGC-Fib	3	1	12

2.8 Static Cell Culture Studies

Hydrogels were statically cultured in cell culture wells containing Chondrogenic Growth Medium (Cell Applications Inc., ABD) supplemented with 10% (v / v) fetal bovine serum (FBS, Sigma Co., Germany) and 1% penicillin-streptomycin (Sigma Co., Germany) at 37°C in a humidified CO2 (95% air and 5% CO_2) atmosphere. The culture medium was refreshed once in every 3 days.

2.9 Dynamic Cell Culture Studies

Prior to beginning dynamic culture studies, to define the appropriate compressive loads that can be applied to the hydrogels during dynamic culture studies, some preliminary tests were performed. For this purpose, 1 MeGC- Fib hydrogels were divided to four groups and were placed into the bioreactor culture chambers containing chondrogenic media. The four groups of hydrogels were subjected to 1 h/day cyclic compressive loading at different loading magnitudes as 7 kPa, 14 kPa, 21 kPa and 28 kPa, with 1 Hz of frequency by the loading pistons which were placed on top of the hydrogels for two weeks (n=3). These loads were chosen on the lineer region of stress-strain curve of 1 MeGC-Fib hydrogels (A representative stress-strain curve is presented in Appendix E). The culture chambers of bioreactor system were maintained in a standard 5% CO_2/95% air CO_2 incubator at 37 °C during all preliminary experiments and the medium flow rate was set at 1 mL/min. At the end of preliminary expriments, all hydrogels were intact and in good physical condition. However, some microcracks were observed in a sample of the group exposed to 28 kPa it was decided not to use this magnitude of loading in further experiments. As a result, 7 kPa, 14 kPa, 21 kPa loadings were chosen for the dynamic culture studies.

Compressive loads were applied using a custom-designed mechanobioreactor (Bimetron, Turkey) that enables cyclic uniaxial compressive loading in conjunction with medium perfusion under controlled cultivation and stimulation conditions. The

bioreactor system has compact, autoclavable, perfused twin culture chambers; a peristaltic pump; a control unit; and a contactless mechanical loading device platform equipped with a linear actuator for compressive loading (Fig. 2.2). Uniaxial compressive loading is controlled by applied magnetic fields and in real time control of the load was achieved by a platform load cell. Each hydrogel (5 mm in diameter and 3 mm in height) was cultivated in a separate well of a polycarbonate 12 well plate-like chamber. Magnetic field movement is controlled by a linear actuator, and compressive force is applied remotely via magnetic particle-containing plungers positioned on top of hydrogels.

Figure 2.2. Mechanical stimulation bioreactor system

After cell entrapment ($2x10^6$ rabbit chondrocytes/mL) all hydrogels were precultured for 24 h in Chondrogenic Growth Medium supplemented with 10% (v/v) fetal bovine serum and 1% (v/v) penicillin-streptomycin at 37°C in a 95% humidified CO_2 (5%) atmosphere (static culture conditions). Following this, two hydrogel groups were placed into the two individual culture chambers of mechanobioreactor while one group of gels remained under static culture conditions as the control group (free swelling, FS). For all dynamic culture studies hydrogels were placed into the bottom

of each well of culture chambers and loading pistons were placed on top of the hydrogels. The culture chambers of bioreactor system were maintained in a standard 5% CO_2/95% air CO_2 incubator at 37 °C for all experiments and the medium flow rate was set at 1 mL/min. In bioreactor studies the same chondrogenic media composition was used with static culture and medium was changed every 3 days. 1 h/day cyclic compressive loading with 1 Hz of frequency was applied to both groups which were subjected to dynamic conditions during 21 days of culture [107, 113]. In bioreactor experiments two different loading regimes as, cyclic compressive loading with constant force and incremental cyclic compressive loading were studied. First group of hydrogels (DC-1) was stimulated with 21 kPa of cyclic compressive loading throughout the culture meanwhile for the second group of hydrogels (DC-2) applied initial cyclic compressive loading (7 kPa) stepwise increased every seven days to the values of 14 kPa and 21 kPa during the culture. At the end of the first 24 h and every seven days of culture Alamar Blue, DMMB, Hoechst, total collagen and collagen II analysis were performed on cultivated hydrogels to investigate the effect of different culturing conditions on the cartilage tissue development.

Considering theresults of previously performed investigations about the effect of different mechanical stimulation conditions on the cartilage tissue development, DC-2 incremental dynamic compressive loading regime was chosen to be applied for cultivation of autologous hydrogels.

2.10 Alamar Blue Assay

Alamar Blue is a cell viability indicator dye which reduced by cellular metabolic activity and cell proliferation [138]. The oxidized (reduced) form of redox indicator changes color from blue to red owing to the reduction process and optical densities of obtained solutions were measured at 570 nm and 600 nm.

Cell viability analyses were performed on different hydrogel groups for different times. At first, as a preliminary cell viability test, AB analysis was performed on rabbit chondrocyte entrapped in MeGC-based hydrogels at the end of 1, 3, and 7 days of incubation. Following this step, for optimization purposes before dynamic cell culture studies, cell viability analysis was performed on primary bovine chondrocytes entrapped in MeGC-based hydrogels at the end of 1, 7, 14 and 21 days of static cell culture.

For AB assay, the medium in each well was removed and the hydrogels were washed with PBS (0.1 M, pH 7.22) twice. Working solution consisting of 10% AB solution (10% Alamar Blue (Invitrogen, USA) & 90% DMEM-F12 (Biowest, France) was added to each well and incubated at dark in CO_2 incubator for 4 h. The optical densities of oxidized solutions were measured at 570 nm and 600 nm via microplate spectrophotometer (μOuant TM, Biotek Instruments Inc., USA) and calculated using the following equation:

$$\text{Percent reduced} = \frac{(\varepsilon_{OX})\lambda_2 A\lambda_1 - (\varepsilon_{OX})\lambda_1 A\lambda_2}{(\varepsilon_{RED})\lambda_1 A'\lambda_2 - (\varepsilon_{RED})\lambda_2 A'\lambda_1} \times 100$$

ε_{ox}: Molar extinction coefficient of AB oxidized form (BLUE),

$\varepsilon_{red:}$ Molar extinction coefficient of AB reduced form (RED),

A: Measured absorbance of test wells,

A: Measured absorbance of negative control well,

λ_1: 570 nm, λ_2: 600 nm.

In general, cell-free hydrogels were used as blank and each data point was an average of four measurements.

2.11 Cytotoxicity Tests

Cytotoxic effects that may result from hydrogel preparation processes were investigated using L929 fibroblast cell line. Cytotoxicity tests were performed with MeGC and 1MeGC-Fib hydrogel groups. In cytotoxicity experiments, the morphology of fibroblasts seeded on the surface of the hydrogel with a seeding density of 10^5 cells / hydrogel was observed by light microscopy and cell viability was evaluated by AB assay. Cell-free hydrogels are used as blank for AB assay. Each group was studied by using four replicates.

2.12 Dimethylmethylene Blue Assay

In order to investigate chondrocytes' potential for cartilagenous regeneration in the hydrogel system (in both the supernatants of cell lysates and the cell medium), the total sulfated glycosaminoglycan (sGAG) content of chondrocyte-entrapped MEGC-based hydrogels was quantified using the Dimethyl methylene blue (DMMB) method [139]. To extract cell lysates, chondrocyte-containing hydrogels were placed in eppendorf tubes and 1 mL of papain digestion solution (1 mg/mL papain in 0.1 M PBS containing 5 mM L-Cysteine HCl and 5 mM EDTA was added to each Eppendorf tube [140, 141]. Following this step, samples were incubated at 60°C for 15 h and then centrifuged at 15000 g for 20 min at RT to prepare cell lysate medium.

DMMB solution was prepared in Glycine/NaCl solution containing 3.04 g Glycine, 2.37 g NaCl, 95 mL 0.1 M HCl, and 905 mL deionized water at a cocentration of 16 g DMMB/mL (pH 3). In a 48-well plate, 20 uL aliquots of specimens were introduced to 200 uL DMMB reagent and the optical densities at 525 nm were recorded. To construct the calibration curve (0-15 ug/ml), chondroitin sulfate (ChS) from shark cartilage was utilized as a standard. The measured s-GAG concentrations were normalized using the dry weight and DNA content of lyophilized hydrogel samples (n=4).

2.13 Hoechst Assay

The concentration of DNA in cell lysates was quantified using a Modulus Fluorometer (9200, Turner Biosytems, USA) and Hoechst 33258 dye . The Hoechst reagent selectively binds selectively to A-T base pairs on DNA, allowing for spectroscopic estimation of the DNA quantity following cell lysis [142].

For the studies, Hoechst 33258 stock dye (1 mg/mL) and 10 X TNE buffer stock solution (containing Tris base [Tris hydroxymethyl aminomethane], EDTA disodium salt dehydrate, and NaCl, at a pH of 7.4) were prepared. To dilute samples for the tests, (1X) TNE buffer was utilized. The dye solution and diluted sample were combined in a 1:1 ratio (10 x 10 mm) and the fluorescence of the specimens was measured using a Modulus Fluorometer (Turner Biosystems, USA) with excitation and emission filters set at 350 and 450 nm, respectively. Various concentrations of calf thymus DNA (ranging from 0-1000 ng/ml) was used to construct the calibration curve in TNE buffer [143]. The DNA concentrations determined were normalized to the dry weight of lyophilized gel samples. (n=4).

2.14 Live-Dead Assay

To assess the distribution of live and dead cells in hydrogels with fluorescence microscopy, bovine chondrocyte-entrapped hydrogels were placed in a 24-well plate at the end of 1 and 21 days of culture. Before analysis, cell culture media were emptied from wells and samples were incubated for 60 min at 37°C in a 5% CO_2 and 95% humidified environment containing ethidium homodimer-1 (6 mM) and calcein-AM (4 mM) solutions [144]. Following this, hydrogels were observed with an inverted fluorescence microscope (Nikon ECLIPSE, TS 100 / TS 100-F, Japan) and images were captured using the microscope's camera (Nikon, Japan).

2.15 Quantitative Analysis of Total Collagen and Collagen II

The amount of collagen and collagen II in cultivated hydrogels and the collected culture media and were measured using a Total Collagen Assay Kit (BioVision, Inc., USA) and Type II Collagen Detection Kit, Multi-Species (Chondrex, USA). Collagen concentrations was calculated in all samples according to the manufacturers' procedures. The absorbances was measured with a Multiscan™ microplate photometer (Radwag, China). The obtained amounts of collagens were normalized to the dry weight of the lyophilized hydrogel samples (n=4).

2.6 In Vivo Studies

This study was performed at Kobay Deney Hayvanları Lab. San. ve Tic. A.S., Ankara, Turkey under the guidelines for animal experiments with the approval of the Local Ethical Committee (Approval no: 329). A total of 28 mature male New Zealand white rabbits age of 8 months were used in the study and two surgical procedures were performed on animals. In both operations, the rabbits were anesthetized with an intramuscular injection of 25 mg/kg ketamin hydrochloride and 5 mg/kg xylasin hydrochloride (Bayer, Turkey). The first operation was performed on the knee joint of the right hind leg to obtain articular cartilage biopsy from a non-weight bearing area of the medial femur condyle. After anesthesia, the operative right hind knees were freed of hair and sterilized and prepared for surgery. Following medial parapatellar incision femoral condyles were exposed and lateral patellar dislocation carried out. Subsequently, the harvested cartilage tissues were taken in individual falcons washed with sterile PBS and transported in serum-free DMEM–F12 medium (supplemented with 0.5 % penicillin–streptomycin) for further cell isolation studies. Then, each joint was washed of debris, the articular capsule and skin were closed. After wound closure, buprenorphine HCl (narcotic analgesic) were subcutaneously administered to the rabbits. After sterilizing and bandaging operated knees securely, rabbits were returned to their cages.

The isolated autologous chondrocytes were expanded until passage 3 and then were entrapped into the hydrogels at a concentration of 2 million cells/mL. The *in-vitro* culture of cells in the hydrogels was continued for 21 days in static or DC-2 dynamic culture conditions. After completion of cultivation time, the second operation was performed for implantation of autologous or cell-free hydrogels using the same clinical procedure as the first operation. For this purpose, 28 rabbits were randomly and equally divided into four experimental groups as follow;

Cell-free hydrogel group: The defects were filled with chondrocyte-free 1MeGC-Fib hydrogels; statically cultured autologous chondrocyte containing hydrogel group: The defects were filled with autologous chondrocyte containing 1 MeGC-Fib hydrogels that were cultured under static conditions. Dynamically cultured autologous chondrocyte containing hydrogel group: The defects were filled with autologous chondrocyte containing 1 MeGC-Fib hydrogels that were cultured under dynamic conditions. Dynamically cultured hydrogels were subjected to incremental cyclic compressive loading (DC-2 regime) in mechanobioreactor. Control group: Spontaneous repair group, created defects left empty.

In the second operation, the femoral condyles were reached by medial parapatellar incision. Osteochondral defects of 3.5 mm diameter and 3 mm deep were created in the central load-bearing region of the right hind leg medial condyle by using a depth gauge and stainless-steel punch and the hydrogels were implanted to the defect site (Fig. 2.3) [135, 145-148]. 4 months after the operation, all animals were sacrificed by administration of a high dose of anesthetic and operated cartilage samples collected. All attached soft tissue was removed and the distal femoral component was excised and placed into 10% paraformaldehyde fixative.

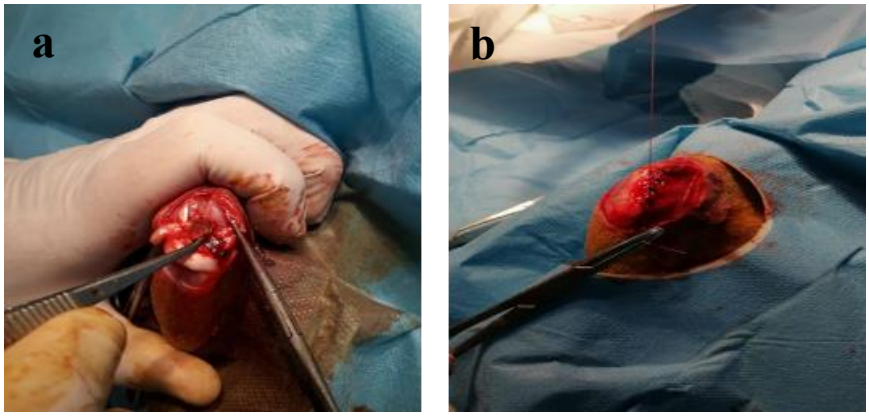

Figure 2.3. Macro images of surgical operations performed on New Zealand white rabbits**. (a)** Hydrogel application to the defect site **(b)** Closure of the operation area with sutures stimulation bioreactor system

2.6.1 Histological and Immunofluorescence Analyses

Explanted tissue samples were fixed in 10% paraformaldehyde for 24 h. and the distal femora were decalcified with 10% Ethylenediaminetetraacetic acid (EDTA) for 21 days. Following this step, all samples were dehydrated by a graded series of alcohol and xylene washes, paraffin embedded and sectioned at 5 µm. For Hematoxylin-Eosin Staining, deparaffinized sections in Harris' Hematoxylin solution for 1 min and the excess dye was washed under top water [149]. Following this step, sections were stained with alkaline Eosin solution for 1 min and incubated in 96 % ((v/v) 2X) and in absolute ethanol (1X) for 3 min. As a next step, proteoglycan content of hydrogels was analyzed with Alcian Blue staining [150]. For this purpose, deparaffinized sections stained by incubating in Alcian Blue solution (1 % (w/v) Alcian Blue in 3% acetic acid solution (v/v), pH 2.5) for 15 min. Slides were then washed twice in the distilled water and rinsed in the top water. Cell nuclei were stained with Harris' Hematoxylin for 1 min and the dye was washed under top water for 1 min. Sections were dehydrated in the alcohol by incubating in ethanol with increasing ethanol concentration (70 %, 80 %, 90 %, 100 %, each for 30 s. All slides were cleared in the xylene and mounted with entellan. (The examination of

samples was performed by light microscopy by using Olympus BX50 advanced inverted phase contrast microscope (USA) and photographed with a Olympus DP camera.

Total collagen content of hydrogels was examined by Sirius Red staining [151]. First sections were deparaffinized and stained with Weigert's Hematoxyline for 8 min. Slides were then washed twice under top water for 10 min and then stained with Picrosirius Red solution (0.1 % (w/v) in saturated aqueous solution of picric acid) for 45 min. Following this step, sections were washed in two changes of acidified water (0.5 % (v/v) acetic acid solution) and dehydrated in three changes of 100 % ethanol. Slides were cleared in xylene and mounted with entellan then examined using a fluorescent microscope (Zeiss Axio observer Z1 microcope (Germany)) by using a Texas red filter [151]. Images were photographed with an Axiocam 506 mono camera (Germany).

For investigation of collagen II expression, sections were deparaffinized with xylene, rehydrated with decreasing ethanol solutions, and rinsed for 10 min in distilled water. Sections were washed with PBS for 5 min then incubated in 0.05 % (v/v) trypsin solution for 10 min at 37ºC for antigen retrieval. Sections were washed 3 times for 5 min with PBS and incubated in 0.1 % Triton X solution for 10 min. Nonspecific antigens were blocked by rinsing sections in 10 % goat serum for 30 min, before incubation for 24 h at 4ºC with primary anti- collagen type II (1:100, Abcam, AB185430). After washing three times for 5 min in PBS, sections were incubated with the goat anti-mouse Alexa Fluor 488 (1:250) secondary antibody for 1 h. in the dark. Following another washing step with PBS, one drop of 4', 6-diamidino-2-phenylindole (DAPI) (Abcam, Ab104139) was added to the sections and the cell nuclei were stained. Negative control staining experiments have been performed by application of only the secondary antibody on healthy cartilage tissue explants and

chondrocyte entrapped hydrogels. The examination of samples was performed by using Zeiss Axio observer Z1 fluoresan microcope (Germany) with Zen-2 software.

2.7 Statistical Analysis

Statistical analysis of the data was done with one-way analysis of variance (ANOVA) with Tukey's post-hoc test for multiple comparisons using SPSS-22 Software (SPSS Inc., USA). Differences were considered significant at $p \leq 0.05$. The results are presented as mean± standard deviation. All tests conducted were performed at least in triplicates.

CHAPTER 3

RESULTS AND DISCUSSION

3.1 Chemical Characterizations

^{1}H-NMR spectra of glycol chitosan (GC) and methacrylated glycol chitosan (MeGC) are provided in Fig. 3.1. Methacrylation is achieved, as evidenced by peaks arising at 5.85 ppm and 6.30 ppm due to protons on the vinyl carbon and a peak at 2.10 ppm due to the methyl group on the methacrylate [129]. In addition, the appearance of a new peak at 5.1 ppm corresponding to H-1 for the N-methacrylated residue proved that methacrylation of glycol chitosan was successful [129].

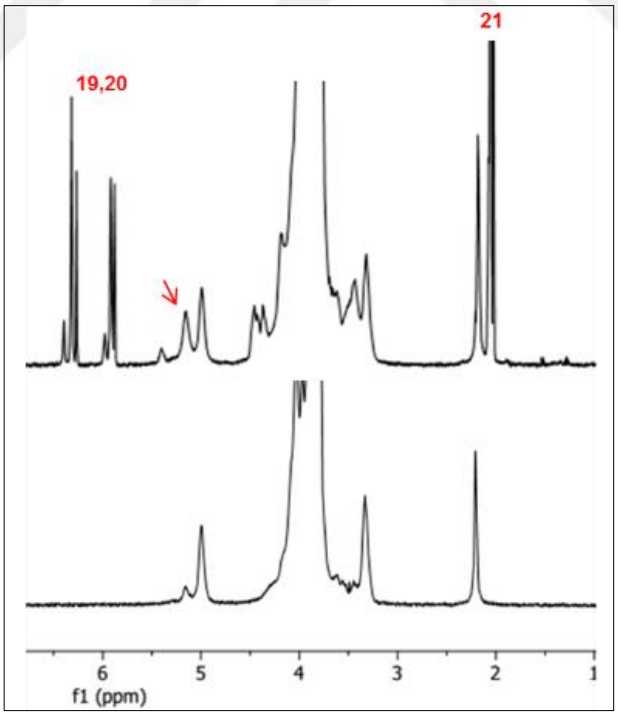

Figure 3.1. ^{1}H-NMR spectra of glycol chitosan and methacrylated glycol chitosan Top; MeGC, Bottom; GC

FTIR analysis (Fig. 3.2) of glycol chitosan, MeGC, Fib, and hydrogels was performed to characterize the chemical composition of the hydrogel samples and compare the chemical structure of Glycol Chitosan before and after functionalization with MA.

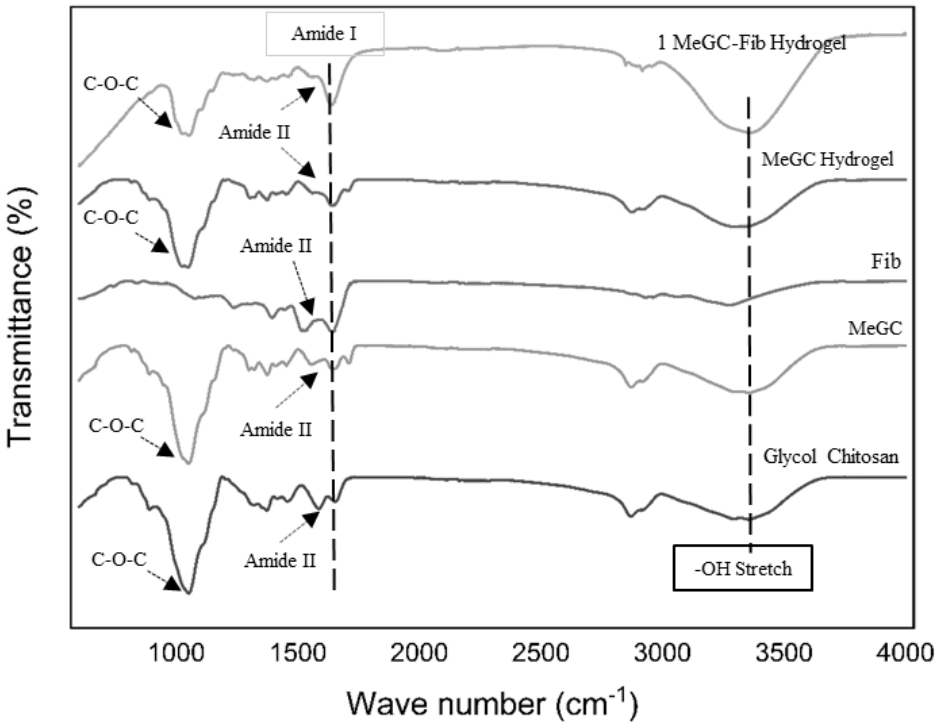

Figure 3.2. FTIR spectra of glycol chitosan, glycol chitosan methacrylate (MeGC), fibrinogen (Fib), glycol chitosan methacrylate hydrogel (MeGC hydrogel) and glycol chitosan methacrylate-fibrinogen (1MeGC-Fib hydrogel) hydrogels.

In the FTIR spectrum of glycol chitosan, C = O stretch band (amide I) at 1652 cm^{-1}, NH bending band (amide II) (1578 cm^{-1}) and CO stretch vibration bands at 1048 cm^{-1} are characteristic peaks of chitosan structure [152, 153]. The large band at 3277 cm^{-1} was attributed to the –OH stretch in the glycol chitosan structure [154]. Transmission bands similar to chitosan are also observed in the spectrum of-glycol chitosan methacrylate. In the FTIR spectrum of fibrinogen, while C = O stretch

vibration of amide I band peptide bonds were observed at 1631 cm^{-1}, the transmission peak of amide II band appeared at 1523 cm^{-1} which arise from in-plane stretch vibrations of N-H, C-N and C-C bonds [155]. Compared to the FTIR spectrum of MeGC hydrogel, the intensity of amide I in 1 MeGC-Fib hydrogel was enhanced at 1626 cm^{-1} after incorporation of Fib. Amide 1 band is known as the major spectral feature in native fibrinogen and the increase in the intensity of this band reveals the successful incorporation of fibrinogen into the MeGC-based hydrogel structure [153].

3.2 Morphological Investigations

SEM images obtained from different hydrogels are given in Fig. 3.3. SEM examinations showed that MeGC- based hydrogels had open porous structure both on the surface and in the cross-section. The micro images demonstrated that all hydrogel groups had pore sizes generally lay between 100 and 300 µm which is suitable for cell penetration [156] Thus, obtained hydrogel structures were suitable for neocartilage formation owing to its pronounced porosity at surface and cross-section.

The average pore diameter of MeGC, 0.25 MeGC-Fib, 0.5 MeGC-Fib and 1 MeGC-Fib groups were determined via ImageJ software as 248 µm ± 49, 214 µm ± 53, 171 ± 42 µm and 145 µm ± 35, respectively. SEM examinations of the hydrogels revealed that as the amount of fibrinogen in the hydrogel structure increased, a tighter network was formed. This might be either due to interpenetrating network formation or an increased cross-linking density in hydrogel structure caused byfibrinogen addition to polymer network [137].

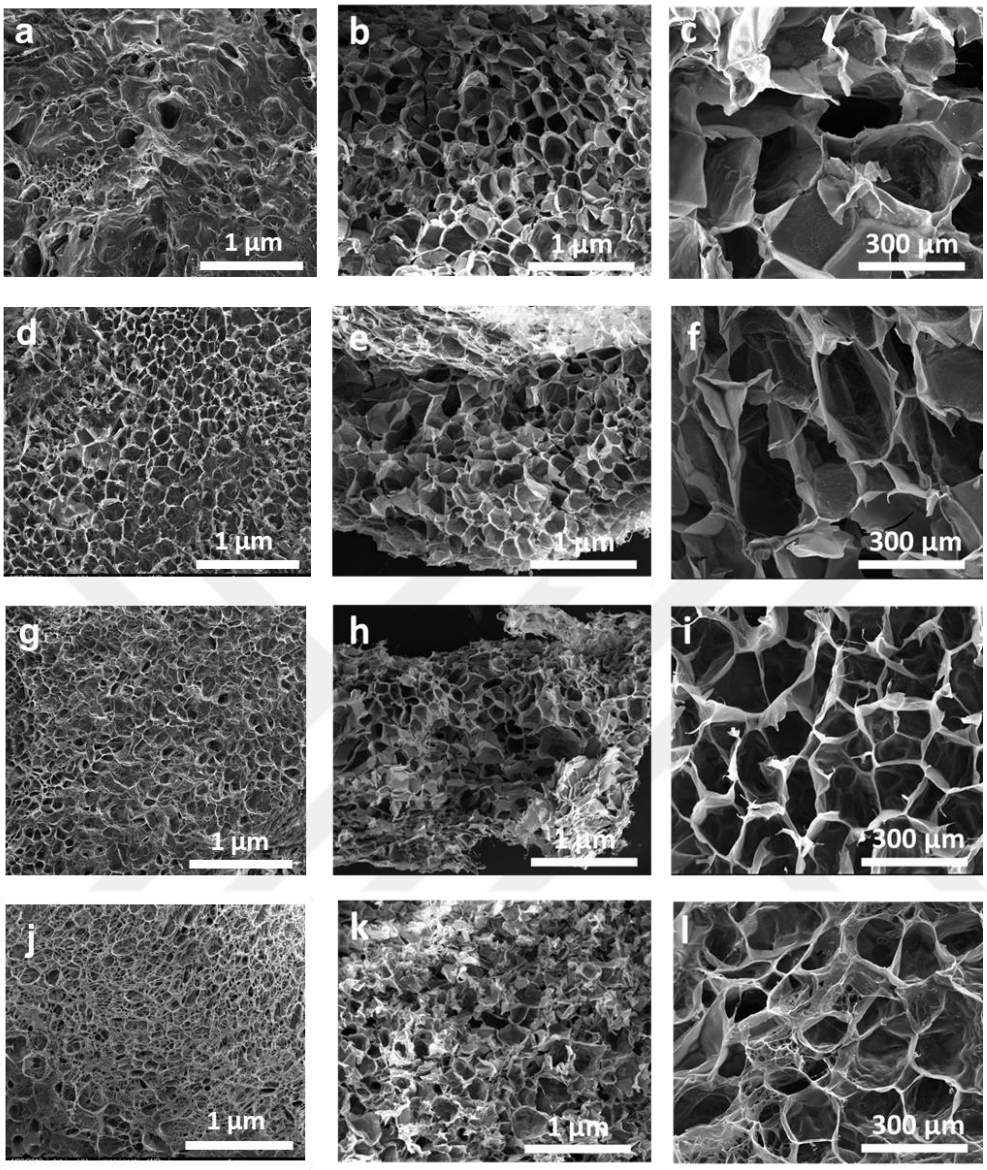

Figure 3.3. Scanning electron microscopy images of the hydrogels. (a) Surface images of MeGC hydrogel; (b,c) cross-sectional image of MeGC hydrogel; (d) surface images of 0.25 MeGC-Fib hydrogel, (e,f) cross-sectional image of 0.25 MeGC-Fib hydrogel, (g) surface images of 0.5 MeGC-Fib hydrogel, (h,i) cross-sectional image of 0.5 MeGC-Fib hydrogel, (j) surface images of 1 MeGC-Fib hydrogel, (k,l) cross-sectional image of 1 MeGC-Fib hydrogel.

3.3 Gelation Time

In this study gelation time of MeGC based hydrogels was determined using vial-tilting method [130, 131]. MeGc-Fib prepolymer solutions with different Fib and photoinitiator concentrations were successfully crosslinked to prepare the hydrogels after exposure to visible blue light.

The effect of different photoinitiator concentration on gelation time of MeGC solutions was investigated. It was found that increasing the amount of riboflavin up to 12 µM accelerated the gelation but increasing the amount of photoinitiator to 24 µM had no significant effect on the gelation time (Table 3.1). Similarly, it was observed that the addition of fibrinogen to the prepolymer solution shortened the gelation time and that the gelation time of fibrinogen-free prepolymer (50.67 s) solution was remarkebly shortened to 32.66 s for 1 % fibrinogen containing 1 MeGC-Fib group. Acceleration of gelation time with the addition of Fib and increase in riboflavin concentration can be attributed to increased amount of free radical formation produced by riboflavin. Riboflavin, as a type II photoinitiator, requires an electron donor when exposed to light radiation and the amine groups are one of the most commonly used electron donor [157]. Together with riboflavin, functional amine groups acts as co-initiators and, this synergistic effect increases the rate of polymerization reaction [157, 158]. It is possible that fibrinogen, as an amine-rich glycoprotein with high lysine content, plays an active role in cross-linking during photopolymerization carried out with riboflavin photoinitiator, which leads to faster gelation [159].

Table 3.1 Gelation time of MeGC based hydrogels (n=3)

DETERMINATION OF GELATION TIME						
Concentration of Riboflavin (µM)	6	12	24	12	12	12
Concentration of Fibrinogen (w/v %)	0	0	0	0.25	0.5	1
Gelation Time (sec)	61.33	52	50.67	43.33	32.66	32.66

Optimization of gelation time is an important step on designing cell entrapped hydrogel systems [160]. Ideally, gelation should occur fast enough to prevent cellular sedimentation but there must be enough time for operator to handle and work on the prepolymer solution throughout the polymerization process [64]. In addition, short gelation times are necessary to achieve encapsulation of viable cells [64]. It is important to keep photopolymerization times as short as possible to minimize cell death and maintain overall cellular activity [161]. It is well known that free radicals which are formed during photopolymerization processes can damage cells, particularly sensitive primary cell types [162].

Our riboflavin-visible blue light-initiated MeGC hydrogel system demonstrated relatively faster sol-gel transition compared to other MEGC, PEG and poly(vinyl alcohol) based hydrogels formed by UV/lithium acylphosphinate or Irgacure 2959 initiators which requires an irradiation time above 180 s [72, 163-165]. Gelation time of photopolymerizable MeGC-based hydrogel systems under visible blue light has previously been investigated. Similar to our findings, addition of biomolecules such as Col II and chondroitin sulphate to MeGC based prepolymer solution was shown to have an accelerating effect on sol-gel phase transition [74, 152]. Addition of both Collagen II (0.4 % w/v) and chondroitin sulphate (1 % w/v) was shown to decrease

the gelation time of MeGC solution (2% w/v) with 3 µM of riboflavin from 80 s to 24 s and 29 s, respectively.

3.4 Mechanical Investigations

Mechanical properties of hydrogels were investigated by uniaxial compression test. Young modulus and ultimate compressive strength results of the hydrogels are given in Table 3. In order to carry out preliminary observations, a series of glycol chitosan solutions were prepared (2%, 3% and 4% (w/v)) in 12 µM riboflavin containing PBS and mechanical investigations were performed. Since the mechanical strength of the obtained 2% (w/v) MeGC hydrogel was very low, mechanical testing with this group could not be performed. The mechanical strength of the hydrogel containing 4% (w/v) MeGC (ε=24.12 kPa) was significantly lower than that of the hydrogel containing 3% (w/v) MeGC (ε=32.81 kPa) which was thought to be due to solubility problems. Decreased transparency at 4% MeGC concentration was observed revealing the solubility problem. Experiments were continued with the hydrogels containing 3 % (w/v) MeGC based on their higher mechanical properties and no solubility problem.

Table 3.2 Compression test results of hydrogels (n=4)

Groups	Elastic Modulus (kPa)	Ultimate Compressive Strength (kPa)
MeGC (4 %w/v)	24.12 ± 1.8	12.18 ± 2.72#
MeGC (3 %w/v)	32.81± 2.62	19.37 ± 3.51*
0.25 MeGC-Fib	44.58 ± 3.21	20.54 ± 4.63 **
0.5 MeGC-Fib	52.94 ± 2.01	26.12 ± 2.4
1 MeGC-Fib	62.65 ± 3.42	37.15 ± 4.14 *- **-#

*For elastic modulus values: All groups are significantly different from eachother, ($p < 0.05$). For ultimate compressive strength values: *,** and # denote statistical significant difference between the groups ($p < 0.05$).*

Combination of chitosan with blood proteins to develop scaffolds for tissue regeneration is a relatively new area of research. Among proteins added to chitosan, fibrinogen (or fibrin) deserves special attention as a coagulation protein [166]. Introducing fibrinogen to the MeGC hydrogel network obviously increased the mechanical properties. Elastic moduli of fibrinogen-free MeGC hydrogels were 32.81 ± 2.62 kPa while the elastic moduli of 0.25 %, 0.5% and 1 % (w/v) fibrinogen containing MeGC groups were 44.58 ± 3.21 kPa, 52.94 ± 2.01 kPa, 62,65 ± 3.42 kPa, respectively. Besides, the results showed that the addition of fibrinogen to the MeGC network significantly increased the ultimate compressive strength of hydrogels. This reinforcement effect of fibrinogen on hydrogel structure might be attributed to two reasons. The first reason is enhancement of mechanical strength of cross-linked MeGC structure by interpenetrating network (IPN) formation by fibrinogen. It was previously demonstrated that, 0.4 % collagen II addition into photopolymerized MeGC hydrogel led to 1.5 fold increase in compressive modulus [73]. In the study, the suggested reason behind this strengthening effect was IPN formation by collagen II in MeGC-based network. The second possible reason is active participation of fibrinogen to cross-linking via its functional thiol groups . It is also known that, radical polymerization can cause cross-linking of thiol moieties in proteins such as cysteine amino acids and, fibrinogen has cysteine residues in its structure [158, 167]. Previously, Huang et. al (2017) prepared knob-grafted hyaluronic acid-based hydrogel by crosslinking knob peptides (GPRPAAC, a mimic peptide of fibrin knob A) with methacrylated hyaluronic acid [168]. Knob-g-HA was synthesized between the methacrylate groups of hyaluronic acid and the thiol groups of knob peptide via Michae-type addition reaction. In another study, Pradhan et. al (2020) prepared poly(ethylene glycol)-fibrinogen hydrogel by covalently coupling fibrinogen to poly(ethylene glycol) diacrylate via thiol groups on fibrinogen cyteins [169]. The hydrogel was formed under visible light by using Eosin Y as photoinitiator.

There are also other literature findings pointing out strenghening effect of fibrinogen addition into chitosan-based biomaterials. A study of Kim et al. (2014) In the study, UV mediated photocrosslinked chitosan-lactide and chitosan-lactide-fibrinogen hydrogels were prepared and the addition of fibrinogen to the photopolymerization system increased the compressive modulus of the hydrogels [153] In another study carried out in 2018 by Laidmae et al. a fibrous scaffold made of fibrinogen and chitosan was produced by electrospinning, and it was observed that addition of fibrinogen to chitosan fiber structure increased the shear modulus of samples subjected to uniaxial compression, a feature that is characteristic of many normal soft tissues [124].

Ideally, a scaffold should be able to withstand the normal loads and stresses of native cartilage, especially in the initial stages, before the cells begin producing their own functional ECM. However, mechanical properties of hydrogel systems that are used in cartilage tissue engineering are considerably lower than that of native cartilage (where Young's modulus ranges from 500 to 1000 kPa) [73, 74, 132, 170, 171]. For example, a fibrin glue which is one of the most commonly used gel to deliver cells to cartilage defects in clinic has a Young's modulus of 30 kPa [172]. A homogeneous GAG distribution and cartilage-like ECM formation were shown in loosely crosslinked PEG gels with a modulus of 30 kPa [40] Photopolymerized Dextran MA-GelMA copolymer hydrogels had elastic modulus of 23.72 kPa [173]. The most commonly used photopolymerized GelMA hydrogel (10 w/v%) had a compression modulus of 26 kPa, elongation at break of 34% and swelling ratio ~800% [134]. Taking into account all of these, mechanical properties of our composite hydrogel system seemed to be sufficient for cartilage tissue engineering applications.

3.5 Water Uptake Properties

For tissue engineering and biomedicine applications, hydrogels are desired to maintain their defined structure while retaining sufficient amounts of water [174]. To determine the effect of Fib content on the water uptake capacity of MeGC-based hydrogels, swelling tests were carried out in PBS at 37°C.The obtained results are presented in Fig. 3.4.

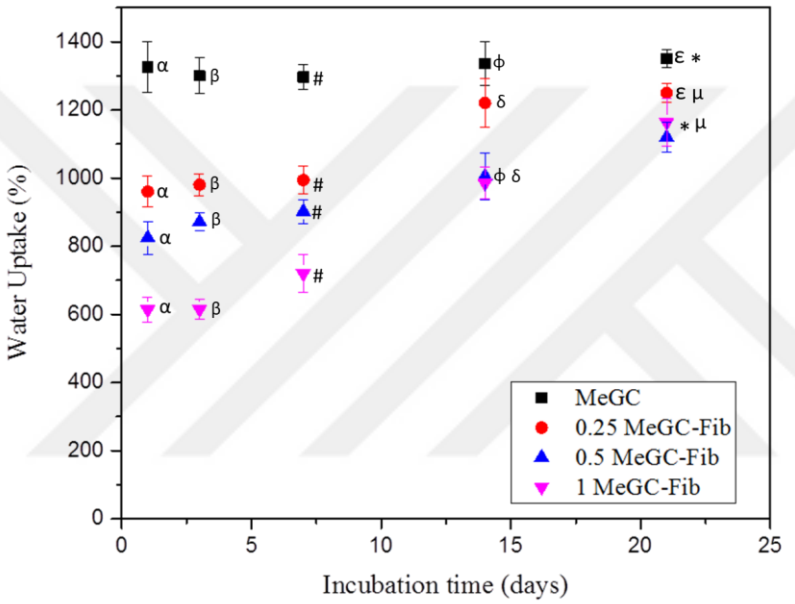

Figure 3.4 Time dependent water uptake (%) values of MeGC based hydrogels in SBF.α,β,δ,μ,Φ,#,π and ∗ denotes statistical significance ($p < 0.05$, n=4).

The initial water uptake of MeGC-based hydrogels was shown to be dependent on concentration of Fib in hydrogel structure. As the Fib concentration was increased from 0.25 wt% to 1 wt%, the initial water uptake significantly decreased from 960.50 ± 45.36 % to 613.92 ± 36.19 %. These results demonstrated that it is possible to adjust initial hydrogel swelling characteristics of MeGC-based hydrogels by varying the Fib content of MeGC prepolymer solution.

The water uptake capacity of MeGC hydrogels on day 1 (1325.73 ± 73.87%) remained almost unchanged with a value of 1350.18 ± 25.84 % at the end of 21 days of incubation. In contrast, swelling values of MeGC-Fib hydrogels obviously changed by time. The water uptake capacity of 0.25 MeGC, 0.5 MeGC, 1 MeGC hydrogels were 960.5 ± 45.36, 825.13 ± 48.35, 613.92 ± 36.19 on day 1; respectively and increased to values of 1250.14 ± 28.36, 1121 ±44.16, ± 1163 ± 49.72, respectively on day 21. The results revealed that, the water uptake of Fib-containing hydrogels increased with time and reached to a similar water retention capacity with Fib-free hydrogels due to loss of water-soluble fibrinogen from hydrogel structure, consequent loosening hydrogel network and increased porosity [175].

According to swelling experiment results, the swelling ratio of Fib containing hydrogels was lower than Fib-free MeGC hydrogels. In general, water uptake (swelling) properties of hydrogel systems are known to vary remarkably with respect to density of crosslinking and a tighter hydrogel network formation [176]. Lower swelling characteristics of Fib containing hydrogels indicate their higher crosslinking density and lower porosity which leads to minimal water uptake into the hydrogel structure [177].

Obtained MeGC-based hydrogels had higher water uptake capacity compared to simple methacrylated chitosan hydrogels which had fairly low swelling degrees in the range of 40–400% in aqueous solutions [178]. Ordinary chitosan-based hydrogels consists of both water absorbing hydrophilic parts and hydrophobic parts which contact with water and prevent the stretching of the network. As a result of introduction of glycol groups into the chitosan structure, the hydrophilicity and water uptake (swelling) capacity of chitosan macromolecules increased [174, 179].

In addition to water uptake behaviour, to characterize the stability of hydrogels during incubation, weight loss of MeGC based hydrogels in SBF swelling medium was investigated over time (Fig.3.5). The initial weight loss of all groups was most likely due to the leaching of uncrosslinked macromers. After this point, the dry weight of the gel did not change much which indicates simulated body-fluid or cell culture medium stability of obtained hydrogel system. A similar time-dependent weight-stability profile of photo-cross-linked MeGC based hydrogel in lysozyme-free PBS medium was demonstrated by Choi et. al [73]. In the mentioned study, incorporation of Col II or chondroitin sulphate did not significantly change the degradation behavior of hydrogels which showed a degradation behavior similar to unmodified MeGC. In the first four days, 3.2% and 6.4% of the loaded Col-II or chondroitin sulphate was released from the hydrogel network. No remarkable change in weight was observed for the hydrogels in PBS for up to 42 days, which indicates that the rest of incorporated ECM molecules remained in the hydrogel structure throughout the incubation period. Another similar result was reported by Wang et. al who observed a significant initial weight loss on photopolymerized acrylated poly(ethylene glycol)-co-poly(xylitol sebacate) hydrogels incubated at 37ºC in enzyme-free PBS [180]. The results showed that prepared hydrogels lost more than 15% of their initial weight with a faster degradation rate during the first 7 days of incubation. This was attributed to the leaching out of uncrosslinked monomers and copolymers from hydrogel network. Later on, no significant hydrogel degradation was detected for the rest of the 28 days incubation period.

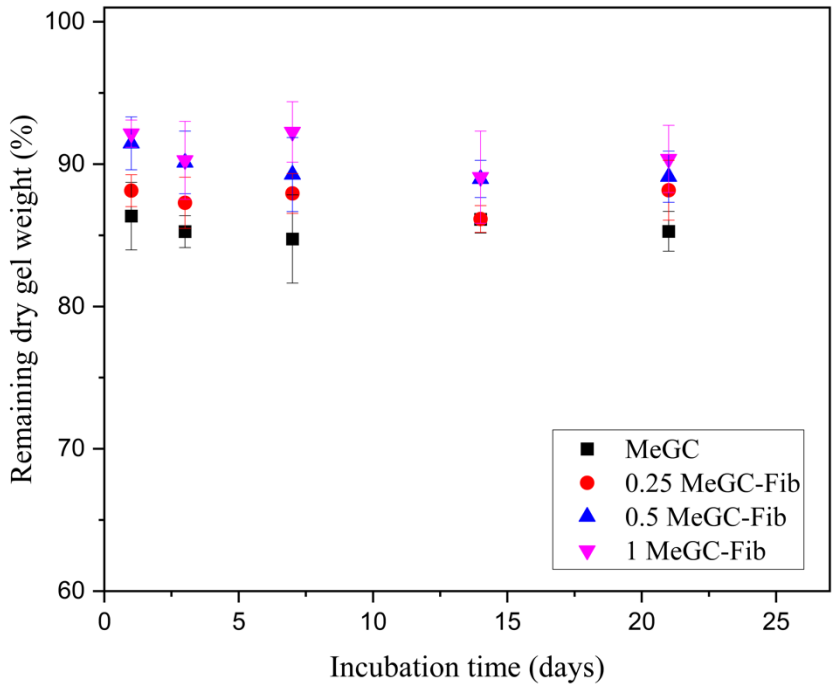

Figure 3.5 Time dependent remaining dry weight (%) values of MeGC based hydrogels incubated in SBF at 37°C (n=4).

3.6 Degradation Properties

Although it is well known that chitosan is completely resorbed in *in vivo*, it is important to characterize the degradation behavior of photocrosslinked chitosan hydrogels. An optimal tissue engineering scaffold is required to degrade gradually at a suitable rate to ensure sufficient cell ingrowth. Following that, cells are expected to build their own extracellular matrix, which will eventually replace the biodegradable hydrogel scaffold [181].

Chitosan is degraded by lysozyme, an enzyme present in a variety of tissues and body fluids including cartilage, through hydrolysis of acetylated residues [10, 11,

182, 183]. The degradation of MeGC hydrogels was evaluated as a function of time by incubating hydrogels in PBS containing 2 mg/mL lysozyme solution at 37˚C for up to 21 days (Fig. 3.6). Lysozyme was used at a concentration of 2 mg/ml in PBS to mimic the physiological conditions in cartilage (lysozyme concentration in human cartilage can increase to levels up to 1000-fold greater than in serum (0.95–2.45 ug /ml) [27].

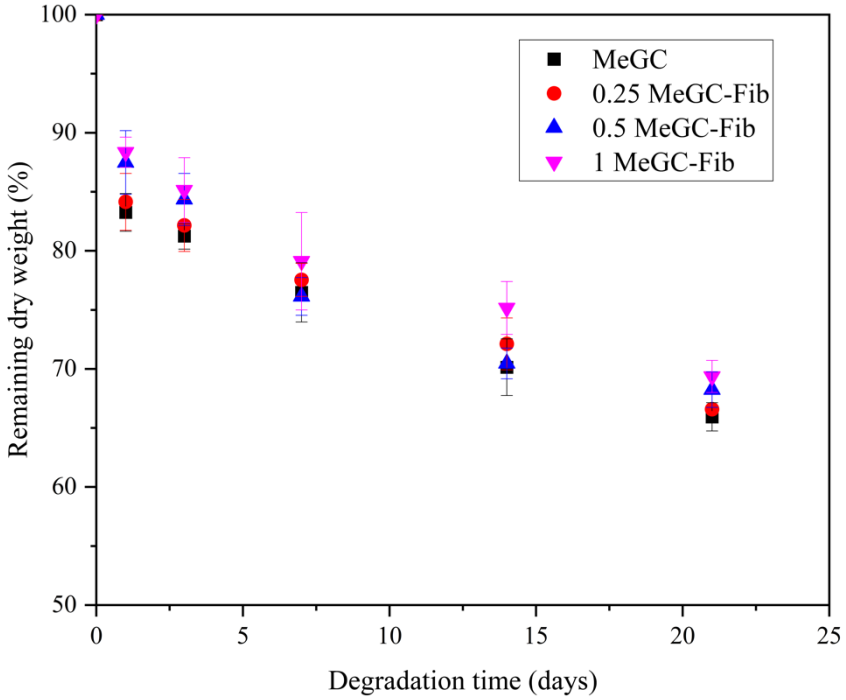

Figure 3.6 Time dependent enzymatic degradation profiles of MeGC based hydrogels in PBS containing 2 mg/mL lysozyme solution (n=4).

The MEGC-based hydrogels had a fast degradation at early stages of incubation, but afterwards the degradation progressed at a significantly slower rate. Approximately 16% mass loss was observed in MeGC-based hydrogels during the first day in the presence of lysozyme, with a cumulative mass loss of 34 % at the end of 21 days of

incubation. The initial mass observed loss was likely due to the degradation of loosely crosslinked chitosan macromolecules from the hydrogel structure [184].

It is also observed that the degradation rate of the MeGC-based hydrogels decreased as the with Fib content of the hydrogels was increased at the early stages of incubation. On the first day, observed mass loss values of MeGC, 0.5 MeGC-Fib and 1 MEGC-Fib groups were 16.74%, 12.52 % and 11.65 %, respectively. The addition of Fib to the MeGC hydrogels slightly slowed down the weight loss rate. Fibrinogen in the hydrogel network formed a tighter network which resulted in lower penetration and accessibility of the lysozyme into the hydrogel, and subsequently slowed initial weight loss. However, the addition of Fib to the MeGC hydrogels did not significantly affect their time-dependent degradation behavior in the long term. After 21 days, the cumulative mass losses of MeGC, 0.25 MeGC-Fib, 0.5 MeGC-Fib and 1 MeGC-Fib hydrogels were 66.58%, 6.24% and 69.36 %, respectively. The obtained results were similar with the enzymatic degradation profile of MeGC/Collagen-II d hydrogels in PBS [152]. The MeGC hydrogel containing 0.4 % (w/v) collagen II lost approximately 30% of its initial weight after 21 days. Considering the fact that a commercially available hyluronan-based cartilage hydrogel scaffold which is used in clinical practice, Hyalograft C, is fully degraded in 3 months after implantation, the slow degradation rate of our MeGC-based hydrogel system seems to be suitable to support new tissue formation during cartilogenesis [185]. The results indicated that 1 MeGC-Fib hydrogel obtained is a suitable candidate to be used in clinical applications.

3.6 Observations on Primary Bovine and Rabbit Chondrocytes

Phase contrast microcopy images of primary bovine and rabbit chondrocytes isolated and cultivated for different time intervals can be seen in Fig. 3.7. Primary articular cartilage chondrocytes were seeded in culture flasks at a density of 1 x 10^4 cells / cm^2. Microscopy images taken from seeded rabbit and bovine chondrocytes after 1 day of incubation are given in Fig. 3.7a and Fig. 3.7b, respectively. Following the

attachment to culture flasks, all the isolated chondrocytes retained cubic-prismatic cell morphology specific to chondrocytes during culture [186].

The growth rate of rabbit articular cartilage chondrocytes during cultivation was found to be slower than the chondrocytes isolated from bovine articular cartilage. Bovine derived chondrocytes reached confluency in approximately 10 days (Fig. 3.7f), while rabbit articular cartilage cells reached confluency in approximately 20 days (Fig. 3.7c) of culture. Primary rabbit chondrocytes' culture time until confluency required a longer time than initially predicted. This unexpected time loss during the cell proliferation process postponed our original in-vitro experiment plan. In order to save time against the delay, bovine primary chondrocytes were used in hydrogel optimization studies.

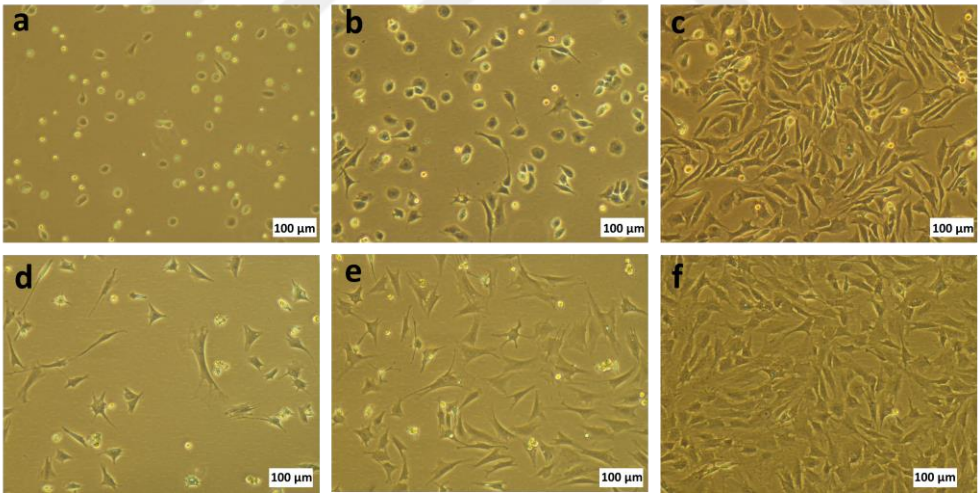

Figure 3.7 Light microscopy images of primary rabbit chondrocytes isolated after (a) 1 day, (b) 3 days, and (c) 10 days of incubation. Light microscopy images of primary bovine chondrocytes isolated after (d) 1 day, (e) 10 days, and (f) 20 days of incubation.

3.7 Static Cell Culture Studies for MeGC-Based Hydrogels

3.8.1 Cell Viability Investigations

Isolated rabbit chondrocytes were suspended in fibrinogen-containing and fibrinogen-free MeGC based prepolymer solutions at a concentration of $2x10^6$ cells/ml, and prepolymer suspensions were photopolymerized with visible blue light for 300 s [72]. Cell viability in the hydrogels was measured by the Alamar Blue viability test (Fig. 3.8). On day 1, cell viability in Fib-free hydrogel group was lower than Fib containing hydrogel groups. As expected, addition of integrin-binding cite rich protein fibrinogen to the hydrogel system improved chondrocyte attachment to the newtwork of the hydrogels [187]. However, there was an unexpected decrease in Alamar Blue Reduction levels of the cells from the first day and the cells lost their viability to a great extent on the seventh day. The cause of this situation was investigated, and it was understood that during the cell encapsulation process 10-fold riboflavin concentration was used instead of 12 µM. Later, the unexpected cell death was found to be consequent of this mistake. It is known that riboflavin has a cytotoxic effect at high concentrations [188].

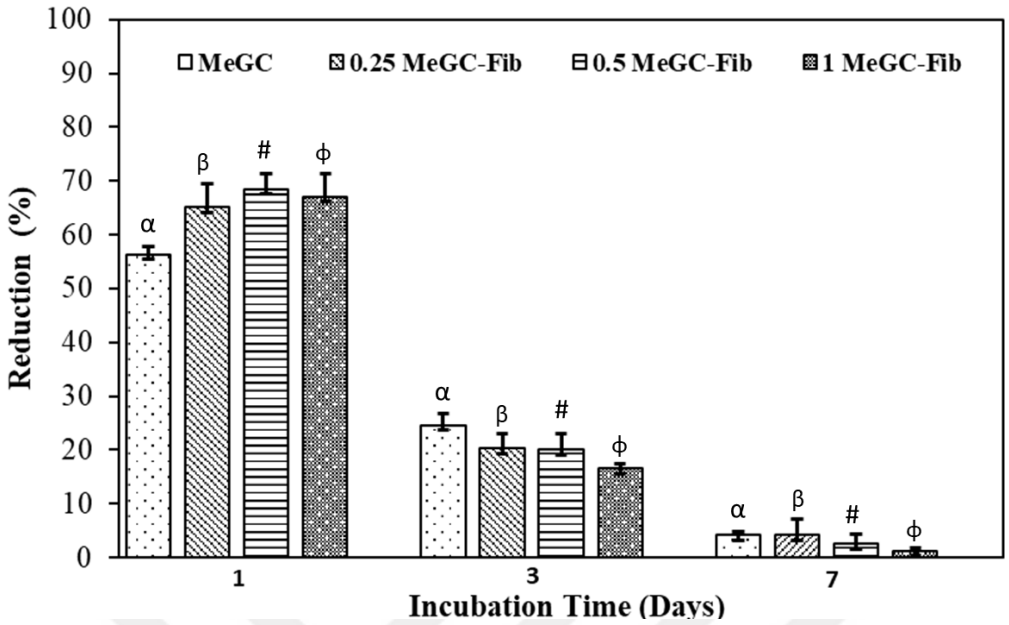

Figure 3.8. Alamar Blue cell viability test results of rabbit chondrocytes that were encapsulated in MeGC based hydrogels and incubated in chondrocyte growth media for different periods of time (n=4).

3.7.2 Cytotoxicity Test

Cytotoxicity of MeGC based hydrogels was investigated by seeding L929 fibroblasts on top of hydrogels and evaluating viability of cells with Alamar Blue assay for one week (Fig. 3.9). Cell viability on MeGC-Fib hydrogels was statistically higher than observed on MeGC on days 3 and 7. Viability of fibroblast on 1 MeGC group almost doubled in seven days showing that fibroblast proliferated on the hydrogels whereas cell viability in MeGC group slightly increased. Results revealed that fibrinogen-free and 1 MeGC hydrogels were cytocompatible.

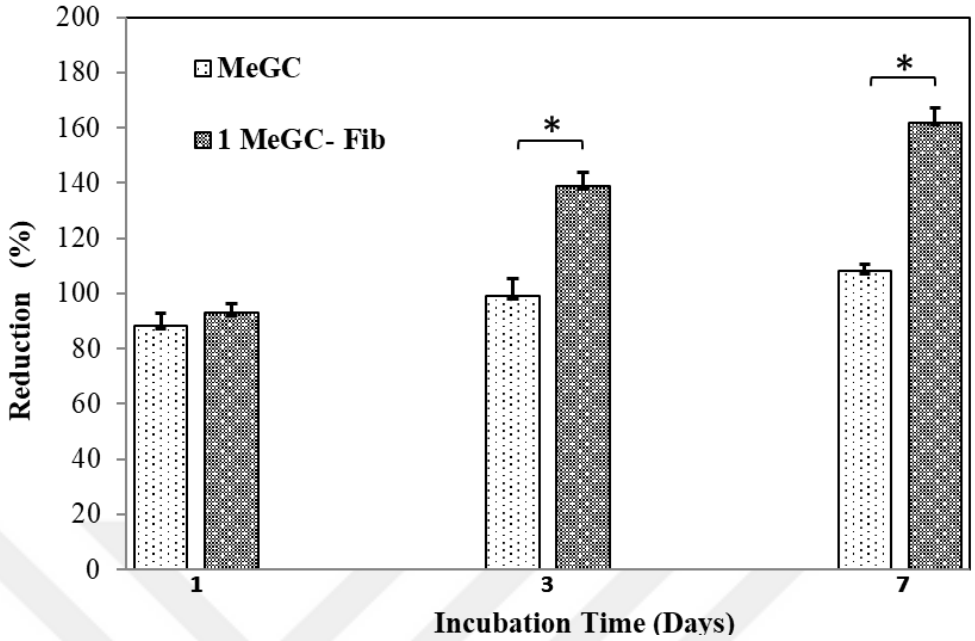

Figure 3.9. Cell viability results of L929 cells cultivated on hydrogels for 7 days (n=4). * denotes statistical significance ($p < 0.05$).

The effect of MeGC based hydrogels on fibroblast morphology was examined by light microscopy (Fig. 3.10). The microscopy images demonstrated that cells on fibrinogen-free MeGC hydrogel surface exhibited spherical morphology at low cell density. This result was in line with the literature, Silva et. al (2011) observed that fibroblasts seeded on chitosan membranes exhibited round morphology, low cell adherence and proliferation [189]. In contrast, Fib containing hydrogels served as a good substrate for the cells to attach, cells on the 1 MeGC-Fib hydrogel were spread on the surface with a remarkably higher cell density. It is well known that when cells adhere poorly to hydrogels they develop a round morphology, whereas, they spread on the surface when they adhere well [49]. Fibrinogen molecules contains RGD sequences which are recognition motifs for cell adhesion. On the other hand, chitosan is highly bioinert and lacks such binding sites so it has a limited cell adhesion compared to fibrinogen [190, 191]. In sum results revealed that, incorporation of Fib into MeGC-based hydrogel system improved cell adhesion to hydrogels.

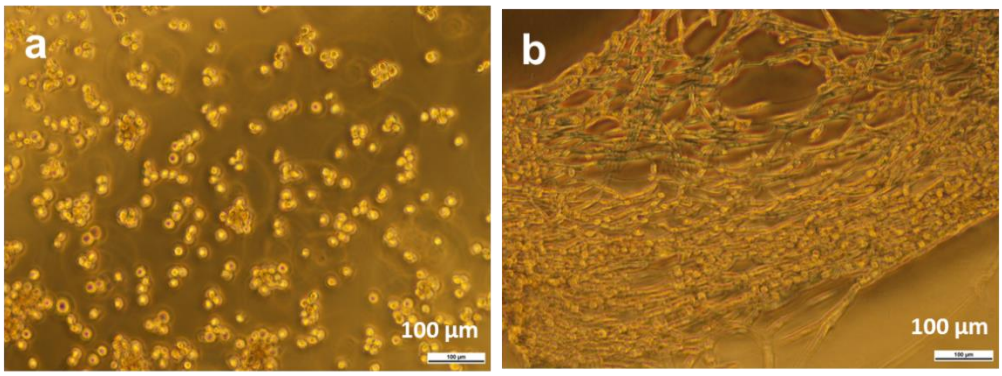

Figure 3.10. Light microscopy images from L929 cells seeded on the obtained (a) MeGC hydrogel surface and (b) 1 MeGC-Fib hydrogel surface.

3.7.3 Cell Viability in MeGC-based Hydrogels

solated bovine chondrocytes were suspended in fibrinogen-containing and fibrinogen-free MeGC based prepolymer solutions at a concentration of $2x10^6$ cells/ml and chondrocytes were entrapped in the hydrogel structure as a result of photopolymerization of the prepared prepolymer suspensions under visible blue light for 300 s [72]. Cell viability within the MeGC based hydrogels was measured via Alamar Blue viability assay. The results are given in Fig. 3.11. After first 24 h of incubation, there was no significant difference among the groups. It is known that the main limitation of chitosan hydrogels in tissue regeneration applications is low cell adhesion to chitosan matrix alone [192]. As expected no significant increase in cell viability was observed in Fib-free MeGC hydrogels during 21 days of culture. Similar to cytotoxicity test results, addition of integrin-binding site rich protein Fib seems to provide cell adhesion motifs for chondrocytes and enhanced cell-chitosan based hydrogel network interaction. Introducing fibrinogen to the MeGC hydrogel network led to a time-dependent increase on the reduction levels which also revealed higher proliferation of chondrocytes. The highest cell viability was observed in 0.5 MeGC and 1 MeGC hydrogel groups resulting from increased number of adhesive

ligands for cell surface integrins in the hydrogel network.. For Fib containing 0.25 MeGC-Fib and 0.5 MeGC-Fib hydrogel groups, proliferation of chondrocytes continued until day 14 days of incubation and then the proliferation rate of cells decreased due to increased number of cells in hydrogel matrix. For 1 Fib- MeGC group, high proliferation profile continued during 21 days of culture. The obtained reduction percentage results of Alamar Blue showed that viability of chondrocytes in the hydrogels was maintained during the 21 days of culture for all hydrogel groups.

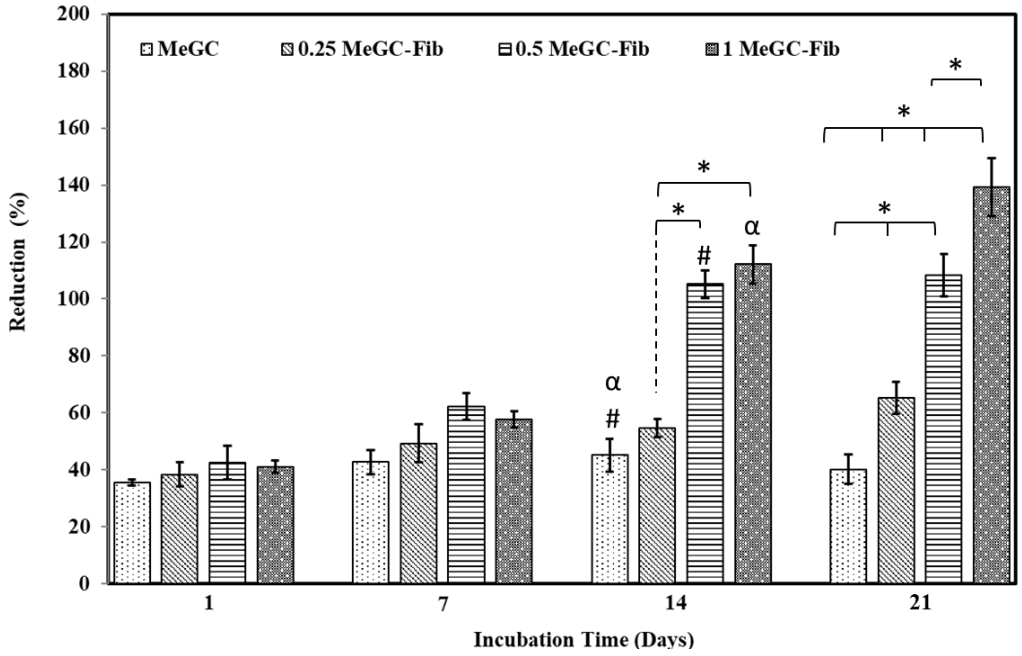

Figure 3.11. Alamar Blue test results of bovine chondrocytes in MeGC hydrogels after incubation in Chondrogenic Growth Medium at 37°C for different periods of time (n=4). * denotes statistical significant difference between the groups ($p < 0.05$).

Fib containing groups 0.5 MeGC-Fib and 1 MeGC-Fib and had significantly higher cell viability on both 14 and 21 days of incubation than that of Fib free MeGC group which was a sign of the positive impact of Fib incorporation into MeGC hydrogel

structure on cell growth. To overcome limited cell attachment problem of chitosan, combination of chitosan with highly cell-adhesive proteins and peptides have been investigated. In 2007, Mochizuki et al. conjugated twelve integrin-binding peptides derived from ECM proteins onto chitosan membranes and examined the biological activity [192]. The results revealed that peptide-chitosan constructs can regulate specific integrin-mediated cell responses and are useful constructs as ECM mimetics. In another study, addition of Collagen II was shown to stimulate chondrocyte attachment in chitosan hydrogels [73]. Among proteins combined with chitosan, Fib deserves special attention as an integrin binding site rich blood protein [166]. Likewise chitosan, Polyethylene glycol is a bioinert material and must be modified to allow cell attachment and proliferation on its surface [193]. For this purpose, Fibrinogen was combined with PEG in a previous study; Dikovski et al. (2006) prepared a biosynthetic 3D hybrid scaffold made of synthetic polyethylene glycol (PEG) and Fib molecules [194]. PEGylated Fib was photo cross-linked by Irgacure under UV light in the presence of smooth muscle cells to form a dense cellularized hydrogel network. Similar to our findings, the results revealed that Fib provides additional biofunctional domains to bioinert PEG due to intergrin-mediated cell adhesion sites on Fib backbone and obtained Fib-containing hydrogel increased cell adhesion to PEG-based matrix [194].

Among Fib containing groups, the highest cell proliferation was observed for 1 MeGC-Fib hydrogels as the group with the highest Fib content at the end of 21 days of incubation. This might be attributed to the fact that when there are more RGD containig protein (Fib) in the hydrogel environment cells could find more sites in the hydrogel structure to adhere and grow. Accordingly, the lowest level of cell proliferation was observed for hydrogels with the lowest amount of Fib, 0.25 MeGC-Fib (among Fib containing groups). Additionally, there was no significant difference between Fib-free MeGC and 0.25 MeGC-Fib groups during the first 14 days of incubation.

3.7.4 DNA Quantification of Hydrogels

DNA contents of MeGC based hydrogels that were incubated for different time periods in chondrogenic growth medium were analyzed using Hoechst dye (Fig. 3.12). No difference in DNA contents was observed among the groups after 24 h of incubation. However, at the end of 14th day DNA content of Fib-free hydrogel group was significantly lower than DNA contents of the other groups. This time-dependent dramatic increase in DNA contents of Fib containing hydrogels was correlated with the trend observed in cell viability results (Fig. 3.11). This can be due to positive effect of Fib on chondrocyte adhesion, migration, and viability of cells in the hydrogels. However, from 14th day to 21st day cell number did not remarkably increase, and cell proliferation rate decreased. This could be caused by the limitation of the transport of nutrients and oxygen to the core of the hydrogels due to the increased cell number and ECM deposited by the cells [195, 196].

Fib-containing groups 0.5 MeGC-Fib and 1 MeGC-Fib had significantly higher DNA content after 14 and 21 days of incubation than Fib-free MeGC group, indicating that Fib incorporation into MeGC hydrogel structure had a favorable impact on cell proliferation. As a result, the hydrogels with the lowest amount of Fib, 0.25 MeGC-Fib, had the lowest level of cell growth together with Fib-free MeGC hydrogels. Similar to viability results, no statistically significant difference exists between the Fib-free MeGC and the 0.25 MeGC-Fib groups throughout the entire culture time.

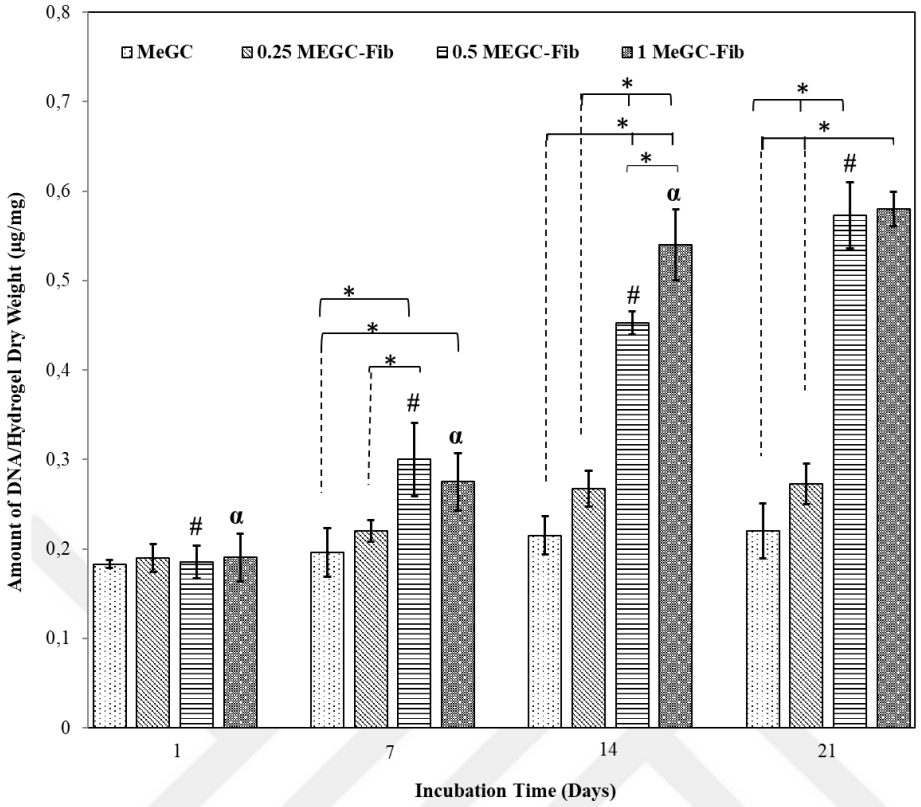

Figure 3.12. DNA amounts in bovine chondrocytes entrapped MeGC based hydrogels after incubation in chondrogenic growth medium containing 10% FBS at 37°C in a carbon dioxide incubator for different periods of time (n=4). * denote significant difference between the groups ($p < 0.05$).

3.7.5 Live/Dead Assay of MeGC-Based Hydrogels

For microscopic investigation of live / dead cell distribution in hydrogels live/dead test was carried out on chondrocytes entrapped constructs at the end of 1st and 21st days of incubation. Since living cells have intracellular esterase activity, Calcein-AM dye that enters the living cell creates a green fluorescent image after its enzymatic transformation [197]. The ethidium homodimer-1, which is used to mark dead cells, can only enter dead cells and binds to nucleic acids in dead cells, producing a red fluorescent signal [197]. Images taken after live / dead cell

fluorescence staining from chondrocyte trapped hydrogels are given in Fig. 3.13. Live-dead assay images indicates that more than 90% of chondrocytes were alive on day 1 for all hydrogel groups. This high cell viability was preserved for 21 days of incubation and a very low number of red stained dead cells was observed in microscope images at the end of 21st day. Consistent with the previously reported findings, MeGC was observed to be nontoxic and, the initiator molecule and free radicals produced during photopolymerization did not cause any noteworthy toxicity [72, 129, 198] Others also reported more than 90% cell viability for visible light-riboflavin initiated MEGC-based hydrogels [72, 152]. In this study, the applied riboflavin dose and light inducing time-dependent cell viability results were similar to previously published viability findings for collagen gels [199]. Similar to Alamar Blue assay and DNA determination results, the highest viable cell number was observed in 0.5 MeGC-Fib and 1 MEGC-Fib groups after 21 days of cultivation. Obtained results indicates the safety of both the visible light and riboflavin-initiated cell entrapment method and the biocompatibility of the biomaterials selected for the design of the MeGC based hydrogel system.

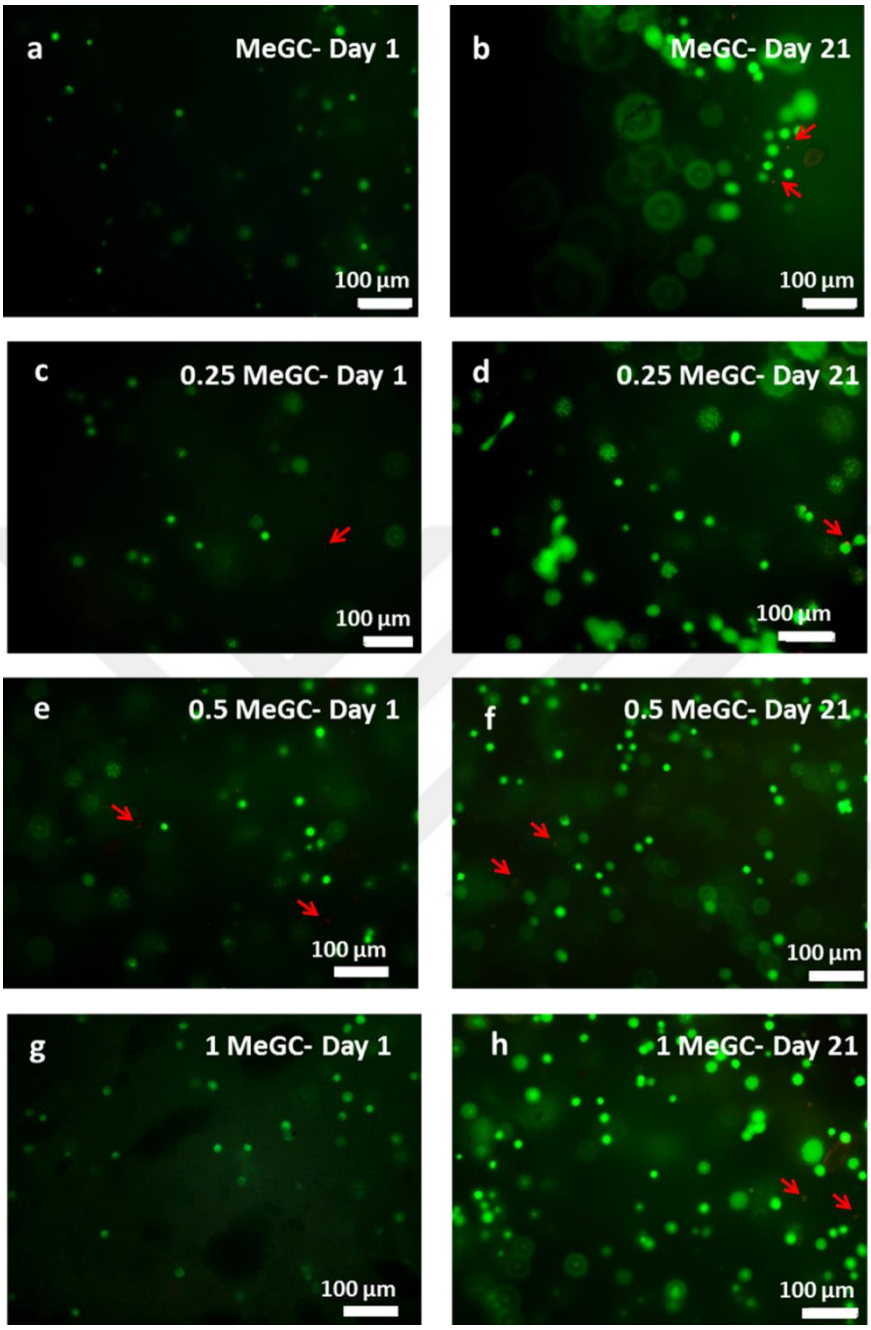

Figure 3.13. Fluorescent microscopy images of Live/Dead assay of primary bovine chondrocytes entrapped in MeGC based hydrogels at 1st (**a, c, e, g**) and 21st **(b, d, f, h**) days of incubation. (**a-b**) MeGC hydrogels, (**c-d**) 0.25 MeGC-Fib hydrogels, (**e-f**) 0.5 MeGC-Fib hydrogels, (**g-h**) 1 MeGC-Fib hydrogels. Green stained cells are live cells, red stained cells are dead cells. Dead cells are shown by red arrows.

3.7.6 Total Sulfated Glucosaminoglycan Content Synthesized by Chondrocytes in MeGC-based Hydrogels

Previous studies have reported that Fib can induce tissue regeneration as a biomaterial. Santos et al. revealed pro-inflammatory and pro-healing roles of fibrinogen in chitosan scaffoldsCumulative GAG concentrations in the culture media collected and the amount of sGAG in the structure of the newly formed extracellular matrix in the cell-entrapped hydrogels were quantitatively determined using the DMMB assay. To rule out the effect of sample size and mass variations, the results were normalized to the dry weights of hydrogels. Time-dependent s-GAG content results are given in Fig. 3.14.The graph shows that GAG content of all hydrogel groups increased during 21 days of incubation. For the Fib-free MeGC group sGAG production increased from 1.69±0.18 (μg/mg) for the 1st day to the 8.70±1.17 (μg/mg) for the 21st day. For the 0.25 MeGC-Fib group increase in sGAG production was similar, it increased from day 1 (1.78±0.32 (μg/mg)) to day 21 (11.23±2.26 (μg/mg)). 0.5 MeGC-Fib group showed a significant increase in production of sGAG from 1.95 ± 0.43 (μg/mg) at 1st day to 27.72 ±1.85 (μg/mg) at the end of 21st day of cultivation. At the end of 21 days, GAG content of 1 MeGC-Fib hydrogels was also as high as 0.5 MeGC- Fib group (31.31 ± 2.60 (μg/mg)). Results revealed that at the end of 14 and 21 days of culture, sGAG content of hydrogel groups containing more than 0.25 % (w/v) fibrinogen was significantly higher than fibrinogen-free hydrogels. Results indicated the positive effect of fibrinogen on sGAG production and therefore, better cartilage specific ECM deposition.

It is well known that material composition of scaffolds has a direct influence on proteoglycan metabolism and GAG production of chondrocytes and accordingly the quality of tissue engineered cartilage [103]. Previously, similar positive effects on s-GAG synthesis of chondrocytes (derived from New Zealand white rabbits) were observed in MeGC-based hydrogels supplemented with Col II [152]. According to

the study, after six weeks in culture, MeGC/Col II hydrogels produced much more s-GAG than MeGC hydrogels (4.6-fold higher compared to MeGC).

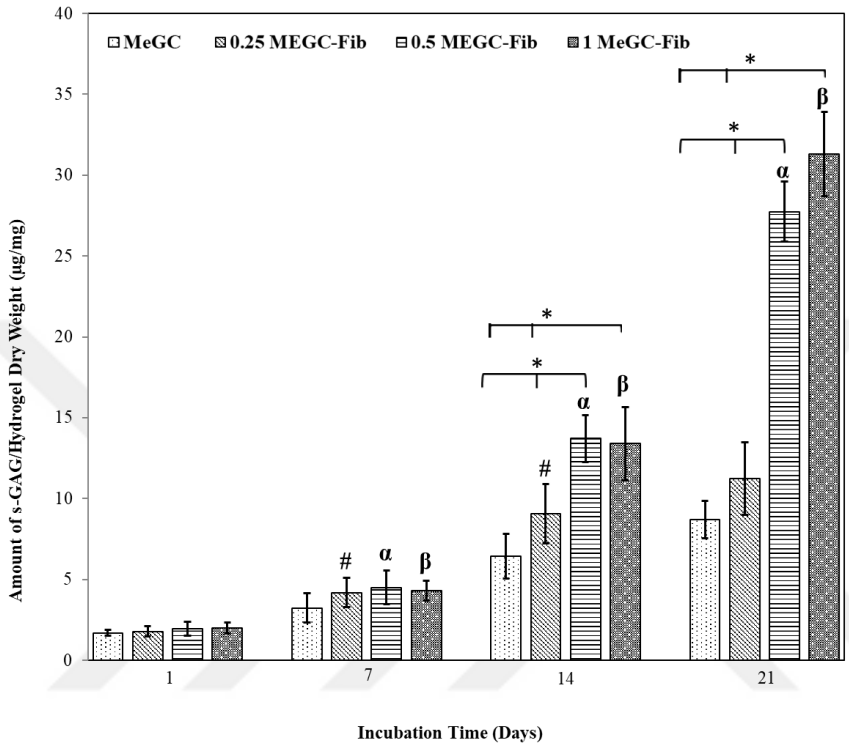

Figure 3.14. Cumulative total GAG amounts synthesized by chondrocytes (in both the supernatants of cell lysates and the cell medium deposited by bovine chondrocytes) after incubation in chondrogenic growth medium containing 10% FBS at 37°C for different periods of time (n=4). *, #, α, β denote significant difference between the groups ($p < 0.05$).

The sGAG/DNA ratios representing s-GAG synthesis capacity of a single chondrocyte in MeGC based hydrogels is given in Figure 3.15.At the end of 21 days of incubation, the levels of s-GAG/ hydrogel dry weight for the groups 0.5 MeGC-Fib and 1 MeGC-Fib were remarkably higher compared to the other groups (Figure 3.14). However, when s-GAG values were normalized to the amount of DNA, the calculated difference got smaller due to the higher number of cells in those hydrogels

(Fig. 3.15). The obtained results indicated that, the level of GAG syntesized per cell was in a similar range for all hydrogel groups. Similar findings were also previously reported for chondrocytes entrapped other hydrogel blends such as alginate-chondroitin sulfate, collagen type I-chitosan, and thiol modified gelatin-hyaluronic acid [200-202].

Although being non-significant at some points, s-GAG/DNA ratio increased with time for all individual hydrogel groups. At the end of 21 days of culture, sGAG/DNA values of MeGC (39.56±5.31) and 0.25 MeGC-Fib (41.24±8.30) hydrogels were almost at the same levels. S-GAG/ DNA ratio of chondrocytes entrapped in 1MeGC-Fib based hydrogels (53.98±4.47) found to be significantly higher than the other groups at the end of the cultivation. The results indicated that 1 MeGC-Fib hydrogel composition could promote the production of cartilaginous matrices more than the other hydrogel groups.

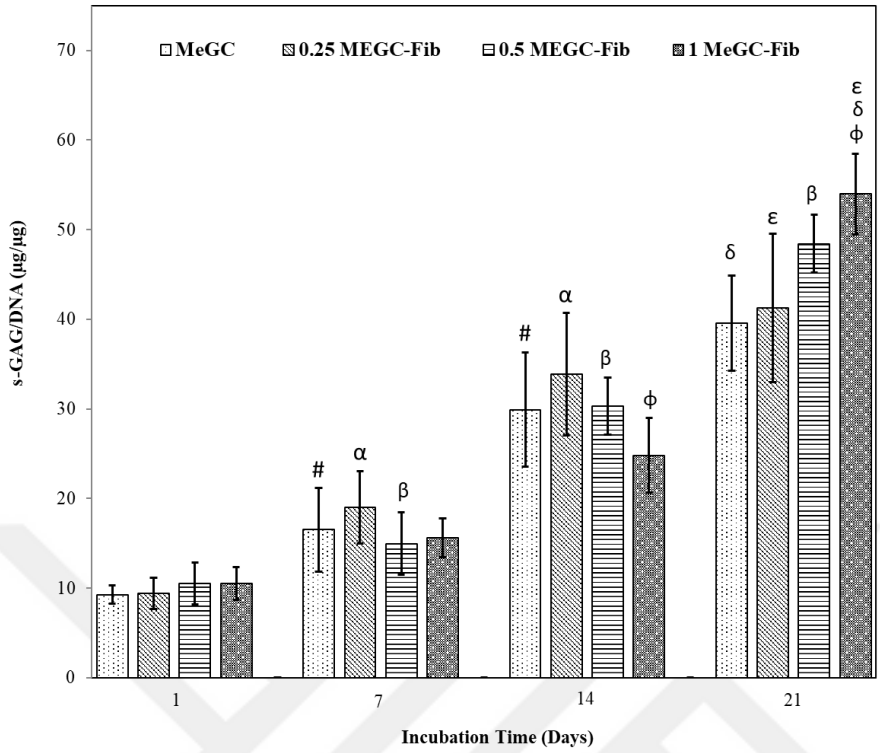

Figure 3.15. Cumulative s-GAG/DNA amounts produced by bovine chondrocytes which were entrapped in MeGC based hydrogels after incubation for different periods of time in chondrogenic growth medium containing 10% FBS at 37°C (n=4). (GAG amounts used in calculations were previously determined in both the supernatants of cell lysates and the cell medium.) *, #, α, β, φ denote significant difference between the groups ($p < 0.05$).

Fibrin, the polymer form of fibrinogen macromolecules, have been used hydrogel scaffolds for cartilage tissue regeneration [203]. Although, platelet rich fibrin (PRF, a naturally derived fibrin scaffold that is easily obtained from peripheral blood) has been applied for clinical procedures such as repair of articular joints and osteoarthritis therapy more than 15 years, there is still very limited number of research on fibrinogen/fibrin containing hydrogels/scaffolds developed for cartilage regeneration [203, 204]. Previously it was shown that MSCs entrapped in fibrin hydrogels differentiated into chondrocytes and produced significantly more cartilaginous ECM with a higher total GAG content compared to fibrin-alginate

hydrogels.[205]. In another study, MSCs encapsulated in fibrin glue demonstrated superior chondrogenic differentiation and superior aggrecan expression compared to control group (ADMSCs without scaffold) [206]. Deepthi et. Al (2016) entrapped hMSCs into a chitosan-fibrin-alginate hydrogel and chondrogenic potential of this hydrogel system was investigated. The results indicated that hMSCs produced a higher level of s-GAG when compared to control group [207].

3.7.7 Total Collagen and Collagen Type-II Contents in MeGC -Based Hydrogels

The amounts of collagen and collagen II in hydrogels cultured under static conditions were measured and calculated using a Total Collagen Assay Kit (BioVision, Inc., USA) and Type- II Collagen Detection Kit (Chondrex, USA), respectively [208, 209]. To eliminate the effect of possible sample size variations, the measured data were normalized to hydrogel dry weights.

Chondrocytes cultured in 1 MeGC hydrogels showed the highest expression level of total collagen and collagen type-II after 21 days of culture indicating that chondrocytes cultured in 1 MeGC hydrogels had the best maintenance capacity of chondrogenic phenotype (Fig. 3.16 and Fig. 3.17). Total collagen and Type II collagen contents were significantly lower in MeGC and 0.25-MeGC based hydrogels than the other two groups. The results revealed that expression of collagen becoming more prominent for fibrinogen amounts more than 0.25 % (w/v) in MeGC hydrogel content.

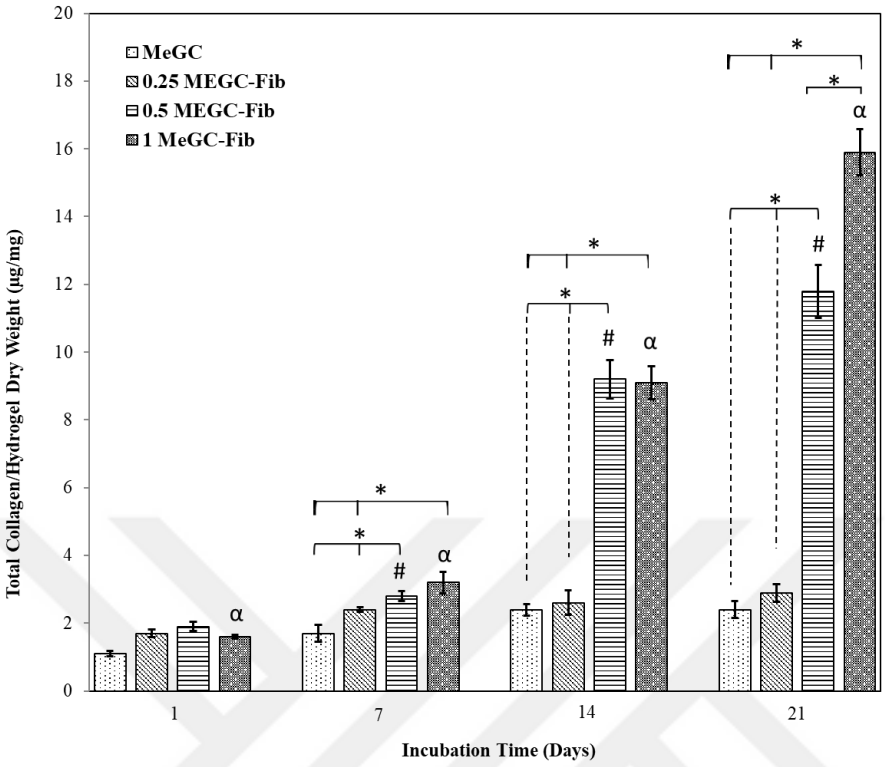

Figure 3.16. Cumulative total collagen amounts produced by bovine chondrocytes entrapped in MeGC based hydrogels which were incubated in chondrogenic growth medium containing 10% FBS at 37°C in a carbon dioxide incubator for different periods of time (n=4). *, #, α denote significant difference between the groups ($p < 0.05$).

Chondrocytes cultured in 1 MeGC hydrogels showed the highest amount of total collagen and collagen type-II after 21 days of culture indicating that these chondrocytes maintained their chondrogenic phenotype and biosynthesis functionality (Fig. 3.16 and Fig. 3.17). Total Collagen and collagen type- II content of 1 MeGC hydrogel significantly increased during 21 days of incubation and reached values of 0.67 µg/mg and 11.2 µg/mg respectively. On the other hand, collagen contents of MeGC and 0.25 MeGC hydrogel groups did not change significantly throughout the culture period. Total collagen and Type II collagen

contents of MeGC and 0.25-MeGC based hydrogels were significantly lower than the other two groups. When the concentration of Fib was increased above 0.25 (% w/v) a more prominent total collagen and collagen type- II expression was observed.

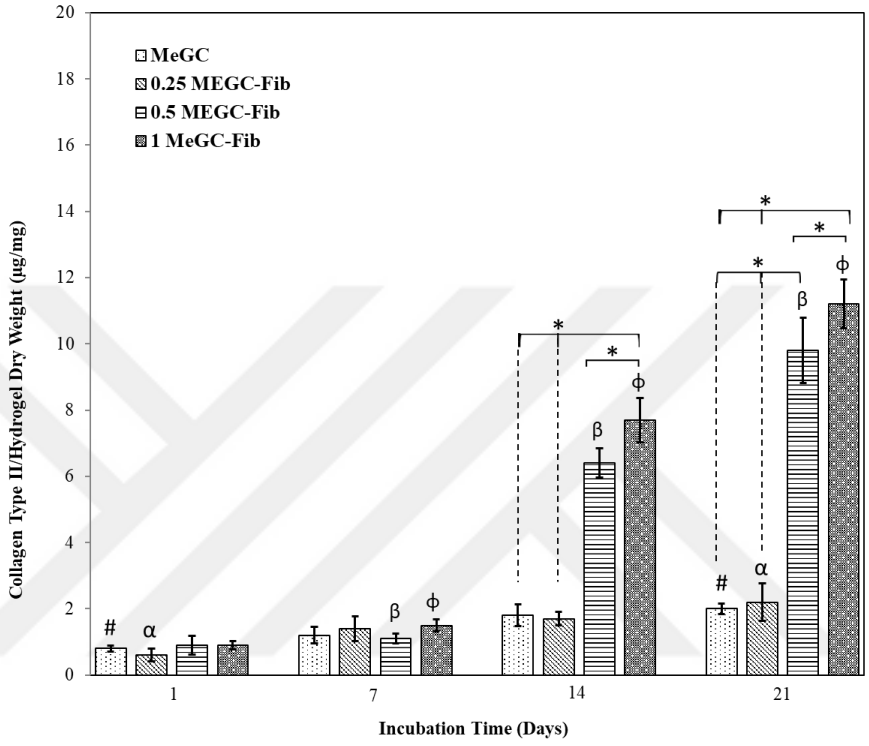

Figure 3.17. Cumulative collagen type II amounts produced by bovine chondrocytes entrapped in MeGC based hydrogels which were incubated in Chondrogenic Growth Medium containing 10 % FBS at 37°C in a carbon dioxide incubator for different periods of time (n=4). *, #, α, β, φ denote significant difference between the groups ($p < 0.05$).

Based on our findings, 1-MeGC-Fib hydrogels appears to be the most promising chondrogenic matrix which is favourable for chondrogenesis and chondrogenic functionality. The elevated total collagen production in 1-MeGC-Fib hydrogels could be a result of the increased amount of the biologic recognition sites , such as RGD sequences, in hydrogel structure due to elevated amount of fibrinogen. Since,

when there are more RGD-containing proteins (Fib) in the hydrogel environment, cells may find more places to adhere which enhances cell adhesion, proliferation and ECM synthesis[190]. At the end of 21 days of culture collagen II level of 1-MeGC-Fib group was 4.5 fold higher compared to MeGC group. Previously collagen-II secretion was shown to increase 3.5 fold for MeGC-Col II hydrogel system, which is lower than our findings for the same culture period [152].

3.8 Dynamic Cell Culture Studies in Mechanobioreactor

Considering the results of previously performed optimization investigations, hydrogels 1 MeGC-Fib hydrogels were chosen to be used in dynamic culture studies.

3.8.1 Cell Viability Profiles and DNA Content of Hydrogels

In this study, viability of the chondrocytes in the hydrogels which were dynamically and statically cultured were measured using Alamar Blue assay (Fig. 3.18a). First group of hydrogels (DC-1) was stimulated with 21 kPa of cyclic compressive loading throughout the culture meanwhile for the second hydrogel group (DC-2) applied initial cyclic compressive loading (7 kPa) stepwise increased every seven days to the values of 14 kPa and 21 kPa during the culture. And the third hydrogel group (FS) was statically cultured.

Culturing hydrogels under DC-2 dynamic mechanical compression regime significantly enhanced the number of cells within the scaffolds when compared to unloaded FS constructs. It is known that in static cultures, chondrocytes in the inner region of AC constructs have limited access to signals and nutrients causing them to lose function and their typical chondrocyte phenotype [210]. As a general approach, higher chondrocyte viability in dynamic cultures is attributed to higher nutrient accessibility and increased diffusion towards the core of tissue constructs compared to passively stimulated or static cultures [210]. However, the lowest cell growth profile was observed for the other mechanically stimulated DC1 group.

It was observed that for most of the MEGC- based hydrogel constructs, cellular metabolic activity increased until Day 14, and subsequently decreased. In general, an increased cell metabolic activity indicates the proliferation of cells, because it is well known that metabolic activity and cell number are correlated. Therefore, the detected decrease on cell viability pointing out a decrease on cell proliferation rate after Day 14, at this point instead of proliferation, cells tend to produce ECM.

Obtained results on the effect of mechanical stimulation on cell viability indicated that, not just dynamic cultivation but applied mechanical stimulation regime is also crucially important on viability of cells [111, 211-213]. At the end of 21 days of mechanical stimulation, when hydrogels were dynamically cultured under the DC-2 mechanical simulation regime almost fivefold increase was observed in viability of rabbit chondrocytes in the hydrogels. But interestingly, chondrocyte proliferation was hampered by DC-1 stimulation compared to free swelling hydrogels. Based on our Alamar Blue test results, it is suggested that starting from a lower-range load at the beginning and application of an incremental compressive loading regime enhances cell growth while instantaneous application of higher magnitude (21 kPa) of loading has a negative effect on the cell proliferation. Although the large body of literature reporting a positive impact of dynamic compressive loading on cell proliferation with chondrocyte entrapped hydrogels, there are some studies demonstrating a decrease in cell number within hydrogels such as agarose, fibrin and collagen [212, 214-216]. Unfortunately comparison of outcomes among these studies is challenging and inconclusive due to lack of standardization on applied dynamic compression protocols (frequencies around 1 Hz, mechanical loading amplitudes within the frame of 5–20%, daily compression periods of 1–4 h/day and loading durations of at least 7 days) and there is almost no data for the magnitude of applied stress on hydrogels. In addition, used cell sources, culture conditions, bioactive molecules and type of hydrogel vary between studies [213, 217]

Differences in the DNA contents were also noted between the different cultivation treatment groups (Fig. 3.19b). After 21 days of culture, the highest DNA content was observed for DC-2 hydrogel group which subjected to incremental loading regime and for this group a fourfold increase in the amount of DNA was observed. Similar to viability results, the DNA content of DC-1 hydrogels which are instantaneously subjected to 21 kPa 1 Hz cyclic compressive loading was significantly lower than the DNA content of hydrogel group which were dynamically cultivated under DC-2 mechanical simulation regime. In addition, no time-dependent decrease was observed on DNA contents of unloaded FS (free swelling) constructs.

Similar to our DC-1 dynamic loading findings, Hunter et. al demonstrated that, dynamic compressive loading has no significant effect on viability and DNA content of bovine chondrocytes entrapped in a fibrin-based hydrogel in comparison with FS or statically compressed control groups [214]. In another previous study, similar to DC-2 protocol, incremental dynamic compressive loading (the magnitude of the load increased in an uncontrolled manner) was applied on bovine synoviocytes seeded on polyethylene terephthalate fiber scaffolds. Results revealed an increased DNA content for dynamically loaded constructs compared to free swelling samples which support the findings of the current study [113].

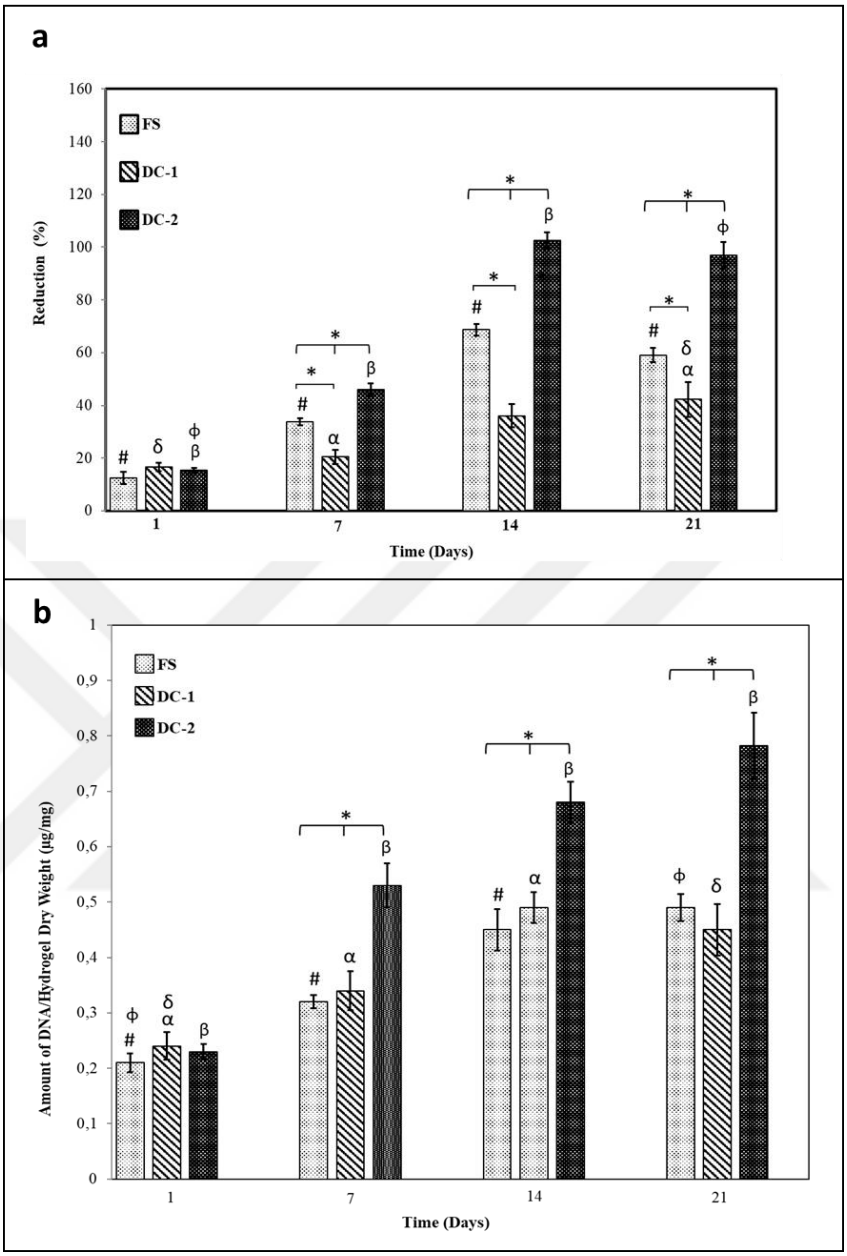

Figure 3.18. (a) Viability and **(b)** DNA contents of rabbit chondrocytes entrapped in the hydrogels with a density of 2 x 10^6 cells/mL. Hydrogels were cultivated under static and dynamically loaded culture conditions as DC-1; 21 kPa of cyclic compressive loading, DC-2; Initial cyclic compressive loading of 7 kPa stepwise increased every seven days to the values of 14 kPa and 21 kPa during the culture and, FS; Free Swelling *, #, α, δ, β and, φ, denote significant difference between the groups ($p < 0.05$). (n=4).

In our findings, the detected dramatic differences in chondrocyte proliferation response to different compressive loading regimes highlights the importance of magnitude of loading applied in early culture periods for cartilage tissue engineering. The reason why 7 kPa stimulation increased DNA content and the cell viability while a direct application of 21 kPa led to a minimal difference compared to free swelling at the end of 7 days of culture is not clear. We suggest that in the early periods of cultivation, due to low level of synthesized ECM, the cells are hypersensitive to mechanostimulation and a higher level of force applied on cells may induce catabolic responses and hamper proliferative activities in chondrocytes. It is known that mechanical loading can induce anabolic behaviors while being subjected to supraphysiological high magnitude forces can drive catabolic responses on chondrocytes [218, 219].

Articular cartilage is routinely exposed to diverse mechanical stimuli, and encounter forces of several times greater the body weight during joint loading by normal physical activity [220]. The unique anisotropic structure of native articular cartilage tissue (depth-dependent variation in alignment of collagen fibrils and confinement of hydrated proteoglycan) allows these forces to be dissipated so that the magnitude of cellular stress experienced by chondrocytes is actually much lower [221, 222]. However, due to the difficulty in replicating the native cartilage's complex architecture in lab environment and lack of highly organized stiff ECM surrounding, chondrocytes entrapped in hydrogels experience much more harsh conditions when subjected to in-vitro dynamic loading. Dynamic loading produces a complex environment involving both cell deformation and fluid flow, which will influence cell response within the hydrogels [223]. The degree of cell deformation and induced fluid flow through the hydrogels is likely to be dependent on applied strain and the correspondence stress on hydrogels [114, 223]. It is possible that at early periods of the culture, due to lack of cell-surrounding and force-dissipating ECM in hydrogels, a direct 21 kPa loading led to high level of fluid flow end cell deformations which resulted in a catabolic shift on chondrocyte metabolism and reduced cell proliferation

rate with DC-1 loading. On the contrary, cells entrapped in the statically cultured FS hydrogel group were not subjected to any dentrimental loading, they continued to significantly proliferate for the first 14 days of culture and after the first day the cell viablity values of FS group was higher than DC-1 group of hydrogels.

3.8.2 Total Sulfated Glucosaminoglycan and Collagen Contents of Hydrogels

Total sGAG amount produced by chondrocytes entrapped in the hydrogels (amount of GAG deposited in hydrogel plus amount released into the culture media) over 21 days of culture was quantitively determined via DMMB assay (Fig. 3.20).

At the end of the first week, there was no statistical difference in s-GAG biosynthesis between the groups except for the hydrogels subjected to DC-2 regime. A statistically significant increase on GAG syntesis of all groups was observed on day 14. At the end of 21 days of culture, s-GAG production of hydrogel-entrapped chondrocytes subjected to DC-1 compressive loading regime was significantly lower than other two groups. This result was parallel with the viability examinations which proved the DC-1 regime was not favoirable for cellular methabolic activity. Compared to other groups, hydrogel-entrapped chondrocytes subjected to incremental dynamic compressive loading (DC-2 regime) showed a significant increase in s-GAG content from day 14, indicating the stimulatory effects of incremental compressive loading regime (DC-2) on s-GAG synthesis.

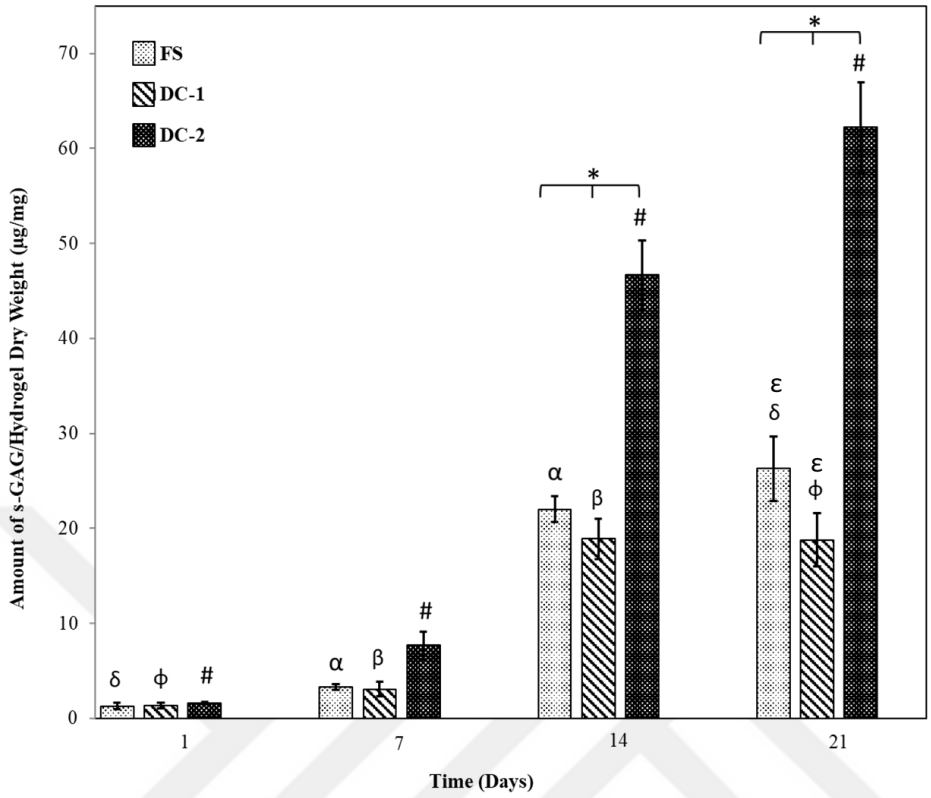

Figure 3.19. Total GAG amounts produced by the rabbit chondrocytes entrapped in the hydrogels with a density of 2 x 10^6 cells/mL (amount of GAG deposited into the gel plus released into medium). Hydrogels were cultivated under static and dynamically loaded culture conditions as DC-1; 21 kPa of cyclic compressive loading, DC-2; Initial cyclic compressive loading of 7 kPa stepwise increased every seven days to the values of 14 kPa and 21 kPa during the culture and, FS; Free Swelling. *, #, α, δ β, φ denote significant difference between the groups ($p < 0.05$, n=4).

As a major component of the extracellular matrix, the quantity of GAG secreted by chondrocytes can reflect the functional status of the cells. According to Fig. 3.21, it was found that cells responded similarly in all groups on day 1 and the proportions of GAG to DNA in both experimental groups increased with the culture time. Rabbit chondrocytes in DC-2 group, secreted significantly more GAG than the other groups

after the first week. . The highest increase on GAG synthesis per cell of all groups was observed at day 14. Both at the end of 14 and 21 days of culture, s-GAG/DNA level of hydrogel-entrapped chondrocytes subjected to DC-1 compressive loading regime was significantly lower than other two groups which was another sign of the negative impact of DC-1 mechanical stimulation regime on GAG biosynthesis. GAG/DNA values of hydrogels in DC-2 group were significantly higher than hydrogels in FS group, from 1.40-fold, to 1.48-fold on day 14 and 21, respectively. In other words, when GAG content of DC-2 group was measured relative to DNA content at day 21, it was determined that 48% more GAG was produced per chondrocyte compared to chondrocytes cultured in free swelling conditions. The obtained result indicated that incremental loadeded chondrocytes synthesized more GAG of cartilage specific tissue ECM. DC-1 group chondrocytes which were directly subjected to 21 kPa cyclic compressive load during dynamic cultivation secreted less GAG from chondrocytes which are statically cultured (FS group) GAG at day 14 and day 21 probably due to dentrimental effect of DC-1 regime on cellular metabolic activities.

For the first 14 days of culture, chondrocytes in all groups continued to produce collagen with a significant increase on collagen levels, except for DC-1. For DC-1 group cells responded differently and no significant change was observed on amount of collagen probably due to negative effect on DC-1 stimulation regime on cellular metabolic activities. During 21 days of culture, total collagen amounts produced by rabbit chondrocytes which were subjected to incremental compression (DC-2) was significantly higher than free swelling hydrogels and DC-1 group (Fig. 3.22). There was no significant difference in the amount of total collagen between free swelling group of hydrogels and hydrogels DC-1 hydrogels which were subjected to the same value of cyclic loading for entire culture time.

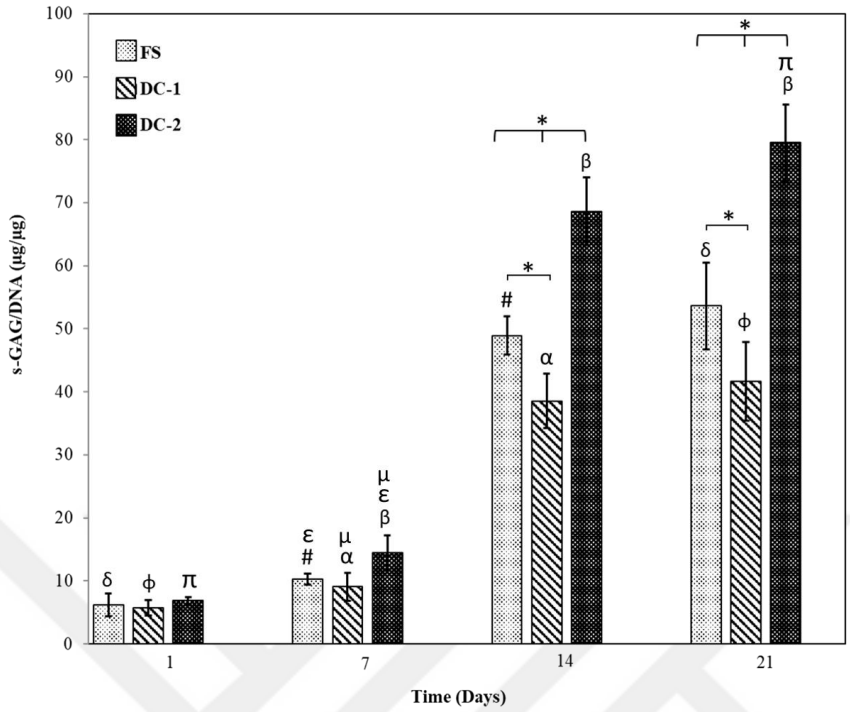

Figure 3.20. Total s-GAG/DNA values produced by the rabbit chondrocytes entrapped in the hydrogels with a density of 2 x 10^6 cells/mL (amount of GAG in the hydrogel deposited plus amount released into the media were normalized to DNA content in the hydrogels). Chondocytes entrapped in the hydrogels were cultivated under static and dynamically loaded culture conditions as DC-1; 21 kPa of cyclic compressive loading, DC-2; Initial cyclic compressive loading of 7 kPa stepwise increased every seven days to the values of 14 kPa and 21 kPa during the culture, FS; Free swelling *, #, α, δ β, φ denote significant difference between the groups ($p < 0.05$, n=4).

Col I, the most abundant collagen in our bodies, is a fibrocartilage marker and is highly expressed by immature cartilage which is later be replaced by Col II [224]. Therefore, an increase in Collagen II level is regarded as an evidence to healthy neocartilage formation in tissue engineering studies. Results revealed that the synthesis and accumulation of collagen II, was remarkably enhanced by the application of incremental compressive loading regime (Fig. 3.23). The highest

cumulative Collagen II synthesis (19.33 µg/mg) was observed in DC-2 group during 21 days of culture period. Although there were no significant difference in GAG and total collagen content between free swelling hydrogels and hydrogels cyclically compressed with the same magnitude of load, collagen II content of DC-1 group was significantly lower than collagen II content of FS group. Even though being non-significant at some points, the culture duration also resulted in an increase in the type II collagen content in all groups.

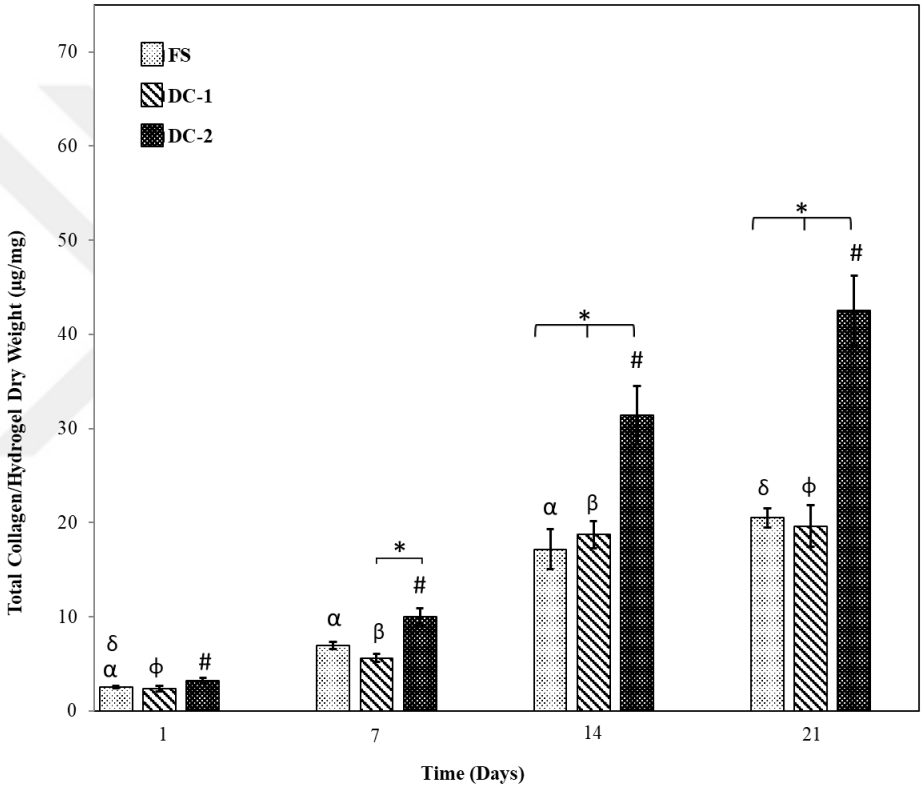

Figure 3.21. Total collagen amounts produced by the rabbit chondrocytes entrapped in the hydrogels with a density of 2 x 10^6 cells/mL (amount of collagen deposited into the gel plus released into medium). Chondocytes entrapped in the hydrogels were cultivated under static and dynamically loaded culture conditions as DC-1; 21 kPa of cyclic compressive loading, DC-2; Initial cyclic compressive loading of 7 kPa stepwise increased every seven days to the values of 14 kPa and 21 kPa during the culture, FS; Free swelling. #, α, δ β, φ denote significant difference between the groups ($p < 0.05$,n=4).

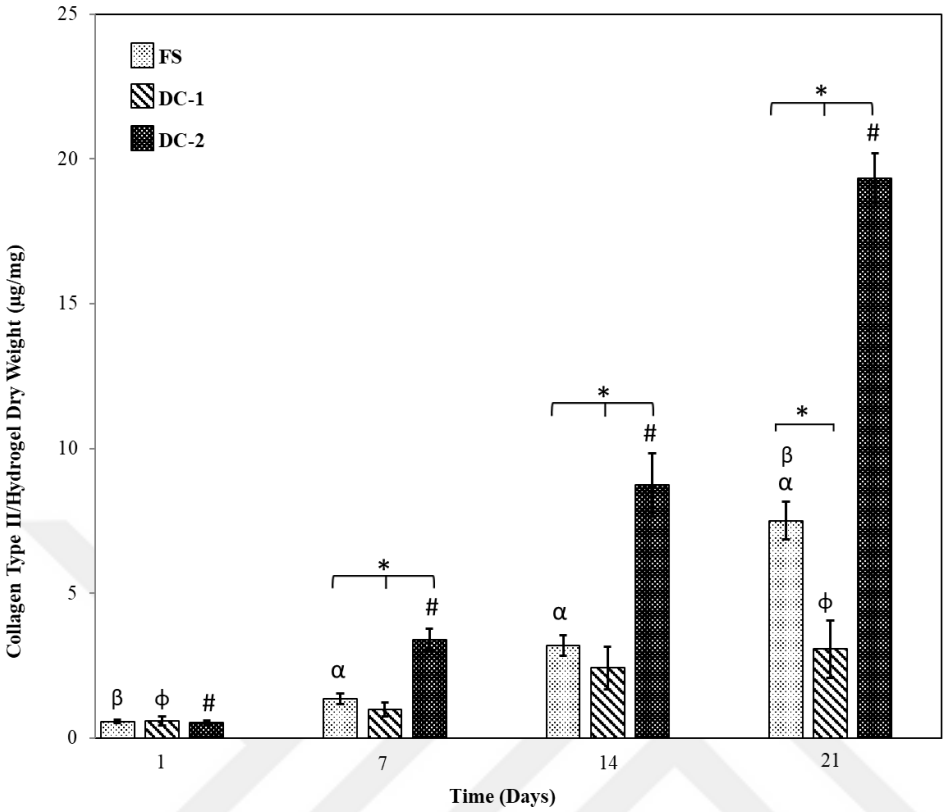

Figure 3.22. Total collagen II amounts produced by the rabbit chondrocytes entrapped in the hydrogels with a density of 2 x 10^6 cells/mL Chondocytes entrapped in the hydrogels were cultivated under static and dynamically loaded culture conditions as DC-1; 21 kPa of cyclic compressive loading, DC-2; Initial cyclic compressive loading of 7 kPa stepwise increased every seven days to the values of 14 kPa and 21 kPa during the culture, FS; Free swelling. . *, #, α, δ β, φ denote significant difference between the groups ($p < 0.05$, n=4).

The findings of the current study indicate that an optimal strategy using well-characterized conditions for the functional tissue engineering of articular cartilage, particularly to induce GAG and collagen II synthesis, may incorporate stepwise application of increasing magnitudes of dynamic compressive loading. The reason why 7 kPa stimulation elevated GAG and collagen II levels while a direct application of 21 kPa load led to a reduction in cartilage specific ECM synthesis compared to

free swelling at the end of 21 days of culture is not clear. In the previous literature, different dynamic compressive loading regimes appears to result in a wide range of chondrogenic outcomes and the reasons of this variations are not fully understood yet. The results obtained for DC-2 regime is in line with the results of previous studies reporting a promoting effect of dynamic mechanical compression on deposition of cartilage-specific ECM synthesis. For instance, Mauck et al. applied a dynamic compressive stimulation regime (10% strain, at a frequency of 1 Hz, 3 x (1 h on, 1 h off)/day, 5 days/week) to chondrocyte entrapped agarose gels for 4 weeks. The results indicated that long-term (∼28 day) dynamic compression of chondrocyte entrapped agarose gels induced cartilagenious matrix synthesis with an increase in both GAG and total collagen contents in hydrogels [225]. In another study, Wang et al. (2013) reported that mechanical loading (dynamic sinusoidal oscillation loading, 0.4 ± 0.2 mm (5% to 15% of scaffold height) at 1 Hz, surface shear at ±25° for 1 h twice a day, with 8 h rest in between loadings, on every second day) for four week promoted GAG and collagen type-II synthesis, and improve ECM accumulation in primary chondrocyte seeded on polyurethane scaffolds [226]. In another study, Nebelung et al. investigated the effect of long-term continuous dynamic compression on primary human chondrocytes entrapped in type -I collagen hydrogels (0.3 Hz frequency, 10% amplitude and 28 days of culture time) and immunohistochemistry results revealed that dynamic compression led to a remarkable increase in collagen II biosynthesis of chondrocytes.[227]. In a recent study, Xie et al. applied dynamic compressive loading on homan chondrocyte entrapped poly-D,L-lactic acid/polyethylene glycol and polycaprolactone(PEG-PDLLA- PCL) hydrogels and demonstrated that dynamic compressive loading (%5 strain, 0.2 Hz, 1 h/day) stimulated the production of cartilage matrix with an increase in GAG and collagen-II synthesis compared to statically cultured hydrogels at the end of 28 days [111]. However, even though in most of the previous studies dynamic compressive stimulation was found to promote biosynthesis of proteoglycans and collagen type-II in chondrocytes, there are some other studies reporting a contrary effect which is similar to our results for DC-1 stimulation regime. Villanueva et. al showed that

dynamic compressive loading (0.3 Hz, 15% amplitude strains, 6 h) of chondrocyte-entrapped PEG-chondroitin sulfate hydrogels led to a decrease in collagen production by 52% compared to free swelling controls [107]. In another study, Lima et. al demonstrated that dynamic compressive loading (1Hz, 3hrs/day, 10% unconfined compression) which applied immediately following cell entrapment caused a remarkable decrease in GAG and collagen-II synthesis after 32 and 51 days of loading when compared to statically cultured control group [228]. When initiation of loading was delayed by 14 days, there was no difference in s-GAG or collagen-II production in comparison with free swelling controls.

In this study, for DC-1 dynamic compressive stimulation, a direct application of 21 kPa dynamic compression may disrupt the accumulation of proteoglycan and collagen II by disrupting newly synthesized matrix at early stages of culture [229, 230]. It is well known that, chondrocytes perceive and respond to the mechanical loading via integrin mediated mechanotransduction [25, 231] External mechanical loads (like tissue compression) are known to alter the metabolic activity of articular chondrocytes and are conveyed through, or imposed on ECM molecules, matrix receptors and intracellular sites through cell-matrix interaction [25, 232]. For tissue engineered cartilage application optimal mechanical loading is essential to deliver appropriate signals to cells to maintain chondrocyte functionality and deposition of a cartilage-specific ECM while a high-magnitude of stress can induce catabolic activity on chondrocytes [218, 233]. For DC-1 mechanical stimulation regime, instantaneously being subjected to a high magnitude dynamic compressive loading may also induce matrix metalloproteinase synthesis which results in increased matrix breakdown [234, 235]. The findings of this study indicate that coordination of the timing and magnitude of compressive mechanical loading according to estimated stage of tissue development may be a good a strategy to optimize production of functional tissue engineered cartilage.

3.9 Histological and Immunofluorescence Analyses of In Vitro Cultured Hydrogels

In order to identify matrix components and provide a visual impression of cellular and matrix distribution within the constructs, histological and immunohistochemical staining were carried out. It is well known that detection of the presence of Collagen Type II and high levels of sGAG, classical markers for cartilage tissue, indicates the deposition of cartilage-like matrix in tissue engineering studies [236]. A histological staining combination of Alcian Blue/Sirius Red was used to visualize sGAG and collagen content, respectively, and immunohistochemistry was used to identify collagen Type II.

At the end of the 1st and 21st days of culture histological and immunofluorescence analyses were performed on the hydrogels to investigate the effect of different culturing conditions on cartilage tissue development.

Hematoxylin & Eosin staining is one of the most abundant method in histological analysis. Hematoxylin is blue purple in color and stains nucleic acids. Eosin, on the other hand, stains proteins and appears in pink tones. In a normal healthy tissue, the nucleus is blue-black and the cytoplasm of the cells and ECM are stained pink [237]. Hematoxylin & Eosin-stained light microscopy images of 1 MeGC-Fib hydrogels containing primary chondrocytes subjected to static, DC-1 and DC-2 dynamic cultivation conditions on days 1 and 21 of culture are presented in Fig. 3.24. The presence of chondrocytes and ECM was clearly seen in all three groups. Cell nuclei are dark purple stained. Isogenous chondrocyte groups specific to cartilage were clearly observed in the sections taken from the hydrogels at the end of 21 days of culture, especially in the hydrogels subjected to DC-2 dynamic mechanical stimulation regime. In addition, results revealed that for hydrogels subjected to DC-

2 mechanical stimulation cells proliferated more than the other two group of hydrogels.

One of the most important cartilage-specific markers, the glycosaminoglycan (GAG) content, is examined by Alcian Blue staining. Sections from the hydrogel samples taken on the 1st and 21st days of culture were stained with Alcian Blue and examined under a light microscope (Fig. 3.24 - a, c, e, g, i, k). Nonspecific blue staining of the hydrogels was observed in all groups. The cytoplasm of cells was stained in lighter blue compared to staining of the hydrogel. During 21 days of culture for all hydrogel groups, the intense blue color due to GAG biosynthesis reveals that chondrocyte functionality was preserved. After 21 days of culture, more sGAG expression was observed in the cells inside the hydrogels subjected to DC-2 mechanical stimulation compared to other groups. On the 21st day images of the DK-2 group (Fig 3.24.k), both the intensity of blue and cell density increased significantly, and the cells begun to form their own cartilage-like matrix. In this group, chondrocytes appeared round within lacunae-like structure and started to form isogeneic groups in ground substance (territorial matrix-like) structures which is a distinct structural and morphological characteristics specific to cartilage.

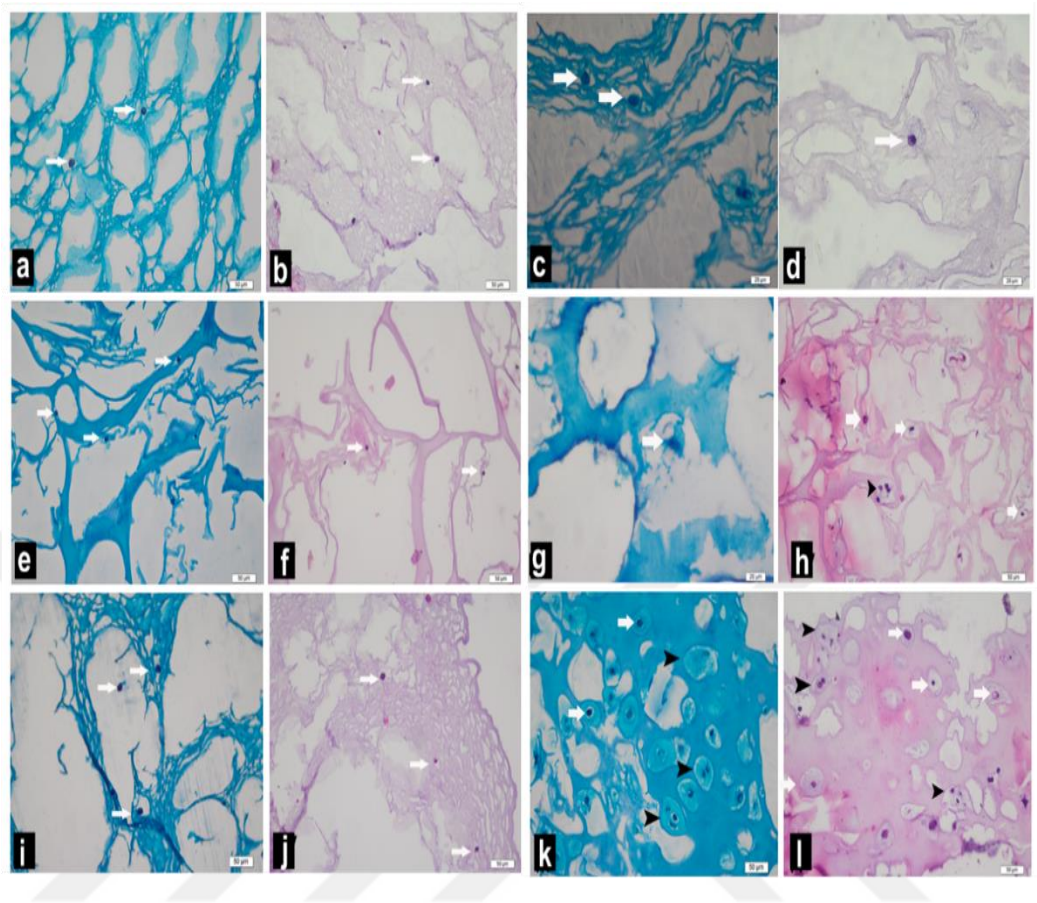

Figure 3.23. Light microscopy images of (a, c, e, g, i, k) Alcian Blue and (b, d, f, h, j, l) Hematoxylin & Eosin staining results of primary rabbit chondrocyte entrapped hydrogels cultured under different conditions. Images were taken at (a, b, e, f, i, j) 1st and (c, d, g, h, k, l) 21st days of cell culture. (a-d) Hydrogels cultivated under static conditions. (e-h) Hydrogels dynamically cultivated under DC-1 mechanical simulation regime. (i-l) Hydrogels dynamically cultivated under DC-2 mechanical simulation regime. Chondrocytes are shown by white arrow, Cartilage-specific isogenic groups are shown by black arrow.

Picrosirius Red staining was performed to investigate the total collagen content in the hydrogels cultured under different conditions for 21 days (Fig. 3.25). Following the first staining with Picro Sirius Red and the distribution of total collagen was visualized under a fluorescent microscope. In this method, areas with collagen

accumulation appear intense bright red. In the given microscopy images, the hydrogel was also slightly stained but the distinct bright red collagen staining around the spherical chondrocytes and the stained cytoplasm are clearly visible. At the end of 21 days of culture the results revealed that, the cells were synthesizing collagen and significant amount of collagen was present in the cytoplasm and in the vicinity of the cells which could be interpreted as ECM deposition by the cells.

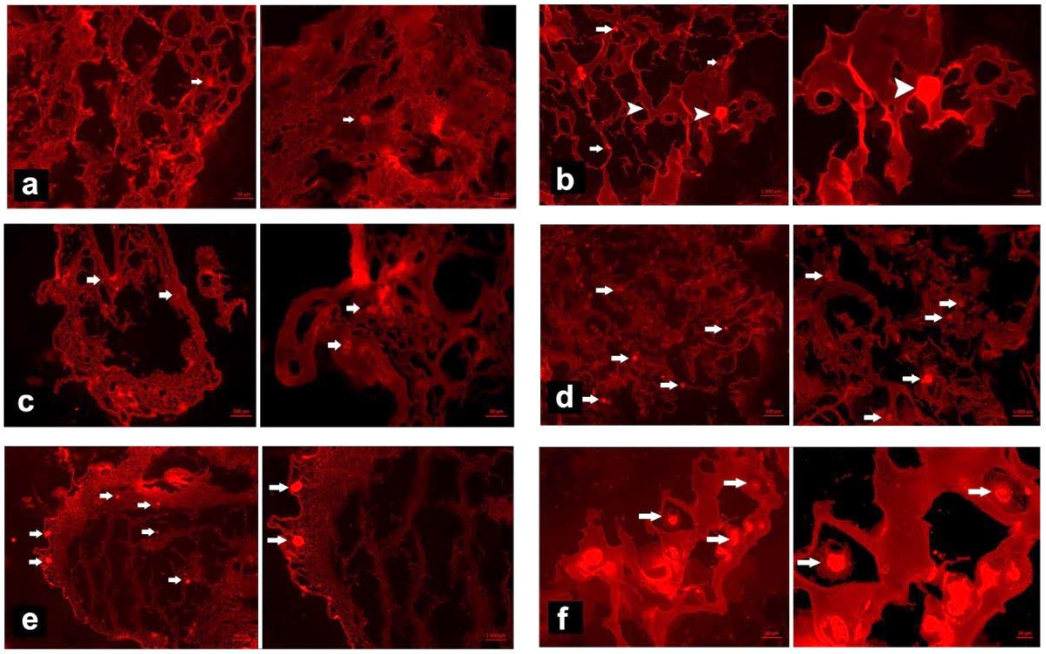

Figure 3.24. Picrosirius Red staining results of primary rabbit chondrocyte-entrapped hydrogels cultured under different conditions**.** (a-b) Fluorescent microscopy images were taken at (a, c, e) 1st and (b, d ,f) 21st days of cell culture. Hydrogels cultivated under static conditions. (c-d) Hydrogels dynamically cultivated under DC-1 mechanical simulation regime**.** (e-f) Hydrogels dynamically cultivated under DC-2 mechanical simulation regime**.** Collagen-expressed chondrocytes are shown by white arrow, cartilage-specific isogenic groups consist of collagen expressing chondrocytes are shown by white arrowhead.

Type II collagen is another major component of the cartilage-specific extracellular matrix and it is used as an important marker of chondrocyte phenotype for cells cultured in vitro [238]. Collagen II immunofluorescence staining was applied to the hydrogel samples on the 1st and 21st days of culture to examine the cartilage development. In the resulting images which are presented in Fig. 3.26, areas of high collagen II deposition appear bright green and DAPI stained cell nuclei appear blue. Immunfloresan staining conforms the findings of total collagen expression detected by Picrosirius Red staining in terms of expression of collagen – II. At the end of 21 days of culture, the intense green color due to collagen II biosynthesis in the cells and surrounding the cells reveals that chondrocyte functionality was preserved and neocartilage formation was observed for all hydrogel groups. The cytoplasm and surroundings of cells, which are spherical in structure, were also stained with an intense bright green color. The results revealed that the amount of collagen II for hydrogels subjected to DC-2 mechanical stimulation regime was higher than the other two groups.

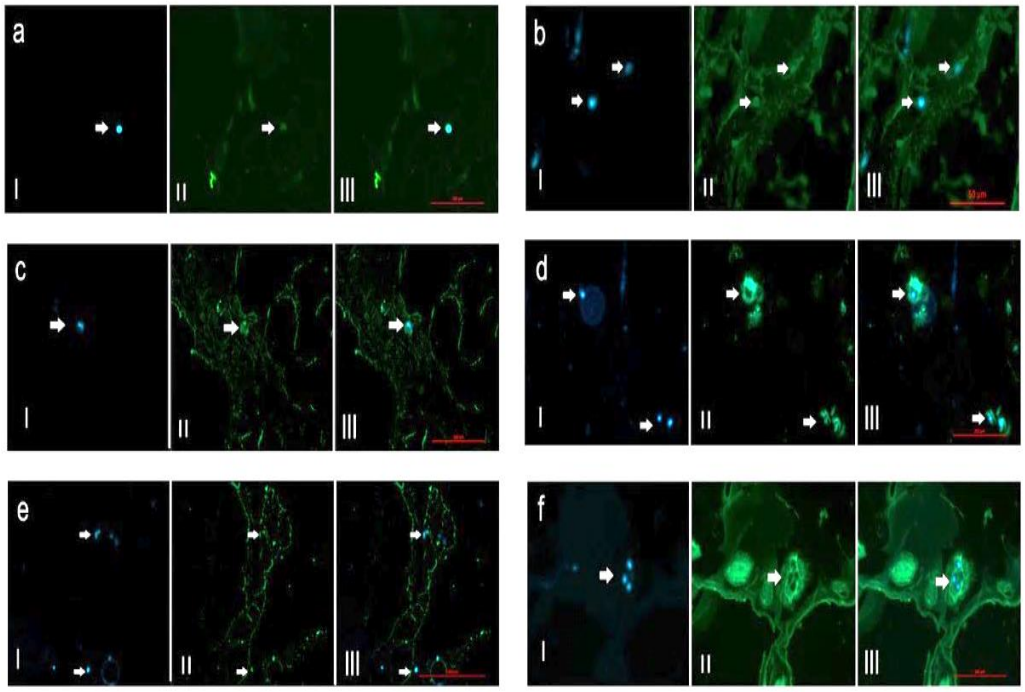

Figure 3.25. Fluorescent microscopy images of immunofluorescence-stained collagen II molecules in primary rabbit chondrocyte-entrapped hydrogels cultured under different conditions. Images were taken at (a, c, e) 1st and (b ,d ,f) 21st days of culture. (a-b) Hydrogels cultivated under static conditions. (c-d) Hydrogels dynamically cultivated under DC-1 mechanical simulation regime**.** (e-f) Hydrogels dynamically cultivated under DC-2 mechanical simulation regime**.** The nuclei were stained blue with DAPI. Collagen II molecules were stained with bright green. Collagen II-expressing cartilage-specific isogenic chondrocyte groups are shown by white arrows.

In native cartilage tissue, chondrocytes are responsible for the synthesis and maintenance of ECM which is mainly composed of proteoglycans and collagen II [106, 239]. Previous studies revealed that dynamic mechanical loading regulate the biosynthetic response of chondrocytes *in vitro*, and *in vivo*, establishing the importance of dynamic mechanical loading on cartilage homeostasis and chondrocyte functionality [107, 240-242]. The histology and immunohistochemical

results of the present study confirmed the previous findings. Although at the end of the 21st day of cell culture there was an increased level of Alcian Blue and collagen type II staining throughout all hydrogel groups compared with day 0, the highest amount cartilage-specific ECM deposition was observed for DC-2 hydrogel group which were subjected to incremental compressive loading regime during dynamic cell culture. Previously, a similar method developed by Finlay et al. used incremental dynamic compressive loading to engineer functional cartilage constructs in vitro but, in the study the magnitude of the load increased in an uncontrolled manner [113]. In the mentioned research, bovine synoviocytes were seeded polyethylene teraphalate fiber scaffolds. During dynamic culture the applied initial strain, which is not fully defined but in the range of 13%-23%, was increased as the construct developed to a maximum strain level (30%) and consequently, the applied load to the constructs was incremented by time. Like our results, histological findings demonstrated a more intense Alcian Blue staining and higher amount of type II collagen immuno-positive staining for the loaded constructs than nonloaded controls. However, in the study, a comparison carried out only between statically and dynamically cultured constructs and no groups of a constant loading throughout the dynamic culture were reported to compare direct effect of the incremental mechanical loading regime to engineer cartilage.

Recently, Kwan et. al investigated effects of incremental tissue compression on cell morphology and deformation in tissue engineered cartilage [114]. In the study, the incremental compressive loading method developed by Finlay *et al* was used on similar synoviocyte/PET scaffold constructs. The applied minimum initial strain, which is in the range of 13%-23%, was increased as the construct developed to a maximum strain level of 28%. In an attempt to explore Finlay's hypothesised mechanism in developing cartilage-like constructs and to address the relationship between applied tissue strain and cellular strain, the researchers developed and used a new confocal-microscopy based methodology to visualize and quantify live cell morphology in tissue constructs which were under static incremental compressive

strain. No significant change was reported in synoviocyte morphology within loaded constructs under the estimated strain experienced by the construct during mechanical loading. However, because of the restricted laser penetration into the cartilage constructs (images were captured from the surface to a depth of approximately 40/50 µm)., this study was limited to the morphometric appearance and distribution of synoviocytes at the periphery of the constructs and it was not possible to visualize synoviocytes in regions near the core. Similar to our findings, in histological investigations, a higher level of collagen type II and s-GAG accumulation was observed within the constructs the loaded constructs compared to unloaded samples.

In parallel to the results obtained from biochemical analyses of hydrogel constructs, the results obtained from histological investigations indicated that starting from a lower-range load at the beginning and application of an incremental dynamic compressive loading regime (from 7 kPa to 21 kPa) enhances chondrocyte functionality and cartilage-specific ECM synthesis while instantaneous application of higher magnitude (21 kPa) of dynamic loading has a similar chondrogenic outcome to statically cultured hydrogels.

3.10 Histology and Immunoflorescent Analysis of In Vivo Studies

The qualitative analysis of physiological structure of the regenerated cartilage was carried out by histological staining investigations. The histological study focus on detailed evaluation of effect of MEGC-based hydrogels for cartilage regeneration in vivo in critical size defects in rabbit knee joints. All animals continued to exhibit normal movements during the 16 week period. Gross signs of inflammation such as swelling, reddening of the joint or infection were not evident upon visual inspection of the joint surface at the time of joint retrieval. The synovial fluid had a normal color.

Crossman's trichrome and Alcian Blue staining results of defect site tissues explanted from New Zealand white rabbits sacrificed 4 months after surgical operations are presented in Fig. 3.27 and Fig. 3.28, respectively. For the empty-defect control group, the defect areas showed very low level of repair, mainly expressed as the slight Crossman's trichrome (Fig. 3.27 a, b), and Alcian Blue staining (Fig 3.28 a, b) and irregular, indistint and very thin layer of fibrous connective tissue formation on the subchondral bone with lack of tissue integration was observed. Very little fibrous connective tissue formation with incomplate or almost complete subchondral bone and no cartilage formation was observed in the healing area (Fig. 3.27 a, b). Alcian blue staining showed that the glycosaminoglycans cantaining was very low because of fibrous connective tissue and no cartilage staining (Fig 3.28 a, b).

To see body response to the hydrogel and to investigate the effect of hydrogels on cartilage repair cell-free hydrogels implanted to the defect site. For this group, subchondral bone tissue healing was almost completed but the majority of the healing area was composed of fibrous connective tissue (Fig. 3.27 c, d). A little fibrous cartilage formation progressing bilaterally from the intact cartilage area to the defect area was also observed. The defect area (Fig 3.27d) was smaller than that of control group (Fig 3.27 b), intact cartilage on both sides of the healing area contained more glycosaminoglycans, while less glycosaminoglycans was seen due to the fibrous connective tissue in the center of the healing area. (Fig 3.28d). This result is very important since it indicates the positive impact of hydrogel on cartilage regeneration even without presence of cells inside it. Previously a similar enhancing effect was reported from in-vivo studies of different hydrogel systems [243-245].

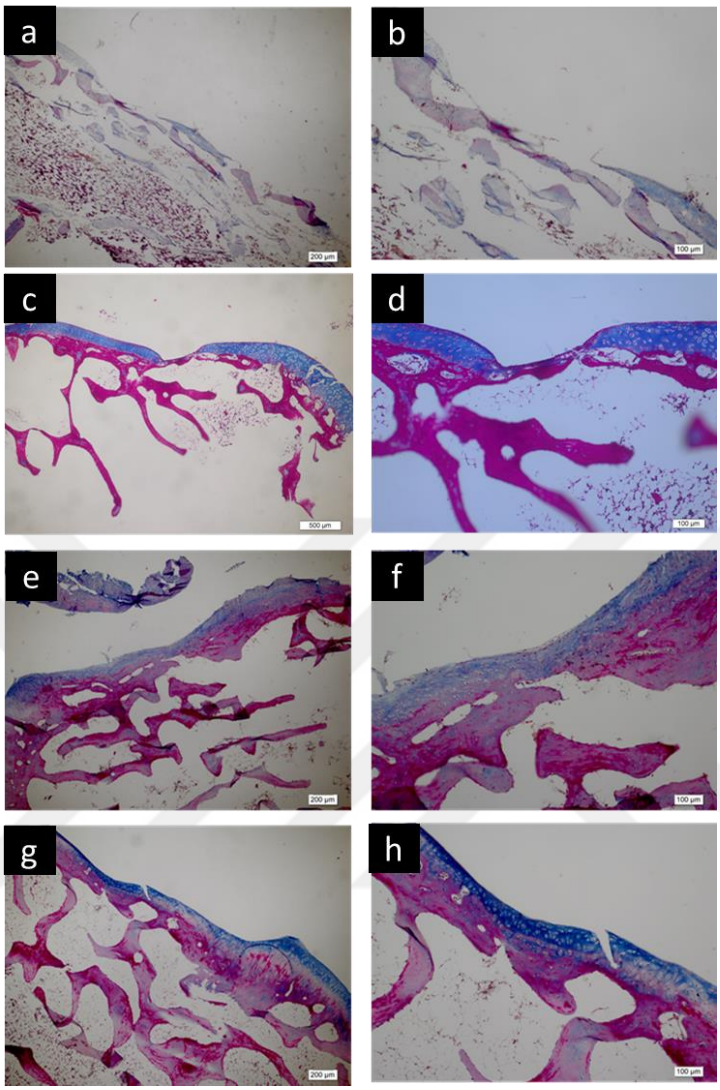

Figure 3.26. Crossman's trichrome staining results of defect site tissue sections obtained from New Zealand white rabbits. **(a)** Control group. **(b)** Cell-free hydrogel group. **(c)** Statically cultured autologous chondrocyte containing hydrogel group **(d)** Dynamically cultured autologous chondrocyte containing hydrogel group.

In animals that received cells along with the hydrogels a mixture of fibrous tissue and cartilage regeneration was observed in the defect area (Fig 3.27 e, f and Fig 3.28 e, f). For statically cultured autologous chondrocyte containing hydrogel group, subchondral bone formation that is a almost completion with little cartilage callus

was observed in the defect site (Fig 3.27 e, f). Bilateral cartilage formation was detected from the intact cartilage tissue towards the defect area, fibrous cartilage consisting of cells of a rounded was seen on both side of healing area, while mixture of fibrous cartilage and connective tissue on the center of healing area (Fig 3.27 e, f). The cartilage tissue was stained more darker blue than fibrous connective tissue in healing zone with alcian blue (Fig 3.28 e, f).

The knees with dynamically cultured autologous chondrocyte containing hydrogel group, the cartilage repair was overall superior than other experimental groups (Fig 3.27 g, h and Fig 3.28 g, h). The defect had high amount of cartilaginous tissue that was well stained with Crossman's Trichrome and Alcian Blue. For this group, subchondral tissue formation was completed (Fig 3.27 g, h). A progressing bilateral cartilage formation was detected from the intact cartilage tissue towards the defect area and neocartilage tissue was almost identical to the surrounding native cartilage tissue with indistinct margins (Fig 3.27 g, h and Fig 3.28 g, h).

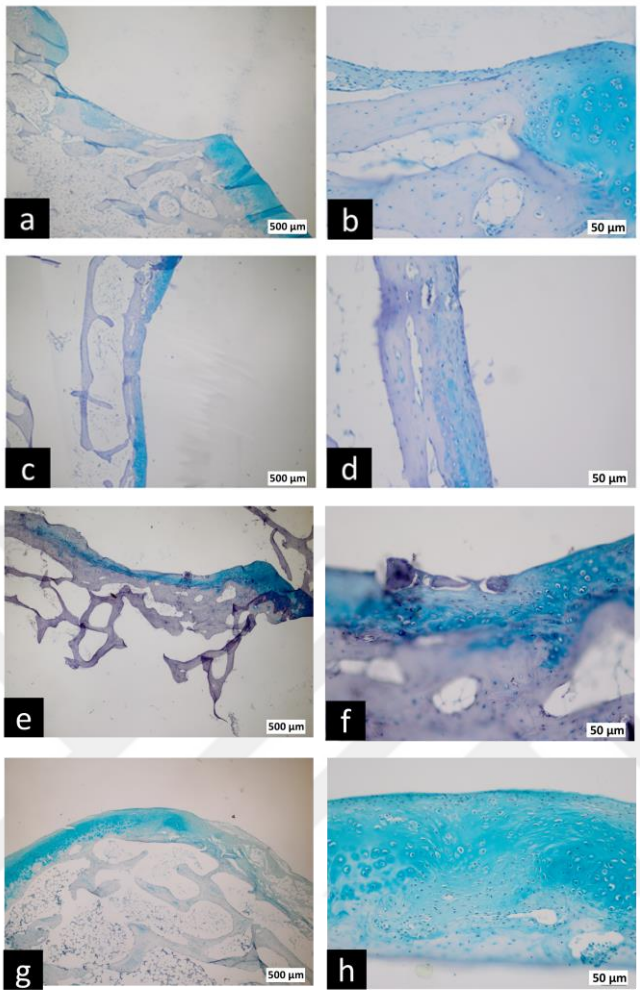

Figure 3.27. Alcian Blue staining results of defect site tissue sections obtained from New Zealand white rabbits. **(a,b)** Control group, **(c,d)** cell-free hydrogel group, **(e,f)** Statically cultured autologous chondrocyte containing hydrogel group, **(g,h)** Dynamically cultured autologous chondrocyte containing hydrogel group.

Immunofluorescent staining was performed on the tissue sections to analyse collagen II contents (Fig. 3.30). Healthy cartilage tissue (Fig. 3.29a) and chondrocyte entrapped hydrogels stained without the inclusion of Collagen type II primary antibodies (Fig. 3.29b) were used as a negative control for secondary antibody and no false-positive labeling was observed. In microscopy images, fluorescent labeled bright green areas indicates collagen II accumulation and cell nuclei were stained

blue with DAPI (Fig 3.29 and Fig. 3.30). Immunohistochemical analysis of untreated defects revealed negligible type II collagen presence in the defect site after 16 weeks postoperatively (Fig. 3.30a). Results revelaed that for hydrogel-implanted groups, cells produced regenerative cartilage matrix which is positive for type II collagen in defect regions (Fig. 3.30 b-d). Especially for autologous chondrocyte entrapped DC-2 hydrogel group (Fig. 3.30d), collagen II synthesis and neocartilage formation was remarkably higher than all other groups.

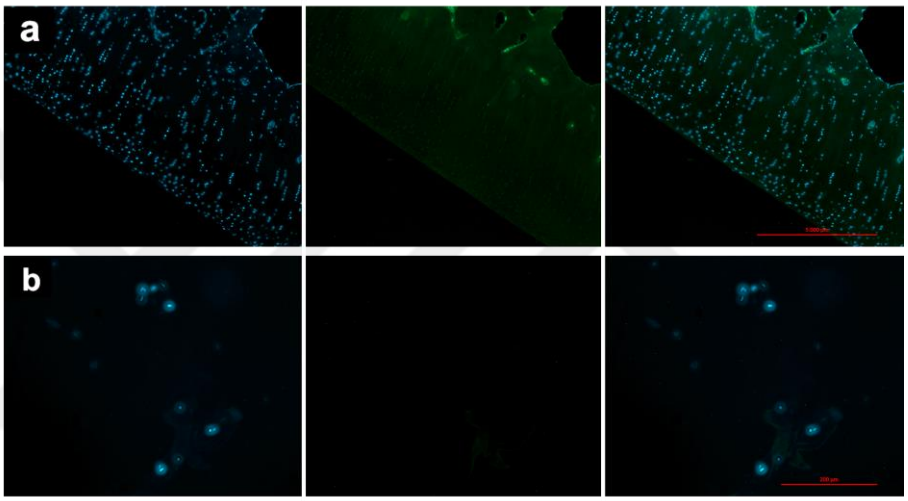

Figure 3.28. Negative controls for immunoflorescent staining. Histological appearance of sections from (a) healthy cartilage tissue explants and (b) chondrocyte entrapped hydrogels stained without the inclusion of Collagen type II primary antibodies.

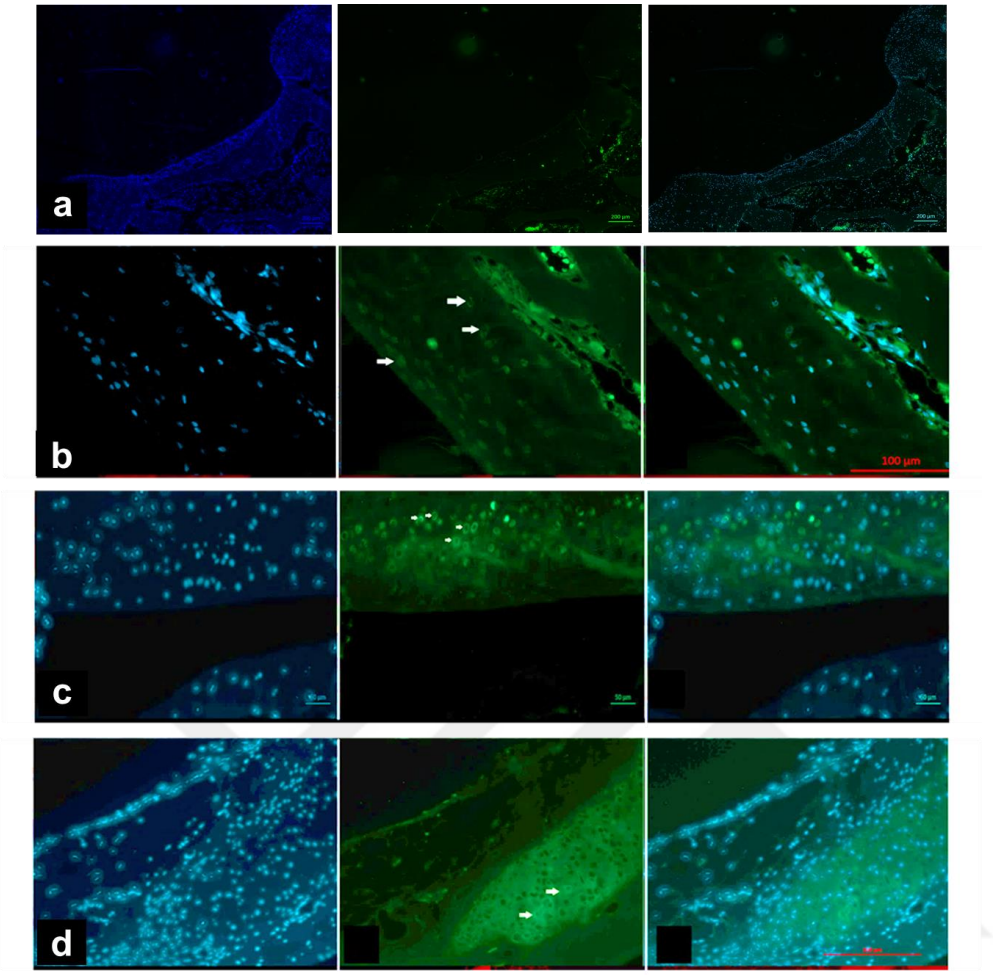

Figure 3.29. Immunofluorescent staining of collagen II on the tissue sections obtained from New Zealand white rabbits. **(a)** Control group, **(b)** Cell-free hydrogel group, **(c)** Statically cultured autologous chondrocyte containing hydrogel group, **(d)** Dynamically cultured autologous chondrocyte containing hydrogel group. Collagen II-expressing chondrocytes are shown by white arrow. **(c1, d1, e1):** The nuclei were stained blue with DAPI. (**b**, **c2, d2, e2)** Collagen II molecules were stained with bright green. (**c3, d3, e3):** merged images.

Together, the present findings indicated that cell-free 1 MeGC-Fib hydrogel system could enhance the neocartilage formation in the in vivo rabbit articular cartilage defect model. Dynamic stimulation of the cell-entrapped hydrogel more significantly supported both tissue ingrowth and chondrogenesis compared to other three groups.

For the dynamically cultured group at week 16, along with the higher amount of cartilage callus and progressing cartilage formation, a more intense cartilage specific ECM formation was detected in the defect site. The obtained results indicating that DC-2 dynamic culture regime can help engineered cartilage maintain better chondrogenic phenotype during cartilage repair in vivo. Based on the present findings, it is possible that greater cartilage production will be achieved in longer implantation periods.

CHAPTER 4

CONCLUSION

In this thesis we developed a new photopolymerizable MeGC-Fib hydrogel that gels under visible blue light irradiation with riboflavin as a photoinitiator. Introduction of fibrinogen to hydrogel structure decreased the swelling, led to increase in stability and improved the mechanical properties of MeGC-based hydrogels. The properties of the MeGC-based hydrogels, such as swellability, stiffness, and pore size, can be readily adjusted by changing Fib content in MeGC prepolymer solution. The photopolymerized hydrogels were shown to be cytocompatible. Incorporation of 1% (w/v) Fib in the hydrogel network improved cell adhesion and significantly increased cell proliferation, sGAG, and total collagen and collagen II synthesis and cartilagenous ECM deposition within hydrogels in vitro. In order to investigate the effect of incremental dynamic compressive loading on the development of cartilage tissue constructs, rabbit chondrocytes were entrapped in 1 MeGC-Fib based hydrogels and cultivated in a custom-built mechanobioreactor. Investigations about the effect of mechanical stimulation on cell viability revealed that, not just dynamic cultivation but applied mechanical stimulation regime is also crucially important on viability of cells. At the end of 21 days of cultivation, incremental cyclic compressive stimulation (DC-2) regime increased chondrocyte viability almost five-folds while chondrocyte proliferation was hampered by constant 21 kPa cyclic compressive loading throughout cultivation (DC-1). Compared to free swelling and DC-1 group, hydrogel-entrapped chondrocytes cultivated under incremental dynamic compressive loading regime showed a remarkable increase in DNA, s-GAG, total collagen and collagen type II content, indicating the stimulatory effects of incremental compressive loading regime on neocartilage formation. In vivo investigations performed by implantation of the hydrogels to critically sized rabbit hindleg articular chondral defects demonstrated that both MeGC-Fib hydrogels and

DC-2 regime enhanced neo-cartilogenesis and, accelerated healing of the cartilage defect with a higher s-GAG, total collagen and collagen-II content compared to other groups. In conclusion, these findings reveals the high potential of the developed MeGC-Fib hydrogels and applied incremental dynamic compressive loading (DC-2) regime to promote cartilage regeneration for the treatment of cartilage damage.

REFERENCES

[1] E.A. Makris, A.H. Gomoll, K.N. Malizos, J.C. Hu, K.A. Athanasiou, Repair and tissue engineering techniques for articular cartilage, Nature reviews. Rheumatology 11(1) (2015) 21-34.

[2] Z. Zhao, C. Fan, F. Chen, Y. Sun, Y. Xia, A. Ji, D.A. Wang, Progress in articular cartilage tissue engineering: a review on therapeutic cells and macromolecular scaffolds, Macromolecular bioscience 20(2) (2020) 1900278.

[3] K.A. Athanasiou, E.M. Darling, J.C. Hu, G.D. DuRaine, A.H. Reddi, Articular Cartilage, Taylor & Francis2013.

[4] M. Sittinger, D.W. Hutmacher, M.V. Risbud, Current strategies for cell delivery in cartilage and bone regeneration, Current opinion in biotechnology 15(5) (2004) 411-8.

[5] M. Wasyłeczko, W. Sikorska, A. Chwojnowski, Review of synthetic and hybrid scaffolds in cartilage tissue engineering, Membranes 10(11) (2020) 348.

[6] R. Cancedda, B. Dozin, P. Giannoni, R. Quarto, Tissue engineering and cell therapy of cartilage and bone, Matrix biology : journal of the International Society for Matrix Biology 22(1) (2003) 81-91.

[7] D. Martínez-Moreno, G. Jiménez, P. Gálvez-Martín, G. Rus, J. Marchal, Cartilage biomechanics: A key factor for osteoarthritis regenerative medicine, Biochimica et Biophysica Acta (BBA)-Molecular Basis of Disease 1865(6) (2019) 1067-1075.

[8] R.M. Schulz, A. Bader, Cartilage tissue engineering and bioreactor systems for the cultivation and stimulation of chondrocytes, European biophysics journal : EBJ 36(4-5) (2007) 539-68.

[9] L.A. McMahon, F.J. O'Brien, P.J. Prendergast, Biomechanics and mechanobiology in osteochondral tissues, Regen Med 3(5) (2008) 743-59.

[10] C.A. Heath, S.R. Magari, Mini-review: Mechanical factors affecting cartilage regeneration in vitro, Biotechnology and bioengineering 50(4) (1996) 430-7.

[11] J.B. Choi, I. Youn, L. Cao, H.A. Leddy, C.L. Gilchrist, L.A. Setton, F. Guilak, Zonal changes in the three-dimensional morphology of the chondron under compression: the relationship among cellular, pericellular, and extracellular deformation in articular cartilage, J Biomech 40(12) (2007) 2596-603.
[12] M.M. Espanha, [Articular cartilage: structure and histochemical composition], Acta reumatologica portuguesa 35(5) (2010) 424-33.
[13] J. Eschweiler, N. Horn, B. Rath, M. Betsch, A. Baroncini, M. Tingart, F. Migliorini, The Biomechanics of Cartilage-An Overview, Life (Basel) 11(4) (2021) 302.
[14] M. Wong, D.R. Carter, Articular cartilage functional histomorphology and mechanobiology: a research perspective, Bone 33(1) (2003) 1-13.
[15] M. Kazemi, J.L. Williams, Depth and strain rate-dependent mechanical response of chondrocytes in reserve zone cartilage subjected to compressive loading, Biomechanics and Modeling in Mechanobiology (2021) 1-17.
[16] J. Eschweiler, N. Horn, B. Rath, M. Betsch, A. Baroncini, M. Tingart, F. Migliorini, The Biomechanics of Cartilage—An Overview, Life 11(4) (2021) 302.
[17] C. Herberhold, S. Faber, T. Stammberger, M. Steinlechner, R. Putz, K.H. Englmeier, M. Reiser, F. Eckstein, In situ measurement of articular cartilage deformation in intact femoropatellar joints under static loading, Journal of biomechanics 32(12) (1999) 1287-95.
[18] W.A. Hodge, R.S. Fijan, K.L. Carlson, R.G. Burgess, W.H. Harris, R.W. Mann, Contact pressures in the human hip joint measured in vivo, Proceedings of the National Academy of Sciences of the United States of America 83(9) (1986) 2879-83.
[19] N.Y. Afoke, P.D. Byers, W.C. Hutton, Contact pressures in the human hip joint, The Journal of bone and joint surgery. British volume 69(4) (1987) 536-41.
[20] V.C. Mow, C.C. Wang, Some bioengineering considerations for tissue engineering of articular cartilage, Clinical orthopaedics and related research (367 Suppl) (1999) S204-23.

[21] R. von Eisenhart, C. Adam, M. Steinlechner, M. Müller-Gerbl, F. Eckstein, Quantitative determination of joint incongruity and pressure distribution during simulated gait and cartilage thickness in the human hip joint, Journal of orthopaedic research : official publication of the Orthopaedic Research Society 17(4) (1999) 532-9.

[22] C. Chen, D.T. Tambe, L. Deng, L. Yang, Biomechanical properties and mechanobiology of the articular chondrocyte, American journal of physiology. Cell physiology 305(12) (2013) C1202-8.

[23] N.D. Leipzig, K.A. Athanasiou, Static Compression of Single Chondrocytes Catabolically Modifies Single-Cell Gene Expression, Biophysical Journal 94(6) (2008) 2412-2422.

[24] K. Zhang, L. Wang, Z. Liu, B. Geng, Y. Teng, X. Liu, Q. Yi, D. Yu, X. Chen, D. Zhao, Mechanosensory and mechanotransductive processes mediated by ion channels in articular chondrocytes: Potential therapeutic targets for osteoarthritis, Channels 15(1) (2021) 339-359.

[25] Z. Zhao, Y. Li, M. Wang, S. Zhao, Z. Zhao, J. Fang, Mechanotransduction pathways in the regulation of cartilage chondrocyte homoeostasis, Journal of cellular and molecular medicine 24(10) (2020) 5408-5419.

[26] G. Zhen, Q. Guo, Y. Li, C. Wu, S. Zhu, R. Wang, X.E. Guo, B.C. Kim, J. Huang, Y. Hu, Mechanical stress determines the configuration of TGFβ activation in articular cartilage, Nature communications 12(1) (2021) 1-16.

[27] T. Seeger-Nukpezah, E.A. Golemis, The extracellular matrix and ciliary signaling, Current opinion in cell biology 24(5) (2012) 652-661.

[28] Y.Y. Shao, L. Wang, J.F. Welter, R.T. Ballock, Primary cilia modulate Ihh signal transduction in response to hydrostatic loading of growth plate chondrocytes, Bone 50(1) (2012) 79-84.

[29] M. Hevesi, G. Jacob, K. Shimomura, W. Ando, N. Nakamura, A.J. Krych, Current hip cartilage regeneration/repair modalities: a scoping review of biologics and surgery, International Orthopaedics 45(2) (2021) 319-333.

[30] Y.-R. Chen, X. Yan, F.-Z. Yuan, J. Ye, B.-B. Xu, Z.-X. Zhou, Z.-M. Mao, J. Guan, Y.-F. Song, Z.-W. Sun, The use of peripheral blood-derived stem cells for cartilage repair and regeneration in vivo: a review, Frontiers in pharmacology 11 (2020) 404.
[31] S. Jiang, W. Guo, G. Tian, X. Luo, L. Peng, S. Liu, X. Sui, Q. Guo, X. Li, Clinical application status of articular cartilage regeneration techniques: tissue-engineered cartilage brings new hope, Stem Cells International 2020 (2020).
[32] W. Wei, Y. Ma, X. Yao, W. Zhou, X. Wang, C. Li, J. Lin, Q. He, S. Leptihn, H. Ouyang, Advanced hydrogels for the repair of cartilage defects and regeneration, Bioactive Materials 6(4) (2021) 998-1011.
[33] F. Migliorini, A. Berton, G. Salvatore, V. Candela, W. Khan, U.G. Longo, V. Denaro, Autologous chondrocyte implantation and mesenchymal stem cells for the treatments of chondral defects of the knee-a systematic review, Current stem cell research & therapy 15(6) (2020) 547-556.
[34] R.L. Davies, N.J. Kuiper, Regenerative medicine: a review of the evolution of autologous chondrocyte implantation (ACI) therapy, Bioengineering 6(1) (2019) 22.
[35] H.B. Schuette, M.J. Kraeutler, J.B. Schrock, E.C. McCarty, Primary autologous chondrocyte implantation of the knee versus autologous chondrocyte implantation after failed marrow stimulation: a systematic review, The American Journal of Sports Medicine (2020) 0363546520968284.
[36] P. Behrens, T. Bitter, B. Kurz, M. Russlies, Matrix-associated autologous chondrocyte transplantation/implantation (MACT/MACI)--5-year follow-up, The Knee 13(3) (2006) 194-202.
[37] V. Rai, M.F. Dilisio, N.E. Dietz, D.K. Agrawal, Recent strategies in cartilage repair: a systemic review of the scaffold development and tissue engineering, Journal of Biomedical Materials Research Part A 105(8) (2017) 2343-2354.
[38] M. Sahranavard, A. Zamanian, F. Ghorbani, M.H. Shahrezaee, A critical review on three dimensional-printed chitosan hydrogels for development of tissue engineering, Bioprinting 17 (2020) e00063.

[39] J. Liu, B. Yang, M. Li, J. Li, Y. Wan, Enhanced dual network hydrogels consisting of thiolated chitosan and silk fibroin for cartilage tissue engineering, Carbohydrate polymers 227 (2020) 115335.
[40] W. Zhao, X. Jin, Y. Cong, Y. Liu, J. Fu, Degradable natural polymer hydrogels for articular cartilage tissue engineering, Journal of Chemical Technology & Biotechnology 88(3) (2013) 327-339.
[41] M.J. Moura, H. Faneca, M.P. Lima, M.H. Gil, M.M. Figueiredo, In situ forming chitosan hydrogels prepared via ionic/covalent co-cross-linking, Biomacromolecules 12(9) (2011) 3275-3284.
[42] J.K. Suh, H.W. Matthew, Application of chitosan-based polysaccharide biomaterials in cartilage tissue engineering: a review, Biomaterials 21(24) (2000) 2589-98.
[43] L. Lin, Y. Wang, L. Wang, J. Pan, Y. Xu, S. Li, D. Huang, J. Chen, Z. Liang, P. Yin, Injectable microfluidic hydrogel microspheres based on chitosan and poly (ethylene glycol) diacrylate (PEGDA) as chondrocyte carriers, RSC Advances 10(65) (2020) 39662-39672.
[44] M. Risbud, J. Ringe, R. Bhonde, M. Sittinger, In Vitro Expression of Cartilage-Specific Markers by Chondrocytes on a Biocompatible Hydrogel: Implications for Engineering Cartilage Tissue, Cell Transplantation 10(8) (2001) 755-763.
[45] Y.L. Cui, A.D. Qi, W.G. Liu, X.H. Wang, H. Wang, D.M. Ma, K.D. Yao, Biomimetic surface modification of poly(l-lactic acid) with chitosan and its effects on articular chondrocytes in vitro, Biomaterials 24(21) (2003) 3859-3868.
[46] I.-C. Lin, T.-J. Wang, C.-L. Wu, D.-H. Lu, Y.-R. Chen, K.-C. Yang, Chitosan-cartilage extracellular matrix hybrid scaffold induces chondrogenic differentiation to adipose-derived stem cells, Regenerative Therapy 14 (2020) 238-244.
[47] J.E. Lee, K.E. Kim, I.C. Kwon, H.J. Ahn, S.-H. Lee, H. Cho, H.J. Kim, S.C. Seong, M.C. Lee, Effects of the controlled-released TGF-β1 from chitosan microspheres on chondrocytes cultured in a collagen/chitosan/glycosaminoglycan scaffold, Biomaterials 25(18) (2004) 4163-4173.

[48] S. Lee, J.H. Choi, A. Park, M. Rim, J. Youn, W. Lee, J.E. Song, G. Khang, Advanced gellan gum-based glycol chitosan hydrogel for cartilage tissue engineering biomaterial, International journal of biological macromolecules 158 (2020) 452-460.
[49] S.C. Beck, T. Jiang, L.S. Nair, C.T. Laurencin, 2 - Chitosan for bone and cartilage regenerative engineering A2 - Jennings, J. Amber, in: J.D. Bumgardner (Ed.), Chitosan Based Biomaterials Volume 2, Woodhead Publishing2017, pp. 33-72.
[50] C.A. Custodio, C.M. Alves, R.L. Reis, J.F. Mano, Immobilization of fibronectin in chitosan substrates improves cell adhesion and proliferation, Journal of tissue engineering and regenerative medicine 4(4) (2010) 316-23.
[51] C.R. Correia, L.S. Moreira-Teixeira, L. Moroni, R.L. Reis, C.A. van Blitterswijk, M. Karperien, J.F. Mano, Chitosan scaffolds containing hyaluronic acid for cartilage tissue engineering, Tissue engineering. Part C, Methods 17(7) (2011) 717-30.
[52] W. Xia, W. Liu, L. Cui, Y. Liu, W. Zhong, D. Liu, J. Wu, K. Chua, Y. Cao, Tissue engineering of cartilage with the use of chitosan-gelatin complex scaffolds, Journal of biomedical materials research. Part B, Applied biomaterials 71(2) (2004) 373-80.
[53] N. Iwasaki, S.T. Yamane, T. Majima, Y. Kasahara, A. Minami, K. Harada, S. Nonaka, N. Maekawa, H. Tamura, S. Tokura, M. Shiono, K. Monde, S. Nishimura, Feasibility of polysaccharide hybrid materials for scaffolds in cartilage tissue engineering: evaluation of chondrocyte adhesion to polyion complex fibers prepared from alginate and chitosan, Biomacromolecules 5(3) (2004) 828-33.
[54] T. Coviello, P. Matricardi, C. Marianecci, F. Alhaique, Polysaccharide hydrogels for modified release formulations, Journal of Controlled Release 119(1) (2007) 5-24.
[55] E. Marsich, M. Borgogna, I. Donati, P. Mozetic, B.L. Strand, S.G. Salvador, F. Vittur, S. Paoletti, Alginate/lactose-modified chitosan hydrogels: A bioactive

biomaterial for chondrocyte encapsulation, Journal of Biomedical Materials Research Part A 84A(2) (2008) 364-376.
[56] I. Donati, S. Stredanska, G. Silvestrini, A. Vetere, P. Marcon, E. Marsich, P. Mozetic, A. Gamini, S. Paoletti, F. Vittur, The aggregation of pig articular chondrocyte and synthesis of extracellular matrix by a lactose-modified chitosan, Biomaterials 26(9) (2005) 987-98.
[57] A. Rogina, M. Pušić, L. Štefan, A. Ivković, I. Urlić, M. Ivanković, H. Ivanković, Characterization of Chitosan-Based Scaffolds Seeded with Sheep Nasal Chondrocytes for Cartilage Tissue Engineering, Annals of biomedical engineering 1-15.
[58] N. Sahai, M. Gogoi, R.P. Tewari, 3D printed Chitosan Composite Scaffold for Chondrocytes differentiation, Current Medical Imaging (2020).
[59] T. Corrales, F. Catalina, C. Peinado, N.S. Allen, Free radical macrophotoinitiators: an overview on recent advances, Journal of Photochemistry and Photobiology A: Chemistry 159(2) (2003) 103-114.
[60] W. Tomal, J. Ortyl, Water-soluble photoinitiators in biomedical applications, Polymers 12(5) (2020) 1073.
[61] J. Shao, Y. Huang, Q. Fan, Visible light initiating systems for photopolymerization: status, development and challenges, Polymer Chemistry 5(14) (2014) 4195-4210.
[62] C. Felipe-Mendes, L. Ruiz-Rubio, J.L. Vilas-Vilela, Biomaterials obtained by photopolymerization: from UV to two photon, Emergent Materials (2020) 1-16.
[63] D. Zhou, Y. Ito, Visible light-curable polymers for biomedical applications, Science China Chemistry 57(4) (2014) 510-521.
[64] G.D. Nicodemus, S.J. Bryant, Cell encapsulation in biodegradable hydrogels for tissue engineering applications, Tissue engineering. Part B, Reviews 14(2) (2008) 149-65.
[65] M.M. Abdul-Monem, E.A. Kamoun, D.M. Ahmed, E.M. El-Fakharany, F.H. Al-Abbassy, H.M. Aly, Light-cured hyaluronic acid composite hydrogels using

riboflavin as a photoinitiator for bone regeneration applications, Journal of Taibah University Medical Sciences (2021).
[66] S. Piluso, D.F. Gomez, I. Dokter, L.M. Texeira, Y. Li, J. Leijten, R. Van Weeren, T. Vermonden, M. Karperien, J. Malda, Rapid and cytocompatible cell-laden silk hydrogel formation via riboflavin-mediated crosslinking, Journal of Materials Chemistry B 8(41) (2020) 9566-9575.
[67] R.H. Koh, Y. Jin, B.-J. Kang, N.S. Hwang, Chondrogenically primed tonsil-derived mesenchymal stem cells encapsulated in riboflavin-induced photocrosslinking collagen-hyaluronic acid hydrogel for meniscus tissue repairs, Acta Biomaterialia 53 (2017) 318-328.
[68] H.J. Lee, G.M. Fernandes-Cunha, D. Myung, In situ-forming hyaluronic acid hydrogel through visible light-induced thiol-ene reaction, Reactive & functional polymers 131 (2018) 29-35.
[69] H. Lee, D. Shin, S. Shin, J. Hyun, Effect of gelatin on dimensional stability of silk fibroin hydrogel structures fabricated by digital light processing 3D printing, Journal of Industrial and Engineering Chemistry 89 (2020) 119-127.
[70] M. Monfared, D. Mawad, J. Rnjak-Kovacina, M.H. Stenzel, 3D bioprinting of dual-crosslinked nanocellulose hydrogels for tissue engineering applications, Journal of Materials Chemistry B (2021).
[71] L.M. Yu, K. Kazazian, M.S. Shoichet, Peptide surface modification of methacrylamide chitosan for neural tissue engineering applications, Journal of biomedical materials research. Part A 82(1) (2007) 243-55.
[72] J. Hu, Y. Hou, H. Park, B. Choi, S. Hou, A. Chung, M. Lee, Visible light crosslinkable chitosan hydrogels for tissue engineering, Acta biomaterialia 8(5) (2012) 1730-8.
[73] B. Choi, S. Kim, B. Lin, B.M. Wu, M. Lee, Cartilaginous Extracellular Matrix-Modified Chitosan Hydrogels for Cartilage Tissue Engineering, ACS Applied Materials & Interfaces 6(22) (2014) 20110-20121.
[74] B. Choi, S. Kim, B. Lin, K. Li, O. Bezouglaia, J. Kim, D. Evseenko, T. Aghaloo, M. Lee, Visible-light-initiated hydrogels preserving cartilage extracellular signaling

for inducing chondrogenesis of mesenchymal stem cells, Acta Biomaterialia 12 (2015) 30-41.
[75] J.W.S. Hayami, S.D. Waldman, B.G. Amsden, Chondrocyte Generation of Cartilage-Like Tissue Following Photoencapsulation in Methacrylated Polysaccharide Solution Blends, Macromolecular Bioscience 16(7) (2016) 1083-1095.
[76] P.M. Chichiricco, R. Riva, J.-M. Thomassin, J. Lesoeur, X. Struillou, C. Le Visage, C. Jérôme, P. Weiss, In situ photochemical crosslinking of hydrogel membrane for Guided Tissue Regeneration, Dental Materials 34(12) (2018) 1769-1782.
[77] Y. Zhou, K. Liang, S. Zhao, C. Zhang, J. Li, H. Yang, X. Liu, X. Yin, D. Chen, W. Xu, P. Xiao, Photopolymerized maleilated chitosan/methacrylated silk fibroin micro/nanocomposite hydrogels as potential scaffolds for cartilage tissue engineering, International Journal of Biological Macromolecules 108 (2018) 383-390.
[78] J. Shao, Z. Ding, L. Li, Y. Chen, J. Zhu, Q. Qian, Improved accumulation of TGF-β by photopolymerized chitosan/silk protein bio-hydrogel matrix to improve differentiations of mesenchymal stem cells in articular cartilage tissue regeneration, Journal of Photochemistry and Photobiology B: Biology 203 (2020) 111744.
[79] X. He, X. Liu, J. Yang, H. Du, N. Chai, Z. Sha, M. Geng, X. Zhou, C. He, Tannic acid-reinforced methacrylated chitosan/methacrylated silk fibroin hydrogels with multifunctionality for accelerating wound healing, Carbohydrate Polymers 247 (2020) 116689.
[80] B.A. De Melo, Y.A. Jodat, E.M. Cruz, J.C. Benincasa, S.R. Shin, M.A. Porcionatto, Strategies to use fibrinogen as bioink for 3D bioprinting fibrin-based soft and hard tissues, Acta Biomaterialia (2020).
[81] S. Bose, C. Koski, A.A. Vu, Additive manufacturing of natural biopolymers and composites for bone tissue engineering, Materials Horizons 7(8) (2020) 2011-2027.

[82] M.W. Mosesson, K.R. Siebenlist, D.A. Meh, The structure and biological features of fibrinogen and fibrin, Annals of the New York Academy of Sciences 936 (2001) 11-30.
[83] S.A. Sell, P.S. Wolfe, K. Garg, J.M. McCool, I.A. Rodriguez, G.L. Bowlin, The Use of Natural Polymers in Tissue Engineering: A Focus on Electrospun Extracellular Matrix Analogues, Polymers 2(4) (2010) 522.
[84] B.J. Rybarczyk, S.O. Lawrence, P.J. Simpson-Haidaris, Matrix-fibrinogen enhances wound closure by increasing both cell proliferation and migration, Blood 102(12) (2003) 4035-43.
[85] A. Sahni, T. Odrljin, C.W. Francis, Binding of basic fibroblast growth factor to fibrinogen and fibrin, The Journal of biological chemistry 273(13) (1998) 7554-9.
[86] C.L. Wu, S.S. Lee, C.H. Tsai, K.H. Lu, J.H. Zhao, Y.C. Chang, Platelet-rich fibrin increases cell attachment, proliferation and collagen-related protein expression of human osteoblasts, Australian Dental Journal 57(2) (2012) 207-212.
[87] M. Naito, C. Funaki, T. Hayashi, K. Yamada, K. Asai, N. Yoshimine, F. Kuzuya, Substrate-bound fibrinogen, fibrin and other cell attachment-promoting proteins as a scaffold for cultured vascular smooth muscle cells, Atherosclerosis 96(2) (1992) 227-234.
[88] J. Gailit, C. Clarke, D. Newman, M.G. Tonnesen, M.W. Mosesson, R.A. Clark, Human fibroblasts bind directly to fibrinogen at RGD sites through integrin alpha(v)beta3, Experimental cell research 232(1) (1997) 118-26.
[89] A. Sahni, C.W. Francis, Vascular endothelial growth factor binds to fibrinogen and fibrin and stimulates endothelial cell proliferation, Blood 96(12) (2000) 3772-8.
[90] I. Woods, A. Black, E.J. Molloy, S. Jockenhoevel, T.C. Flanagan, Fabrication of blood-derived elastogenic vascular grafts using electrospun fibrinogen and polycaprolactone composite scaffolds for paediatric applications, Journal of Tissue Engineering and Regenerative Medicine 14(9) (2020) 1281-1295.
[91] S. Li, L. Su, X. Li, L. Yang, M. Yang, H. Zong, Q. Zong, J. Tang, H. He, Reconstruction of abdominal wall with scaffolds of electrospun poly (l-lactide-co

caprolactone) and porcine fibrinogen: An experimental study in the canine, Materials Science and Engineering: C 110 (2020) 110644.
[92] T. Wu, X. Mo, Y. Xia, Moving electrospun nanofibers and bioprinted scaffolds toward translational applications, Advanced healthcare materials 9(6) (2020) 1901761.
[93] M. Wehrle, F. Koch, S. Zimmermann, P. Koltay, R. Zengerle, G.B. Stark, S. Strassburg, G. Finkenzeller, Examination of hydrogels and mesenchymal stem cell sources for bioprinting of artificial osteogenic tissues, Cellular and Molecular Bioengineering 12(6) (2019) 583-597.
[94] L. Almany, D. Seliktar, Biosynthetic hydrogel scaffolds made from fibrinogen and polyethylene glycol for 3D cell cultures, Biomaterials 26(15) (2005) 2467-2477.
[95] S.A. DeLong, J.J. Moon, J.L. West, Covalently immobilized gradients of bFGF on hydrogel scaffolds for directed cell migration, Biomaterials 26(16) (2005) 3227-34.
[96] J. Pei, H. Hall, N.D. Spencer, The role of plasma proteins in cell adhesion to PEG surface-density-gradient-modified titanium oxide, Biomaterials 32(34) (2011) 8968-78.
[97] B. Mollon, R. Kandel, J. Chahal, J. Theodoropoulos, The clinical status of cartilage tissue regeneration in humans, Osteoarthritis and Cartilage 21(12) (2013) 1824-1833.
[98] Q. Chen, D. Zhang, W. Zhang, H. Zhang, J. Zou, M. Chen, J. Li, Y. Yuan, R. Liu, Dual mechanism β-amino acid polymers promoting cell adhesion, Nature Communications 12(1) (2021) 562.
[99] C. Loebel, A. Ayoub, J.H. Galarraga, O. Kossover, H. Simaan-Yameen, D. Seliktar, J.A. Burdick, Tailoring supramolecular guest–host hydrogel viscoelasticity with covalent fibrinogen double networks, Journal of Materials Chemistry B 7(10) (2019) 1753-1760.
[100] S.G. Santos, M. Lamghari, C.R. Almeida, M.I. Oliveira, N. Neves, A.C. Ribeiro, J.N. Barbosa, R. Barros, J. Maciel, M.C.L. Martins, R.M. Gonçalves, M.A. Barbosa, Adsorbed fibrinogen leads to improved bone regeneration and correlates

with differences in the systemic immune response, Acta biomaterialia 9(7) (2013) 7209-7217.
[101] E. Peled, J. Boss, J. Bejar, C. Zinman, D. Seliktar, A novel poly(ethylene glycol)-fibrinogen hydrogel for tibial segmental defect repair in a rat model, Journal of biomedical materials research. Part A 80(4) (2007) 874-84.
[102] L. Kock, C.C. van Donkelaar, K. Ito, Tissue engineering of functional articular cartilage: the current status, Cell and Tissue Research 347(3) (2012) 613-627.
[103] T.P. Appelman, J. Mizrahi, J.H. Elisseeff, D. Seliktar, The influence of biological motifs and dynamic mechanical stimulation in hydrogel scaffold systems on the phenotype of chondrocytes, Biomaterials 32(6) (2011) 1508-16.
[104] I. Villanueva, C.A. Weigel, S.J. Bryant, Cell-matrix interactions and dynamic mechanical loading influence chondrocyte gene expression and bioactivity in PEG-RGD hydrogels, Acta Biomater 5(8) (2009) 2832-46.
[105] T. Mesallati, C.T. Buckley, T. Nagel, D.J. Kelly, Scaffold architecture determines chondrocyte response to externally applied dynamic compression, Biomech Model Mechanobiol 12(5) (2013) 889-99.
[106] L. Fu, P. Li, H. Li, C. Gao, Z. Yang, T. Zhao, W. Chen, Z. Liao, Y. Peng, F. Cao, The application of bioreactors for cartilage tissue engineering: advances, limitations, and future perspectives, Stem Cells International 2021 (2021).
[107] R.L. Mauck, M.A. Soltz, C.C.B. Wang, D.D. Wong, P.-H.G. Chao, W.B. Valhmu, C.T. Hung, G.A. Ateshian, Functional Tissue Engineering of Articular Cartilage Through Dynamic Loading of Chondrocyte-Seeded Agarose Gels, Journal of Biomechanical Engineering 122(3) (2000) 252-260.
[108] J.D. Kisiday, M. Jin, M.A. DiMicco, B. Kurz, A.J. Grodzinsky, Effects of dynamic compressive loading on chondrocyte biosynthesis in self-assembling peptide scaffolds, Journal of biomechanics 37(5) (2004) 595-604.
[109] N. Sawatjui, T. Limpaiboon, K. Schrobback, T. Klein, Biomimetic scaffolds and dynamic compression enhance the properties of chondrocyte- and MSC-based tissue-engineered cartilage, Journal of Tissue Engineering and Regenerative Medicine 12(5) (2018) 1220-1229.

[110] P.P. Chong, P. Panjavarnam, W.N.H.W. Ahmad, C.K. Chan, A.A. Abbas, A.M. Merican, B. Pingguan-Murphy, T. Kamarul, Mechanical compression controls the biosynthesis of human osteoarthritic chondrocytes in vitro, Clinical Biomechanics 79 (2020) 105178.
[111] M. Xie, M. Fritch, Y. He, H. Fu, Y. Hong, H. Lin, Dynamic loading enhances chondrogenesis of human chondrocytes within a biodegradable resilient hydrogel, Biomaterials Science 9(14) (2021) 5011-5024.
[112] M. Khoshgoftar, W. Wilson, K. Ito, C.C. van Donkelaar, The effects of matrix inhomogeneities on the cellular mechanical environment in tissue-engineered cartilage: an in silico investigation, Tissue engineering. Part C, Methods 20(2) (2014) 104-15.
[113] S. Finlay, B.B. Seedhom, D.O. Carey, A.J. Bulpitt, D.E. Treanor, J. Kirkham, In vitro engineering of high modulus cartilage-like constructs, Tissue Engineering - Part C: Methods 22(4) (2016) 382-397.
[114] C.K. Kwan, A Methodology to Study Cell Deformation Behaviour within Native and Tissue Engineered Cartilage Subjected to Incremental Compression Using Confocal Microscopy, University of Leeds, 2020.
[115] https://ocugen.com/expanded-access-policy/neocart-policy/.
[116] H.R. Jones, D.C. Crawford, An Autologous Tissue Implant, NeoCart, for Treatment of Hyaline Cartilage Injury in the Knee, Operative Techniques in Orthopaedics 24(4) (2014) 264-270.
[117] A. Ravichandran, Y. Liu, S.-H. Teoh, Review: bioreactor design towards generation of relevant engineered tissues: focus on clinical translation, Journal of Tissue Engineering and Regenerative Medicine 12(1) (2018) e7-e22.
[118] L. Fu, P. Li, H. Li, C. Gao, Z. Yang, T. Zhao, W. Chen, Z. Liao, Y. Peng, F. Cao, X. Sui, S. Liu, Q. Guo, The Application of Bioreactors for Cartilage Tissue Engineering: Advances, Limitations, and Future Perspectives, Stem Cells International 2021 (2021) 6621806.

[119] M.F. Rai, M.J. Stoddart, F. Guilak, Mechanical Signals as Regulators of Cartilage Degeneration and Regeneration, JAAOS-Journal of the American Academy of Orthopaedic Surgeons 25(4) (2017) e87-e89.
[120] J.C.-T. Lu, Novel Multi-Axial Cartesian Bioreactor Engineered for Stimulation of Mechanically Regulated Gene Promoters in Human Chondrocytes, University of California, Davis2017.
[121] S.J. Gilbert, E.J. Blain, Cartilage mechanobiology: how chondrocytes respond to mechanical load, Mechanobiology in Health and Disease, Elsevier2018, pp. 99-126.
[122] B. Blombäck, Fibrinogen to fibrin transformation, Blood clotting enzymology, Academic Press New York and London1967, p. 143.
[123] R. Goldshmid, S. Cohen, Y. Shachaf, I. Kupershmit, O. Sarig-Nadir, D. Seliktar, R. Wechsler, Steric Interference of Adhesion Supports In-Vitro Chondrogenesis of Mesenchymal Stem Cells on Hydrogels for Cartilage Repair, Scientific Reports 5(1) (2015) 12607.
[124] I. Laidmäe, K. Ērglis, A. Cēbers, P.A. Janmey, R. Uibo, Salmon fibrinogen and chitosan scaffold for tissue engineering: in vitro and in vivo evaluation, J Mater Sci Mater Med 29(12) (2018) 182-182.
[125] M.M. Islam, M. Shahruzzaman, S. Biswas, M. Nurus Sakib, T.U. Rashid, Chitosan based bioactive materials in tissue engineering applications-A review, Bioactive Materials 5(1) (2020) 164-183.
[126] E.P. Brennan-Pierce, I. MacAskill, R.B. Price, J.M. Lee, Riboflavin-sensitized photo-crosslinking of collagen using a dental curing light, Bio-medical materials and engineering 24(4) (2014) 1659-71.
[127] J.-Y. Lai, L.-J. Luo, Effect of riboflavin concentration on the development of photo-cross-linked amniotic membranes for cultivation of limbal epithelial cells, RSC Advances 5(5) (2015) 3425-3434.
[128] S.-h. Kim, C.-C. Chu, Visible light induced dextran-methacrylate hydrogel formation using (−)-riboflavin vitamin B2 as a photoinitiator and L-arginine as a co-initiator, Fibers and Polymers 10(1) (2009) 14-20.

[129] B.G. Amsden, A. Sukarto, D.K. Knight, S.N. Shapka, Methacrylated glycol chitosan as a photopolymerizable biomaterial, Biomacromolecules 8(12) (2007) 3758-66.
[130] C. Lu, L. Liu, S.-R. Guo, Y. Zhang, Z. Li, J. Gu, Micellization and gelation of aqueous solutions of star-shaped PEG–PCL block copolymers consisting of branched 4-arm poly(ethylene glycol) and polycaprolactone blocks, European Polymer Journal 43(5) (2007) 1857-1865.
[131] E. Elizalde-Pena, D. Zarate-Trivino, S. Nuno-Donlucas, L. Medina-Torres, J. Gough, I. Sanchez, F. Villasenor, G. Luna-Barcenas, Synthesis and characterization of a hybrid (chitosan-g-glycidyl methacrylate)–xanthan hydrogel, Journal of Biomaterials Science, Polymer Edition 24(12) (2013) 1426-1442.
[132] P.A. Levett, D.W. Hutmacher, J. Malda, T.J. Klein, Hyaluronic Acid Enhances the Mechanical Properties of Tissue-Engineered Cartilage Constructs, PLoS ONE 9(12) (2014) e113216.
[133] E.L. Bortel, B. Charbonnier, R. Heuberger, Development of a Synthetic Synovial Fluid for Tribological Testing, Lubricants 3(4) (2015) 664-686.
[134] X. Zhao, Q. Lang, L. Yildirimer, Z.Y. Lin, W. Cui, N. Annabi, K.W. Ng, M.R. Dokmeci, A.M. Ghaemmaghami, A. Khademhosseini, Photocrosslinkable Gelatin Hydrogel for Epidermal Tissue Engineering, Advanced healthcare materials 5(1) (2016) 108-118.
[135] C. Willers, J. Chen, D. Wood, J. Xu, M. Zheng, Autologous chondrocyte implantation with collagen bioscaffold for the treatment of osteochondral defects in rabbits, Tissue engineering 11(7-8) (2005) 1065-1076.
[136] P. Roughley, C. Hoemann, E. DesRosiers, F. Mwale, J. Antoniou, M. Alini, The potential of chitosan-based gels containing intervertebral disc cells for nucleus pulposus supplementation, Biomaterials 27(3) (2006) 388-396.
[137] H. Park, B. Choi, J. Hu, M. Lee, Injectable chitosan hyaluronic acid hydrogels for cartilage tissue engineering, Acta Biomater 9(1) (2013) 4779-4786.

[138] J. O'Brien, I. Wilson, T. Orton, F. Pognan, Investigation of the Alamar Blue (resazurin) fluorescent dye for the assessment of mammalian cell cytotoxicity, European journal of biochemistry 267(17) (2000) 5421-6.
[139] R.W. Farndale, C.A. Sayers, A.J. Barrett, A direct spectrophotometric microassay for sulfated glycosaminoglycans in cartilage cultures, Connective tissue research 9(4) (1982) 247-8.
[140] C. Hoemann, J. Sun, V. Chrzanowski, M. Buschmann, A Multivalent Assay to Detect Glycosaminoglycan, Protein, Collagen, RNA, and DNA Content in Milligram Samples of Cartilage or Hydrogel-Based Repair Cartilage, Analytical biochemistry 300 (2002) 1-10.
[141] R.W. Farndale, D.J. Buttle, A.J. Barrett, Improved quantitation and discrimination of sulphated glycosaminoglycans by use of dimethylmethylene blue, Biochimica et biophysica acta 883(2) (1986) 173-7.
[142] C. Labarca, K. Paigen, A simple, rapid, and sensitive DNA assay procedure, Analytical biochemistry 102(2) (1980) 344-352.
[143] E. Pazarçeviren, Ö. Erdemli, D. Keskin, A. Tezcaner, Clinoptilolite/PCL–PEG–PCL composite scaffolds for bone tissue engineering applications, Journal of Biomaterials Applications 31(8) (2016) 1148-1168.
[144] Chitosan Scaffolds Containing Hyaluronic Acid for Cartilage Tissue Engineering, Tissue Engineering Part C: Methods 17(7) (2011) 717-730.
[145] H. Pulkkinen, V. Tiitu, P. Valonen, T. Silvast, J. Jurvelin, J. Töyräs, I. Kiviranta, M. Lammi, Repair of osteochondral defects with recombinant human type II collagen gel and autologous chondrocytes in a rabbit model, European Cells and Materials 20(2) (2010) 58.
[146] B.J. Ahern, J. Parvizi, R. Boston, T.P. Schaer, Preclinical animal models in single site cartilage defect testing: a systematic review, Osteoarthritis and Cartilage 17(6) (2009) 705-713.
[147] X. Wei, K. Messner, Maturation-dependent durability of spontaneous cartilage repair in rabbit knee joint, Journal of biomedical materials research 46(4) (1999) 539-48.

[148] C.W. Han, C.R. Chu, N. Adachi, A. Usas, F.H. Fu, J. Huard, Y. Pan, Analysis of rabbit articular cartilage repair after chondrocyte implantation using optical coherence tomography, Osteoarthritis and cartilage / OARS, Osteoarthritis Research Society 11(2) (2003) 111-21.
[149] C.-C. Yang, L. Jenkins, K. Burg, Adapted cryosectioning method for hydrogels used in regenerative medicine, Journal of Histotechnology 30(3) (2007) 185-191.
[150] K. Miyamoto, M. Sasaki, Y. Minamisawa, Y. Kurahashi, H. Kano, S.i. Ishikawa, Evaluation of in vivo biocompatibility and biodegradation of photocrosslinked hyaluronate hydrogels (HADgels), Journal of Biomedical Materials Research Part A: An Official Journal of The Society for Biomaterials, The Japanese Society for Biomaterials, and The Australian Society for Biomaterials and the Korean Society for Biomaterials 70(4) (2004) 550-559.
[151] K.A. Wegner, A. Keikhosravi, K.W. Eliceiri, C.M. Vezina, Fluorescence of picrosirius red multiplexed with immunohistochemistry for the quantitative assessment of collagen in tissue sections, Journal of Histochemistry & Cytochemistry 65(8) (2017) 479-490.
[152] B. Choi, S. Kim, B. Lin, B.M. Wu, M. Lee, Cartilaginous extracellular matrix-modified chitosan hydrogels for cartilage tissue engineering, ACS Appl Mater Interfaces 6(22) (2014) 20110-21.
[153] S. Kim, K. Bedigrew, T. Guda, W.J. Maloney, S. Park, J.C. Wenke, Y.P. Yang, Novel osteoinductive photo-cross-linkable chitosan-lactide-fibrinogen hydrogels enhance bone regeneration in critical size segmental bone defects, Acta biomaterialia 10(12) (2014) 5021-5033.
[154] A.A. Mansur, H.S. Mansur, Quantum dot/glycol chitosan fluorescent nanoconjugates, Nanoscale Res Lett 10 (2015) 172-172.
[155] D. Tripathi, A. Sharma, P. Tyagi, C.S. Beniwal, G. Mittal, A. Jamini, H. Singh, A. Tyagi, Fabrication of Three-Dimensional Bioactive Composite Scaffolds for Hemostasis and Wound Healing, AAPS PharmSciTech 22(4) (2021) 138.

[156] C. Vaquette, J.J. Cooper-White, Increasing electrospun scaffold pore size with tailored collectors for improved cell penetration, Acta Biomaterialia 7(6) (2011) 2544-2557.
[157] S.-H. Kim, C.-C. Chu, Fabrication of a biodegradable polysaccharide hydrogel with riboflavin, vitamin B2, as a photo-initiator and L-arginine as coinitiator upon UV irradiation, Journal of Biomedical Materials Research Part B: Applied Biomaterials 91B(1) (2009) 390-400.
[158] M.V. Encinas, A.M. Rufs, S. Bertolotti, C.M. Previtali, Free Radical Polymerization Photoinitiated by Riboflavin/Amines. Effect of the Amine Structure, Macromolecules 34(9) (2001) 2845-2847.
[159] J.H. Sobel, M.A. Gawinowicz, Identification of the α Chain Lysine Donor Sites Involved in Factor XIIIa Fibrin Cross-linking, Journal of Biological Chemistry 271(32) (1996) 19288-19297.
[160] J. Lam, S.T. Carmichael, W.E. Lowry, T. Segura, Hydrogel design of experiments methodology to optimize hydrogel for iPSC-NPC culture, Adv Healthc Mater 4(4) (2015) 534-9.
[161] A. Heirani-Tabasi, S. Hosseinzadeh, S. Rabbani, S.H.A. Tafti, K. Jamshidi, M. Soufi-Zomorrod, M. Soleimani, Cartilage tissue engineering by co-transplantation of chondrocyte extracellular vesicles and mesenchymal stem cells, entrapped in chitosan-hyaluronic acid hydrogel, Biomedical Materials (2021).
[162] S.R. Caliari, J.A. Burdick, A practical guide to hydrogels for cell culture, Nat Methods 13(5) (2016) 405-414.
[163] Y. Wang, M. Ma, J. Wang, W. Zhang, W. Lu, Y. Gao, B. Zhang, Y. Guo, Development of a Photo-Crosslinking, Biodegradable GelMA/PEGDA Hydrogel for Guided Bone Regeneration Materials, Materials (Basel, Switzerland) 11(8) (2018).
[164] M. Fathi-Achachelouei, D. Keskin, E. Bat, N.E. Vrana, A. Tezcaner, Dual growth factor delivery using PLGA nanoparticles in silk fibroin/PEGDMA hydrogels for articular cartilage tissue engineering, Journal of biomedical materials research. Part B, Applied biomaterials 108(5) (2020) 2041-2062.

[165] E.H. Nafea, L.A. Poole-Warren, P.J. Martens, Structural and permeability characterization of biosynthetic PVA hydrogels designed for cell-based therapy, Journal of biomaterials science, polymer edition 25(16) (2014) 1771-1790.
[166] W. Zhang, D. Zhong, Q. Liu, Y. Zhang, N. Li, Q. Wang, Z. Liu, W. Xue, Effect of chitosan and carboxymethyl chitosan on fibrinogen structure and blood coagulation, Journal of biomaterials science. Polymer edition 24(13) (2013) 1549-63.
[167] A. Gennari, J. Wedgwood, E. Lallana, N. Francini, N. Tirelli, Thiol-based michael-type addition. A systematic evaluation of its controlling factors, Tetrahedron 76(47) (2020) 131637.
[168] S. Huang, C. Wang, J. Xu, L. Ma, C. Gao, In situ assembly of fibrinogen/hyaluronic acid hydrogel via knob-hole interaction for 3D cellular engineering, Bioactive materials 2(4) (2017) 253-259.
[169] S. Pradhan, I. Hassani, W.J. Seeto, E.A. Lipke, PEG-fibrinogen hydrogels for three-dimensional breast cancer cell culture, Journal of Biomedical Materials Research Part A 105(1) (2017) 236-252.
[170] S.J. Bryant, K.S. Anseth, Hydrogel properties influence ECM production by chondrocytes photoencapsulated in poly (ethylene glycol) hydrogels, Journal of Biomedical Materials Research Part A 59(1) (2002) 63-72.
[171] H. Shin, B.D. Olsen, A. Khademhosseini, The mechanical properties and cytotoxicity of cell-laden double-network hydrogels based on photocrosslinkable gelatin and gellan gum biomacromolecules, Biomaterials 33(11) (2012) 3143-3152.
[172] S.C. Mastbergen, D.B. Saris, F.P. Lafeber, Functional articular cartilage repair: here, near, or is the best approach not yet clear?, Nature reviews rheumatology 9(5) (2013) 277.
[173] H. Wang, L. Zhou, J. Liao, Y. Tan, K. Ouyang, C. Ning, G. Ni, G. Tan, Cell-laden photocrosslinked GelMA–DexMA copolymer hydrogels with tunable mechanical properties for tissue engineering, Journal of Materials Science: Materials in Medicine 25(9) (2014) 2173-2183.

[174] M. Mu, X. Li, A. Tong, G. Guo, Multi-functional chitosan-based smart hydrogels mediated biomedical application, Expert Opinion on Drug Delivery 16(3) (2019) 239-250.
[175] F. Ganji, S. Vasheghani Farahani, E. Vasheghani-Farahani, Theoretical Description of Hydrogel Swelling: A Review, Iranian Polymer Journal 19 (2010) 375-398.
[176] N.A. Peppas, J.Z. Hilt, A. Khademhosseini, R. Langer, Hydrogels in biology and medicine: from molecular principles to bionanotechnology, Advanced Materials 18(11) (2006) 1345-1360.
[177] H. Hu, B. Ye, Y. Lv, Q. Zhang, Preparing antibacterial and in-situ formable double crosslinking chitosan/hyaluronan composite hydrogels, Materials Letters 254 (2019) 17-20.
[178] S. Samani, S. Bonakdar, A. Farzin, J. Hadjati, M. Azami, A facile way to synthesize a photocrosslinkable methacrylated chitosan hydrogel for biomedical applications, International Journal of Polymeric Materials and Polymeric Biomaterials 70(10) (2021) 730-741.
[179] F. Lin, H.-R. Jia, F.-G. Wu, Glycol Chitosan: A Water-Soluble Polymer for Cell Imaging and Drug Delivery, Molecules 24(23) (2019) 4371.
[180] Y. Wang, Y. Li, X. Yu, Q. Long, T. Zhang, Synthesis of a photocurable acrylated poly (ethylene glycol)-co-poly (xylitol sebacate) copolymers hydrogel 3D printing ink for tissue engineering, RSC advances 9(32) (2019) 18394-18405.
[181] F.J. O'Brien, Biomaterials & scaffolds for tissue engineering, Materials Today 14(3) (2011) 88-95.
[182] S.H. Pangburn, P.V. Trescony, J. Heller, Lysozyme degradation of partially deacetylated chitin, its films and hydrogels, Biomaterials 3(2) (1982) 105-108.
[183] K.M. Varum, M.M. Myhr, R.J. Hjerde, O. Smidsrod, In vitro degradation rates of partially N-acetylated chitosans in human serum, Carbohydr Res 299(1-2) (1997) 99-101.

[184] M. Zhang, T. Wan, P. Fan, K. Shi, X. Chen, H. Yang, X. Liu, W. Xu, Y. Zhou, Photopolymerizable chitosan hydrogels with improved strength and 3D printability, International Journal of Biological Macromolecules 193 (2021) 109-116.
[185] J. Iwasa, L. Engebretsen, Y. Shima, M. Ochi, Clinical application of scaffolds for cartilage tissue engineering, Knee Surgery, Sports Traumatology, Arthroscopy 17(6) (2009) 561-577.
[186] A. Hall, The Role of Chondrocyte Morphology and Volume in Controlling Phenotype—Implications for Osteoarthritis, Cartilage Repair, and Cartilage Engineering, Current Rheumatology Reports 21 (2019).
[187] E. Dejana, M.G. Lampugnani, M. Giorgi, M. Gaboli, P.C. Marchisio, Fibrinogen induces endothelial cell adhesion and spreading via the release of endogenous matrix proteins and the recruitment of more than one integrin receptor, Blood 75(7) (1990) 1509-17.
[188] J.T. Pinto, J. Zempleni, Riboflavin, Advances in nutrition (Bethesda, Md.) 7(5) (2016) 973-975.
[189] S. M Luna, S. Silva, M. Gomes, J.F. Mano, R.L. Reis, Cell Adhesion and Proliferation onto Chitosan-based Membranes Treated by Plasma Surface Modification, 2011.
[190] H. Li, R.-Q. Ma, H.-Y. Cheng, X. Ye, H.-L. Zhu, X.-H. Chang, Fibrinogen alpha chain promotes the migration and invasion of human endometrial stromal cells in endometriosis through focal adhesion kinase/protein kinase B/matrix metallopeptidase 2 pathway, Biology of Reproduction 103(4) (2020) 779-790.
[191] K. Singha, V. Kumar, S. Maity, P. Pandit, 19 - Development and processing of bioinert polymers and composites, in: S. Ahmed (Ed.), Advanced Green Materials, Woodhead Publishing2021, pp. 411-421.
[192] M. Mochizuki, N. Yamagata, D. Philp, K. Hozumi, T. Watanabe, Y. Kikkawa, Y. Kadoya, H.K. Kleinman, M. Nomizu, Integrin-dependent cell behavior on ECM peptide-conjugated chitosan membranes, Biopolymers 88(2) (2007) 122-30.
[193] R.R. Asawa, J.C. Belkowski, D.A. Schmitt, E.M. Hernandez, A.E. Babcock, C.K. Lochner, H.N. Baca, C.M. Rylatt, I.S. Steffes, J.J. VanSteenburg, Transient

cellular adhesion on poly (ethylene-glycol)-dimethacrylate hydrogels facilitates a novel stem cell bandage approach, Plos one 13(8) (2018) e0202825.
[194] D. Dikovsky, H. Bianco-Peled, D. Seliktar, The effect of structural alterations of PEG-fibrinogen hydrogel scaffolds on 3-D cellular morphology and cellular migration, Biomaterials 27(8) (2006) 1496-1506.
[195] Y. Li, T. Ma, D.A. Kniss, L.C. Lasky, S.-T. Yang, Effects of Filtration Seeding on Cell Density, Spatial Distribution, and Proliferation in Nonwoven Fibrous Matrices, Biotechnology Progress 17(5) (2001) 935-944.
[196] G. Bahcecioglu, N. Hasirci, B. Bilgen, V. Hasirci, A 3D printed PCL/hydrogel construct with zone-specific biochemical composition mimicking that of the meniscus, Biofabrication 11(2) (2019) 025002.
[197] S. Sanfilippo, M. Canis, L. Ouchchane, R. Botchorishvili, C. Artonne, L. Janny, F. Brugnon, Viability assessment of fresh and frozen/thawed isolated human follicles: reliability of two methods (Trypan blue and Calcein AM/ethidium homodimer-1), J Assist Reprod Genet 28(12) (2011) 1151-1156.
[198] Z.-K. Cui, S. Kim, J.J. Baljon, B.M. Wu, T. Aghaloo, M. Lee, Microporous methacrylated glycol chitosan-montmorillonite nanocomposite hydrogel for bone tissue engineering, Nature Communications 10(1) (2019) 3523.
[199] S. Ibusuki, G.J. Halbesma, M.A. Randolph, R.W. Redmond, I.E. Kochevar, T.J. Gill, Photochemically Cross-Linked Collagen Gels as Three-Dimensional Scaffolds for Tissue Engineering, Tissue Engineering 13(8) (2007) 1995-2001.
[200] S. Jahangir, D. Eglin, N. Pötter, M. Khozaei Ravari, M.J. Stoddart, A. Samadikuchaksaraei, M. Alini, M. Baghaban Eslaminejad, M. Safa, Inhibition of hypertrophy and improving chondrocyte differentiation by MMP-13 inhibitor small molecule encapsulated in alginate-chondroitin sulfate-platelet lysate hydrogel, Stem Cell Research & Therapy 11(1) (2020) 436.
[201] F. Chicatun, C.E. Pedraza, N. Muja, C.E. Ghezzi, M.D. McKee, S.N. Nazhat, Effect of chitosan incorporation and scaffold geometry on chondrocyte function in dense collagen type I hydrogels, Tissue Eng Part A 19(23-24) (2013) 2553-2564.

[202] Q.G. Wang, N. Hughes, S.H. Cartmell, N.J. Kuiper, The composition of hydrogels for cartilage tissue engineering can influence glycosaminoglycan profile, European cells & materials 19 (2010) 86-95.
[203] M. Pourentezari, M. Anvari, M. Yadegari, A. Abbasi, H. Dortaj, A Review of Tissue-Engineered Cartilage Utilizing Fibrin and Its Composite, International Journal of Medical Laboratory (2021).
[204] R.J. Miron, Y. Zhang, Autologous liquid platelet rich fibrin: A novel drug delivery system, Acta biomaterialia 75 (2018) 35-51.
[205] S.T. Ho, S.M. Cool, J.H. Hui, D.W. Hutmacher, The influence of fibrin based hydrogels on the chondrogenic differentiation of human bone marrow stromal cells, Biomaterials 31(1) (2010) 38-47.
[206] M. Sheykhhasan, R.T. Qomi, M. Ghiasi, Fibrin Scaffolds Designing in order to Human Adipose-derived Mesenchymal Stem Cells Differentiation to Chondrocytes in the Presence of TGF-β3, International journal of stem cells 8(2) (2015) 219-27.
[207] S. Deepthi, A.A.A. Gafoor, A. Sivashanmugam, S.V. Nair, R. Jayakumar, Nanostrontium ranelate incorporated injectable hydrogel enhanced matrix production supporting chondrogenesis in vitro, Journal of Materials Chemistry B 4(23) (2016) 4092-4103.
[208] K. Dibdiakova, A. Svec, Z. Majercikova, M. Adamik, M. Grendar, J. Vana, A. Ferko, J. Hatok, Associations between matrix metalloproteinase, tissue inhibitor of metalloproteinase and collagen expression levels in the adjacent rectal tissue of colorectal carcinoma patients, Molecular and Clinical Oncology 16(2) (2022) 1-9.
[209] A. Nakamura, D. Murata, R. Fujimoto, S. Tamaki, S. Nagata, M. Ikeya, J. Toguchida, K. Nakayama, Bio-3D printing iPSC-derived human chondrocytes for articular cartilage regeneration, Biofabrication 13(4) (2021) 044103.
[210] E.Y. Salinas, J.C. Hu, K. Athanasiou, A Guide for Using Mechanical Stimulation to Enhance Tissue-Engineered Articular Cartilage Properties, Tissue Eng Part B Rev 24(5) (2018) 345-358.

[211] C. Paggi, J. Hendriks, L. Moreira Teixeira Leijten, S. Le Gac, M. Karperien, Mechanical stimulation is a key component in the development of pericellular matrix around human chondrocytes, Osteoarthritis and Cartilage 29 (2021) S134.
[212] J.D. Kisiday, J.H. Lee, P.N. Siparsky, D.D. Frisbie, C.R. Flannery, J.D. Sandy, A.J. Grodzinsky, Catabolic responses of chondrocyte-seeded peptide hydrogel to dynamic compression, Annals of biomedical engineering 37(7) (2009) 1368-75.
[213] I. Uzieliene, D. Bironaite, P. Bernotas, A. Sobolev, E. Bernotiene, Mechanotransducive Biomimetic Systems for Chondrogenic Differentiation In Vitro, International journal of molecular sciences 22(18) (2021) 9690.
[214] C.J. Hunter, J.K. Mouw, M.E. Levenston, Dynamic compression of chondrocyte-seeded fibrin gels: effects on matrix accumulation and mechanical stiffness, Osteoarthritis and Cartilage 12(2) (2004) 117-130.
[215] J.L. Puetzer, J.J. Ballyns, L.J. Bonassar, The effect of the duration of mechanical stimulation and post-stimulation culture on the structure and properties of dynamically compressed tissue-engineered menisci, Tissue engineering. Part A 18(13-14) (2012) 1365-75.
[216] J.J. Ballyns, L.J. Bonassar, Dynamic compressive loading of image-guided tissue engineered meniscal constructs, Journal of Biomechanics 44(3) (2011) 509-516.
[217] D.E. Anderson, B. Johnstone, Dynamic Mechanical Compression of Chondrocytes for Tissue Engineering: A Critical Review, Frontiers in bioengineering and biotechnology 5 (2017) 76.
[218] S. Santos, K. Richard, M.C. Fisher, C.N. Dealy, D.M. Pierce, Chondrocytes respond both anabolically and catabolically to impact loading generally considered non-injurious, Journal of the Mechanical Behavior of Biomedical Materials 115 (2021) 104252.
[219] D.J. Leong, Y.H. Li, X.I. Gu, L. Sun, Z. Zhou, P. Nasser, D.M. Laudier, J. Iqbal, R.J. Majeska, M.B. Schaffler, M.B. Goldring, L. Cardoso, M. Zaidi, H.B. Sun, Physiological loading of joints prevents cartilage degradation through CITED2,

FASEB journal : official publication of the Federation of American Societies for Experimental Biology 25(1) (2011) 182-91.
[220] Y. Kuang, M. Fan, S. Liu, W. Ma, Dynamical Models of Biology and Medicine, MDPI-Multidisciplinary Digital Publishing Institute2019.
[221] C.L. Thompson, S. Fu, H.K. Heywood, M.M. Knight, S.D. Thorpe, Mechanical Stimulation: A Crucial Element of Organ-on-Chip Models, Frontiers in bioengineering and biotechnology 8 (2020).
[222] G. Bergmann, F. Graichen, A. Rohlmann, Hip joint loading during walking and running, measured in two patients, J Biomech 26(8) (1993) 969-90.
[223] I. Villanueva, D.S. Hauschulz, D. Mejic, S.J. Bryant, Static and dynamic compressive strains influence nitric oxide production and chondrocyte bioactivity when encapsulated in PEG hydrogels of different crosslinking densities, Osteoarthritis and cartilage 16(8) (2008) 909-918.
[224] T. Tallheden, C. Karlsson, A. Brunner, J. Van Der Lee, R. Hagg, R. Tommasini, A. Lindahl, Gene expression during redifferentiation of human articular chondrocytes, Osteoarthritis Cartilage 12(7) (2004) 525-35.
[225] R.L. Mauck, M.A. Soltz, C.C. Wang, D.D. Wong, P.H. Chao, W.B. Valhmu, C.T. Hung, G.A. Ateshian, Functional tissue engineering of articular cartilage through dynamic loading of chondrocyte-seeded agarose gels, Journal of biomechanical engineering 122(3) (2000) 252-60.
[226] N. Wang, S. Grad, M.J. Stoddart, P. Niemeyer, N.P. Südkamp, J. Pestka, M. Alini, J. Chen, G.M. Salzmann, Bioreactor-Induced Chondrocyte Maturation Is Dependent on Cell Passage and Onset of Loading, Cartilage 4(2) (2013) 165-176.
[227] S. Nebelung, K. Gavenis, B. Rath, M. Tingart, A. Ladenburger, M. Stoffel, B. Zhou, R. Mueller-Rath, Continuous cyclic compressive loading modulates biological and mechanical properties of collagen hydrogels seeded with human chondrocytes, Biorheology 48(5-6) (2011) 247-261.
[228] E.G. Lima, L. Bian, K.W. Ng, R.L. Mauck, B.A. Byers, R.S. Tuan, G.A. Ateshian, C.T. Hung, The beneficial effect of delayed compressive loading on tissue-

engineered cartilage constructs cultured with TGF-beta3, Osteoarthritis and cartilage 15(9) (2007) 1025-1033.
[229] P.-Y. Wang, W.-B. Tsai, Modulation of the proliferation and matrix synthesis of chondrocytes by dynamic compression on genipin-crosslinked chitosan/collagen scaffolds, Journal of biomaterials science. Polymer edition 24 (2013) 507-19.
[230] A.M. McDermott, E.A. Eastburn, D.J. Kelly, J.D. Boerckel, Effects of chondrogenic priming duration on mechanoregulation of engineered cartilage, Journal of Biomechanics 125 (2021) 110580.
[231] T. Chowdhury, D. Salter, D. Bader, D. Lee, Integrin-mediated mechanotransduction processes in TGFβ-stimulated monolayer-expanded chondrocytes, Biochemical and biophysical research communications 318(4) (2004) 873-881.
[232] J.D. Humphrey, E.R. Dufresne, M.A. Schwartz, Mechanotransduction and extracellular matrix homeostasis, Nature reviews Molecular cell biology 15(12) (2014) 802-812.
[233] A.C. Hall, The role of chondrocyte morphology and volume in controlling phenotype—implications for osteoarthritis, cartilage repair, and cartilage engineering, Current Rheumatology Reports 21(8) (2019) 1-13.
[234] J. De Croos, B. Jang, S. Dhaliwal, M. Grynpas, R. Pilliar, R. Kandel, Membrane type-1 matrix metalloproteinase is induced following cyclic compression of in vitro grown bovine chondrocytes, Osteoarthritis and cartilage 15(11) (2007) 1301-1310.
[235] G.D. Nicodemus, S.J. Bryant, Mechanical loading regimes affect the anabolic and catabolic activities by chondrocytes encapsulated in PEG hydrogels, Osteoarthritis Cartilage 18(1) (2010) 126-37.
[236] H.J. Yoon, S.B. Kim, D. Somaiya, M.J. Noh, K.-B. Choi, C.-L. Lim, H.-Y. Lee, Y.-J. Lee, Y. Yi, K.H. Lee, Type II collagen and glycosaminoglycan expression induction in primary human chondrocyte by TGF-β1, BMC Musculoskelet Disord 16 (2015) 141-141.

[237] J.D. Bancroft, C. Layton, The hematoxylins and eosin, Bancroft's theory and practice of histological techniques (2012) 173-186.
[238] A. Frazer, R.A. Bunning, M. Thavarajah, J.M. Seid, R.G. Russell, Studies on type II collagen and aggrecan production in human articular chondrocytes in vitro and effects of transforming growth factor-beta and interleukin-1beta, Osteoarthritis Cartilage 2(4) (1994) 235-45.
[239] A. Mobasheri, S.D. Carter, P. Martín-Vasallo, M. Shakibaei, Integrins and stretch activated ion channels; putative components of functional cell surface mechanoreceptors in articular chondrocytes, Cell biology international 26(1) (2002) 1-18.
[240] W.B. Valhmu, E.J. Stazzone, N.M. Bachrach, F. Saed-Nejad, S.G. Fischer, V.C. Mow, A. Ratcliffe, Load-controlled compression of articular cartilage induces a transient stimulation of aggrecan gene expression, Archives of Biochemistry and Biophysics 353(1) (1998) 29-36.
[241] J. Yao, B. Seedhom, Mechanical conditioning of articular cartilage to prevalent stresses, Rheumatology 32(11) (1993) 956-965.
[242] M.D. Buschmann, Y.A. Gluzband, A.J. Grodzinsky, E.B. Hunziker, Mechanical compression modulates matrix biosynthesis in chondrocyte/agarose culture, Journal of cell science 108(4) (1995) 1497-1508.
[243] E. Ruvinov, T. Tavor Re'em, F. Witte, S. Cohen, Articular cartilage regeneration using acellular bioactive affinity-binding alginate hydrogel: A 6-month study in a mini-pig model of osteochondral defects, Journal of Orthopaedic Translation 16 (2019) 40-52.
[244] Y. Hua, H. Xia, L. Jia, J. Zhao, D. Zhao, X. Yan, Y. Zhang, S. Tang, G. Zhou, L. Zhu, Q. Lin, Ultrafast, tough, and adhesive hydrogel based on hybrid photocrosslinking for articular cartilage repair in water-filled arthroscopy, Science Advances 7(35) eabg0628.
[245] R. Barbucci, S. Lamponi, A. Borzacchiello, L. Ambrosio, M. Fini, P. Torricelli, R. Giardino, Hyaluronic acid hydrogel in the treatment of osteoarthritis, Biomaterials 23(23) (2002) 4503-4513.

APPENDICES

APPENDIX A

STANDART CURVE FOR GAG QUANTIFICATION

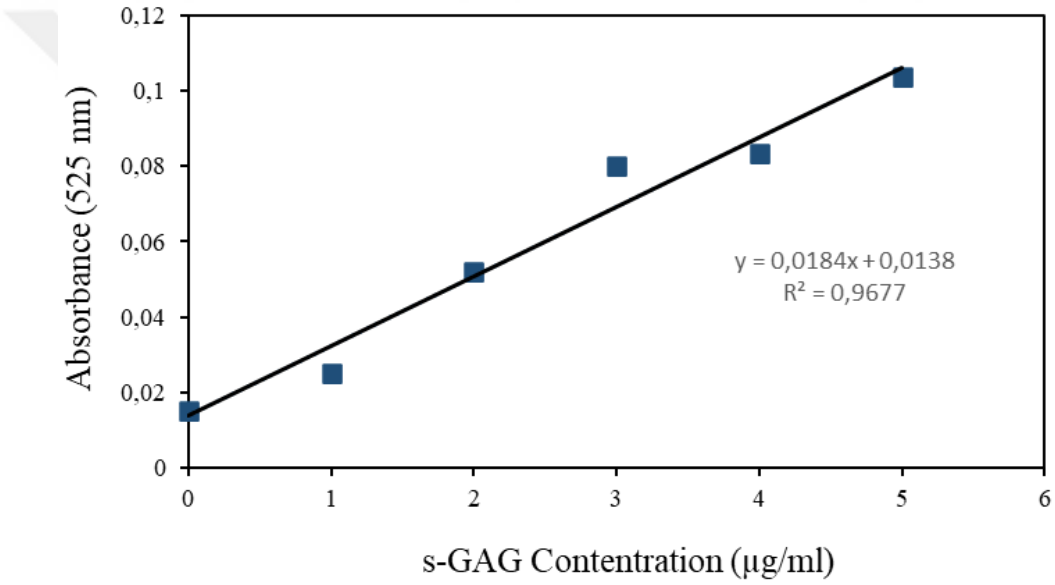

Figure A.1 A representative standart curve for s-GAG quantification using DMMB assay

.

APPENDIX B

STANDART CURVE FOR TOTAL COLLAGEN QUANTIFICATION

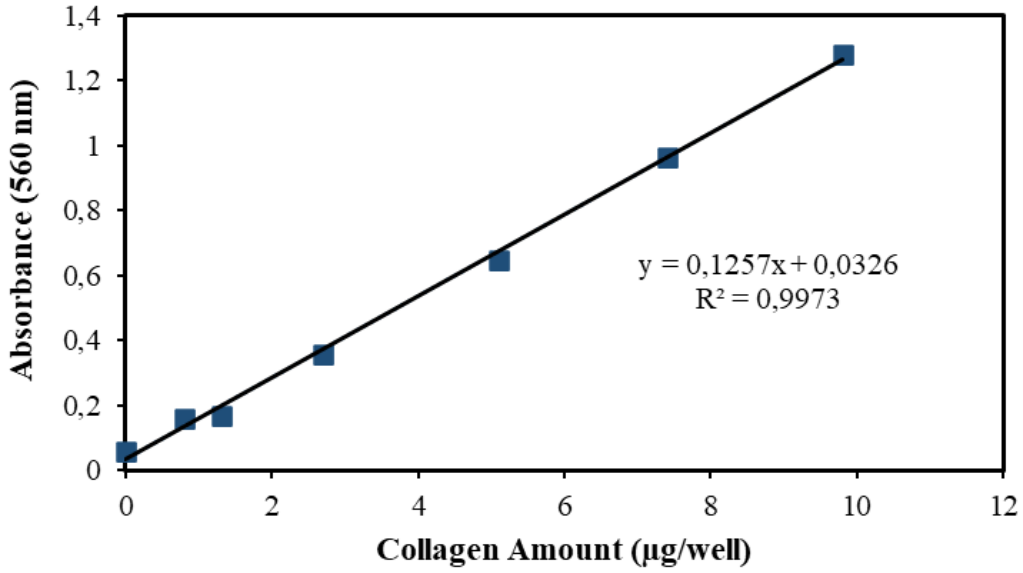

Figure B.1 A representative standart curve for collagen quantification using Total Collagen Assay Kit (Biovision Inc., USA)

APPENDIX C

STANDART CURVE FOR COLLAGEN TYPE II QUANTIFICATION

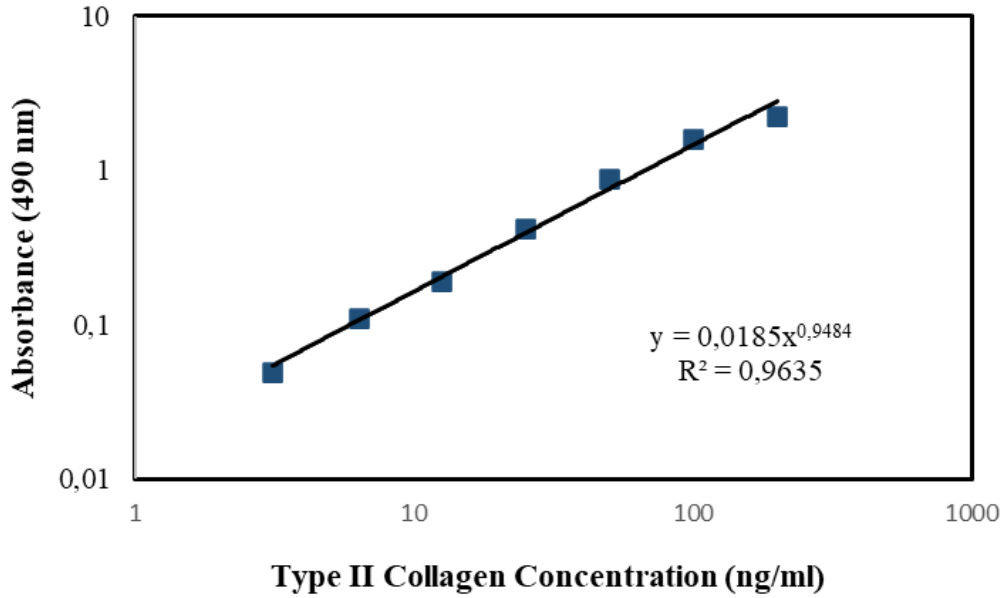

Figure C.1 A representative standart curve for collagen type II determination using Type II Collagen Detection Kit, Multi-Species (Chondrex, USA).

APPENDIX D

REPRESENTATIVE IMAGES FOR AVERAGE PORE SIZE MEASUREMENT

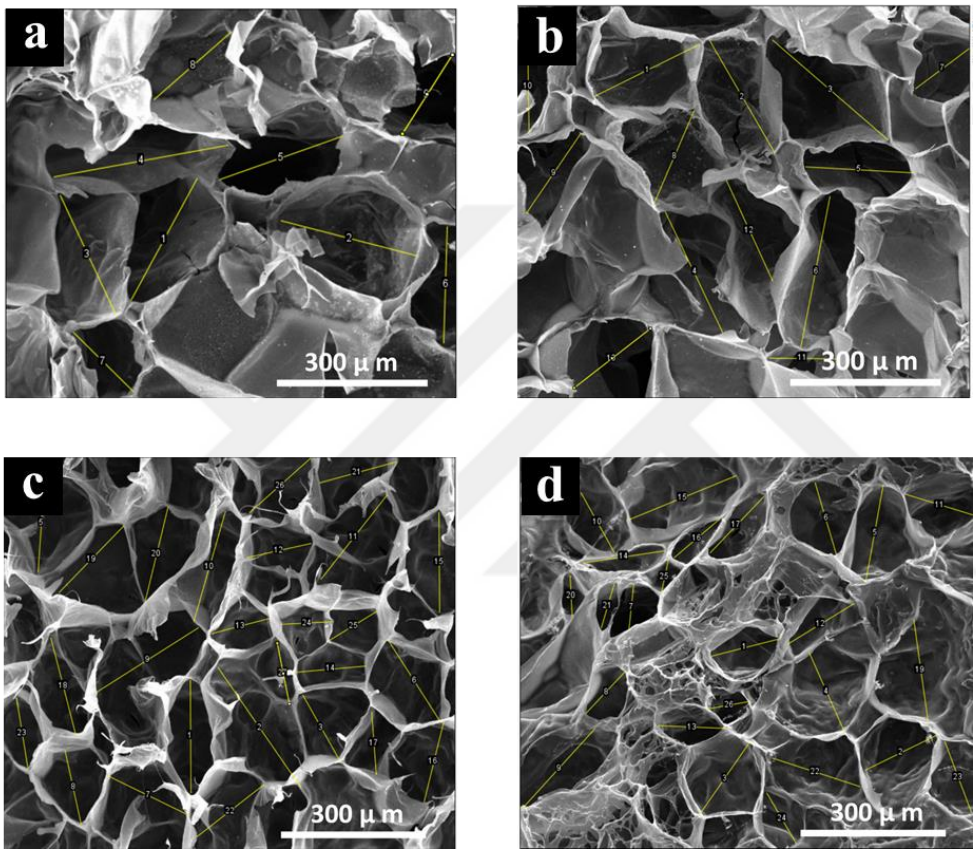

Figure D.1 Representative images for the average pore size diameter measurements on cross-sectional SEM images of (a) MeGC, (b) 0.25 MeGC-Fib, (c) 0.5 MeGC-Fib, (d) 1 MeGC-Fib hydrogels. Average pore sizes were calculated using over 50 measurements obtained from SEM images via ImageJ software (National Institutes of Health, Bethesda, USA).

APPENDIX E

REPRESENTATIVE STRESS-STRAIN CURVE FOR 1 MEGC-FIB HYDROGELS

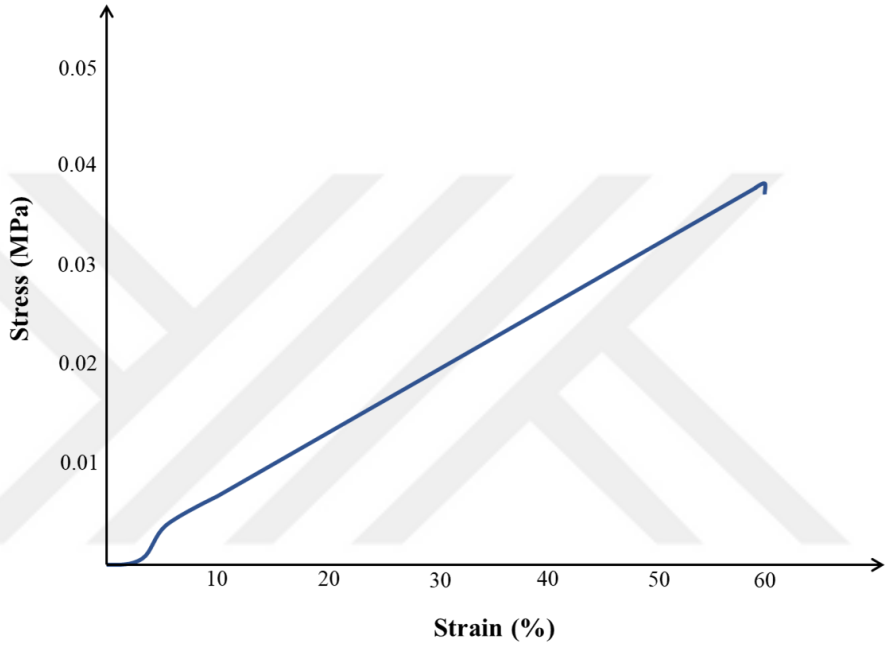

Figure E.1 A representative stress-strain graph for 1 MeGC-Fib hydrogels.